Aus dem Institute

BIH Center for Regenerative Therapies

der Medizinischen Fakultät Charité – Universitätsmedizin Berlin

DISSERTATION

Induced cardiomyocyte precursor cells obtained by direct reprogramming of cardiac fibroblasts

zur Erlangung des akademischen Grades

Doctor of Philosophy (PhD)

vorgelegt der Medizinischen Fakultät

Charité – Universitätsmedizin Berlin

von

Dipthi Bachamanda Somesh

aus Kodagu, India

Datum der Promotion: 18.12.2020

The presented work was performed from August 2014 to April 2019 in the framework of the graduate school Berlin-Brandenburg School for Regenerative Therapies (BSRT).

I, Dipthi Bachamanda Somesh performed most of the practical work under the supervision and guidance of Prof. Dr. Christof Stamm, Dr. Manfred Gossen and Prof. Andreas Kurtz at the Berlin-Brandenburg Center for Regenerative Therapies (BCRT).

Currently, a journal paper is underway summarizing the findings from this thesis. I, Dipthi Bachamanda Somesh am the first co-author along with contributions,

Cell sorting was done by, Dr. rer. nat. Désiree Kunkel, at the BCRT FACS core facility.
RNA sequencing was done by, M.Sc. Ulrike Krüger of the BIH core facility Genomics at Charité – Universitätsmedizin Berlin.
The RNA sequencing data was analyzed by, Dr. rer. nat. Karsten Jürchott, Bioinformatician of Development & Exploratory Lab (DEL), Charité – Universitätsmedizin Berlin.
Janita Aline Maring performed all animal surgeries while I assisted, at Forschungeinrichtung für Experimentelle Medizin (FEM) the animal housing facility, Charité – Universitätsmedizin Berlin.

Additionally, partial results of the presented work have been published as Abstracts:

- Generating proliferative induced cardiomyocyte precursor cells
- Proliferative induced cardiomyocyte precursor cells obtained by direct reprogramming and transcriptional selection
- Maturation of Induced Cardiomyocyte Precursor Cells Created by Direct Reprogramming
- Induced cardiomyocyte progenitor cells created by direct reprogramming and transcriptional selection
- Next generation sequencing reveals a committed but immature phenotype of induced cardiomyocyte progenitor cells
- Maintenance and expansion of induced cardiomyocyte precursor cells created by direct reprogramming
- Transcriptional selection and maintenance of induced cardiomyocyte precursor cells created by direct reprogramming
- Transcriptional selection of induced cardiomyocyte precursor cells

For details please refer to Section 14 of the thesis “Declaration of your own contribution to any publications”

TABLE OF CONTENTS

LIST OF FIGURES AND TABLES

1. ABBREVIATIONS

5-Aza	5-Azacytidine
α-actinin	Alpha actinin, sarcomeric
α-SMA	Alpha smooth muscle actin
AA	Ascorbic acid
AHT	Adult heart tissue
BSA	Bovine serum albumin
CRM	Cardiac reprogramming medium
CDM	Cardiac differentiation medium
cDNA	Complimentary deoxyribonucleic acid
cECM	Cardiac extracellular matrix
CFs	Cardiac fibroblasts
CMs	Cardiomyocytes
CPCs	Cardiac progenitor cells
cTnT	Cardiac troponin
CY5	Cyanine 5
DELC	Delivery control
DM	Differentiation medium
DMEM	Dulbecco's Modified Eagle Medium
DNA	Deoxyribonucleic acid
eGFP	Enhanced green fluorescent protein
ECM	Extracellular matrix
EF	Ejection Fraction
ESCs	Embryonic stem cells
FACS	Fluorescence activated cell sorting
FBS	Fetal bovine serum
FCS	Fetal calf serum
Gata4	GATA binding protein 4
GFP	Green fluorescence protein
GMTMy	Gata4, Mef2c, Tbx5, Myocd
GO	Gene ontology
G418	Geneticin Antibiotic
Hek293	Human embryonic kidney cells

HI-FBS	Heat-inactivated fetal bovine serum
HL1	HL1 cardiac muscle cell line
HT1080	Human fibrosarcoma cell line
ICC	Immunocytochemistry
iCMPs	Induced cardiomyocyte precursors
iPSCs	Induced pluripotent stem cells
IRES	Internal ribosome entry site
LeV	Lentivirus
LV	Left Ventricle
MBs	Molecular Beacons
mEH	Mouse embryonic heart
Mef2a	Myocyte-specific enhancer factor 2a
Mef2c	Myocyte-specific enhancer factor 2c
MI	Myocardial infarction
mNH	Mouse neonatal heart
MOI	Multiplicity of infection
MYH6	Myosin heavy chain 6, cardiac muscle alpha (αMHC)
MYH7	Myosin heavy chain 7, cardiac muscle beta (βMHC)
MYH6/7	Myosin heavy chain 6/7 (α/βMHC)
Myocd	Myocardin
NEGC	Negative control
PCR	Polymerase chain reaction
PEI	Polyethylenimine
RNA	Ribonucleic acid
RNA-Seq	RNA sequencing
RT	Room temperature
SFDM	Serum free differentiation medium
SFFV	Spleen focus forming virus
Tbx5	T-box transcription factor 5
TNNT2	Troponin T
qPCR	Quantitative real time polymerase chain reaction

2. ABSTRACT

Cardiovascular diseases are the leading cause of death globally. Cardiomyocytes (CMs) have poor proliferative capacity, and the therapeutic options to restore heart function are limited. However, there are several promising strategies for cardiac regeneration. The most promising approach is cell transplantation therapy using newly generated CMs. Induced cardiomyocytes (iCMs) generated from cardiac fibroblasts (CFs) represent a potential cell population. However, the iCM reprogramming efficiency is low and mature iCMs do not proliferate. Here I report the generation of proliferative iCM precursor cells (iCMPs) with CM lineage commitment by genetic reprogramming.

CFs were reprogrammed into iCMPs via transduction with cardiomyogenesis-related transcription factors Gata4, Mef2c, Tbx5 and Myocd. Global transcriptome profiling of iCMPs, CFs and mouse adult CMs was performed by RNA sequencing. For differentiation into iCMs, the effectiveness of previously established differentiation conditions was tested. I then extended the approach to the native heart environment. The therapeutic potential of iCMPs was evaluated in a in a rodent model of ischemic heart disease.

iCMPs expressed α-actinin, cTnT and myosin protein as observed by immunocytology. The iCMPs were a heterogenous population of cTnT positive cells, most of which showed a round epithelial like cells morphology. These iCMPs could robustly proliferative and when supplemented with ascorbic acid could maintain a stable phenotype. Pure populations of iCMPs were obtained by transcriptional selection with Myh6/7-targeting molecular beacons. Maturation studies showed that iCMPs displayed elongated sarcomere-like structures after stimulation with 5-Azacytidine a general demethylating agent, which has previously been described for differentiation toward cardiomyocytes. Gene expression pattern suggests that these iCMPs displayed a unique gene expression profile that move towards CM development. In addition, when transplanted into rodent hearts following myocardial infarction (MI), they show improved cardiac function such as left ventricular ejection fraction.

In conclusion I can transdifferentiate fibroblasts into cardiomyogenic cells that can be purified using a clinically compatible molecular beacon technique, can be expanded to yield therapeutic cell doses and exert therapeutic benefits.

Thus, iCMPs are a potential candidate for cardiac cell therapy.

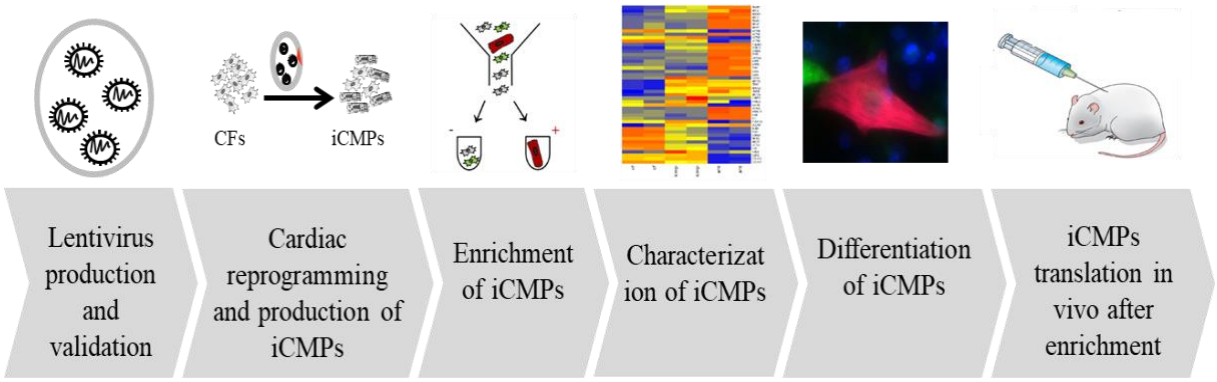

Figure 1: Graphical abstract of the project

3. ZUSAMMENFASSUNG

Herz-Kreislauf-Erkrankungen sind weltweit die häufigste Todesursache. Kardiomyozyten (CMs) haben eine geringe Proliferationskapazität und die therapeutischen Möglichkeiten zur Wiederherstellung der Herzfunktion sind begrenzt. Der wohl vielversprechendste Ansatz zur Herzregeneration ist die Transplantation von CMs. Eine mögliche Zielpopulation sind induzierte Kardiomyozyten (iCMs), die aus Herzfibroblasten (CFs) erzeugt werden. Allerdings ist die Effizienz der iCM-Reprogrammierung gering und reife iCMs sind nicht in der Lage, sich zu vermehren. Eine Lösung dieses Problems ist gleichfalls das Ziel der vorliegenden Arbeit: die Erzeugung proliferativer iCM-Vorläuferzellen (iCMPs) mit CM-Abstammung durch genetische Reprogrammierung.

CFs wurden durch Transduktion verschiedener Transkriptionsfaktoren, die im Zusammenhang mit der Kardiomyogenese stehen, beispielsweise Gata4, Mef2c, Tbx5 und Myocd, in iCMPs umprogrammiert. Die Untersuchung des Transkriptoms erfolgte durch RNA-Sequenzierung. Weiterhin wurde die Effizienz bereits etablierter Kultivierungsbedingungen bezüglich der Differenzierung dieser Zellen in CMs untersucht. Dieser Ansatz wurde anschließend auf die native Herzumgebung ausgedehnt. Schließlich wurde das therapeutische Potenzial von iCMPs in einem Nagetiermodell für ischämische Herzerkrankungen bewertet.

Immunzytologische Untersuchungen zeigten, dass die generierten iCMPs α-Actinin und Myosin exprimieren. Sie stellen eine heterogene Population von cTnT-positiven Zellen dar, von denen die meisten eine kreisförmige epitheliale Zellmorphologie aufwiesen. Sie waren in der Lage, sich zu vermehren und unter Zugabe von Ascorbinsäure wiesen sie einen stabilen Phänotyp auf. Nach Transkriptionsselektion mit Myh6/7-abzielender molecular beacons wurde eine reine Population an iCMPs gewonnen. Reifungsstudien zeigten, dass iCMPs nach Stimulation mit 5-Azacytidin verlängerte sarkomerartige Strukturen haben. Zudem legt das Genexpressionsmuster nahe, dass diese iCMPs ein einzigartiges Genexpressionsprofil besitzen. Wurden sie nach einem Myokardinfarkt (MI) in Nagetierherzen transplantiert, übten sie darüber hinaus therapeutische Vorteile, wie eine verbesserte Herzfunktion, aus.

Zusammenfassend war es möglich, Fibroblasten in kardiomyogene Zellen zu transdifferenzieren und sie unter Verwendung einer klinisch kompatiblen molecular beacon-Technik zu isolieren. Anschließend wurden sie kultiviert, um therapeutische Zelldosen zu erzielen und therapeutische Vorteile, wie eine verbesserte Herzfunktion, zu ermöglichen.

Insgesamt stellen iCMPs einen aussichtsreichen Kandidaten für eine Herzzelltherapie dar.

4. KEY WORDS

Cardiomyocytes, cardiac fibroblasts, direct reprogramming, global transcriptome profile, induced cardiomyocyte precursors, lentivirus, molecular beacons, myosin heavy chain, cardiac regeneration.

5. INTRODUCTION

5.1. HEART FAILURE

Heart failure is the ultimate fate of many patients with various forms of heart disease. One of the major underlying causes is the irreversible loss of cardiomyocytes (CMs). After heart injury, myocardial infarction or chronic inflammation, deleterious remodeling of the heart wall ensues, which leads to the formation of a scar composed of myofibroblasts since adult CMs have little or no ability to regenerate. This scar tissue replacing the lost CMs supports the cardiac structure after injury. Over time, however, this dysfunctional fibrotic tissue leads to progressive deterioration of the heart function followed by heart failure and death, as the heart is unable to meet the workload demand (1).

The treatment options to restore heart function in case of end-stage heart failure are heart transplantation or a ventricular assist device that can be attached to the weakened left ventricle of the heart to help increase blood flow to the body called the left ventricular assist device (LVAD) implantation. These treatment options have huge limitations, e.g. the limited number of donor hearts available, heart transplant rejection, and with LVAD right ventricular failure due to setting of loading changes, physical functional limitations, more psychological distress and reduced quality of life (2-4).

Current therapeutic means are therefore mostly palliative, relieving symptoms and prolonging life for a limited period (5). To date, the medical and surgical therapies are unable to address the main issue causing decreased function in the diseased or aging heart: loss of CMs (6). Moreover, the regeneration capacity of the heart although it seems to exist is insufficient in most patients with severe forms of heart disease (7, 8).

Due to these major limitations, there is a significant clinical need for cardiac regenerative therapy. The main aim of cardiac regenerative therapies is to generate new contractile cells, to replace the damaged cells lost during injury and to restore normal structure and function of the heart. A considerable amount of research has been performed and is still underway to develop cardiac regenerative therapies. Somatic stem cells and progenitor cells from non-cardiac sources such as bone marrow, blood, placenta, and adipose tissue have had some beneficial effect when

transplanted into the heart but are unable to remodel or heal the scar tissue, nor have they been able to activate differentiation of resident cardiac stem cells to support regeneration (9).

Scientists in this era of regenerative medicine are focusing on actually curing heart problems, and not just treating them and delaying the vicious cycle leading to heart failure. Various approaches have been proposed thereafter such as induced pluripotent stem cell (iPSC) derived CMs.

Regeneration of the myocardium can be potentially accomplished by focusing on one of the promising approaches like iPSC reprogramming followed by differentiation to desired cell types such as iPSC-CMs.

5.2. INDUCED PLURIPOTENT STEM CELL DERIVED CARDIOMYOCYTES

In 2006, ESC like cells named induced pluripotent stem cells (iPSCs) could be generated from fibroblasts using a cocktail of transcription factors, Oct4, Klf4, Sox2 and c-myc (OSKM) (10). This discovery of four transcription factors that made a huge cellular change was a major breakthrough. The rationale underlying the reprogramming strategy of Takahashi et al. was that ectopic expression of the transcription factors, which determine the pluripotent phenotype, would convert mature cells back into the pluripotent state (10). Starting out with 24 transcription factors, single factors successively being eliminated and resulting in a combination of OSKM to be sufficient to induce pluripotent reprogramming. iPSCs have come a long way ever since. Lately, iPSCs differentiation has also been induced by chemical means (11).

iPSCs have been hailed as an ideal replacement for ESCs and have become an important tool providing an unlimited supply of once-inaccessible tissues for research. They can be differentiated into any desired cell type. Directed differentiation methods have been developed to obtain CMs efficiently from iPSCs (12-16). Additionally, an autologous cell therapy setting is possible with patient-specific iPSC derived CMs. However, CM maturity, tissue regeneration, heterogeneity, feasibility, and safety remain an issue for cardiac regenerative therapy (17).

Nevertheless, iPSCs brought regenerative medicine closer to its aim. Reprogramming to pluripotent cells convincingly proved that end-stage differentiated cells can be reprogrammed and pushed back up to the top of Waddington's epigenetic landscape.
Besides reprogramming to iPSCs raised the possibility that somatic cells could transdifferentiate into desired cell types without passing through a stem cell stage in a process called direct reprogramming.

5.3. DIRECT CARDIAC REPROGRAMMING

About 30 years ago Davis et al. showed that overexpression of a single transcription factor MyoD, could convert fibroblasts to skeletal muscle in vitro (18) proving that the marbles could take different routes and dedifferentiate or transdifferentiate moving in different routes of the epigenetic landscape. Transcription factors (TFs) like MyoD were discovered for various cell types and direct lineage conversions have since been reported for some cell types. For example, CEBP TF can convert B Lymphocytes to macrophages; GATA-1 transformed myeloblasts to erythroid megakaryocytic cells, and; inner ear cells can be reprogrammed to hair cells by Math1 (19-22).

Unfortunately, for CMs, no single "master regulator" has been, identified. Nevertheless, the discovery and ability to transdifferentiate has paved the path for new treatment approaches.

Thus, lessons from iPSCs generation paved the way to direct reprogramming by forced expression of a cocktail of transcription factors. Direct cardiac reprogramming strategy involves reprogramming cells from the vast pool of non-myocytes, such as cardiac fibroblasts (CFs) in the heart. CFs in the healthy heart account for up to 10% of the total cell population, while endothelial cells are 44%, cardiomyocytes 30% and other non-myocytes 15% (23). Myocardial infarction leads to irreversible loss of CMs followed by a reparative response in which the damaged tissue is replaced with a fibrotic scar produced by CFs proliferation (24). Thus, acknowledging that CFs are activated and increased by replication in an injured heart tissue makes them an ideal candidate for cardiac reprogramming (25). Moreover, reprogramming from neighboring tissue or resident cell types has the advantage of being physically proximal to the injury site, will favor tissue integration and reprogramming in ideal conditions (26).

Applying the concept of iPSC reprogramming, Ieda et al. tested fourteen different factors and identified a combination of three transcription factors Gata4, Mef2c and Tbx5 (GMT) sufficient for reprogramming mouse post-natal fibroblasts into a cardiomyocyte-like cell state (27).
Varieties of approaches have ever since been designed to steer fibroblast cells directly into a cardiomyogenic fate, each employing a unique combination of cardiac-specific transcription factors, miRNAs and/or chemical molecules. Following the initial report by Ieda et al., other groups also reported the generation of cardiomyocyte-like cells from mouse fibroblasts based on the same factors or microRNAs plus additional factors (28-37).

To advance cardiac reprogramming technology, the knowledge gained from studies using mouse system was translated into human cells. GMT alone was insufficient for cardiac induction in human fibroblast. However, in combination with Mesp and Myocd (GMTMM) or with Mesp and Esrrg (GMTEM), human CFs could be reprogrammed into CMs (38-40). Furthermore, following the proof-of-concept in vitro. Qian et al. and Mathison et al. showed that reprogramming of fibroblasts into CMs can be achieved in situ, by delivering reprogramming genes directly into the myocardium following myocardial infarction (MI) (41, 42). This strategy involves reprogramming cells from the vast pool of non-myocytes in the heart (25, 43-45). In vivo, cardiac reprogramming technology circumvents cell therapy associated challenges such as cell retention and homing. However, it brings with it a different set of challenges such as virus toxicity - immunogenicity towards virus or induced cell product, immaturity, cell heterogeneity, and low reprogramming efficiency.

Mature functional iCMs do not proliferate as converted cells rapidly exited the cell cycle, making the regeneration of the heart even more challenging. Regardless of all the huge efforts such as modifications of stoichiometry, transcription factors, small molecules, micro-RNAs and epigenetic factors the reprogramming efficiency and maturity of the iCMs remain an important obstacle to overcome before clinical applications (28-36, 46-50).

Therefore, to generate effective regenerative therapy, we need to reprogram cardiac fibroblasts into a cardiomyogenic cell type with proliferative capacity.

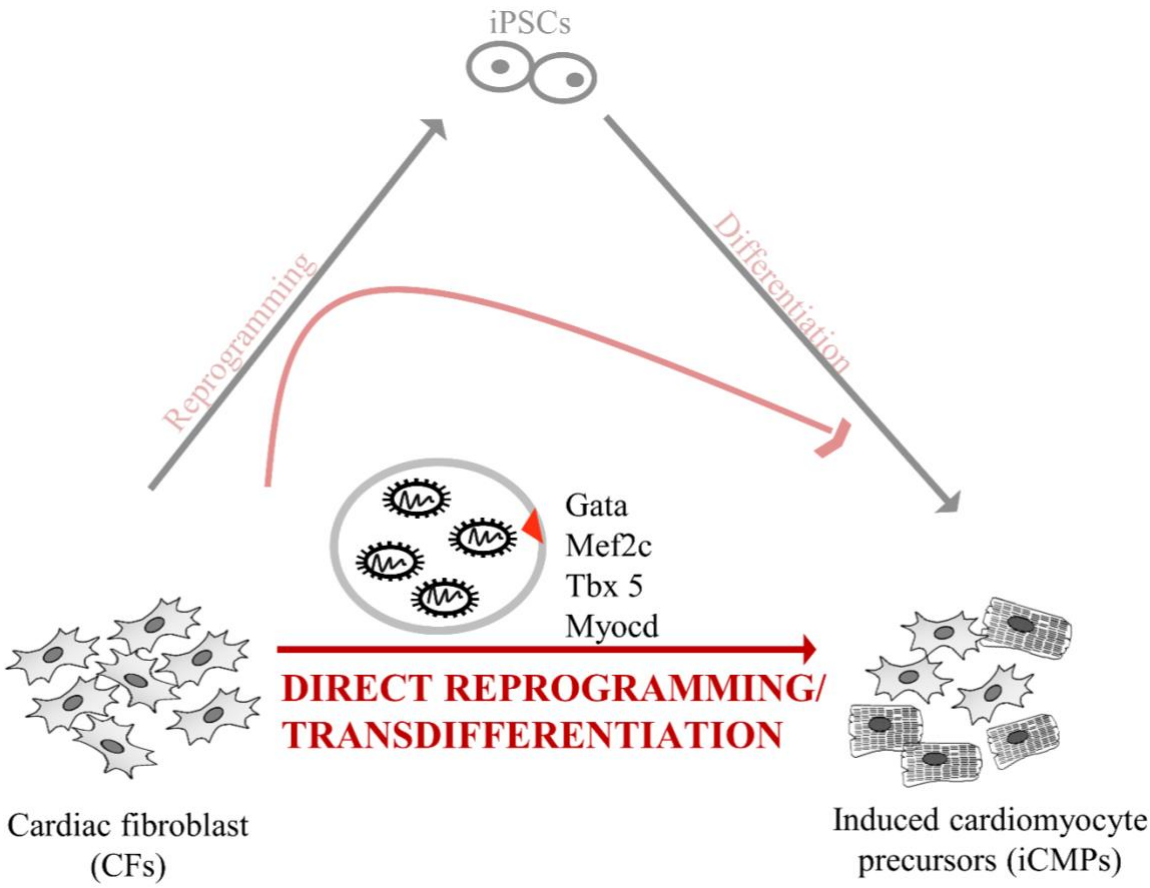

Figure 2: Schematic of direct reprogramming of cardiac fibroblasts into cardiomyocyte like cells, bypassing the iPSC state of reprogramming.

5.4. LENTIVIRAL SYSTEM

Successful reprogramming of cells requires short-term overexpression of transcription factors and efficient vectors. The sufficient presence of these exogenous transcriptional factors activates the endogenous gene regulatory networks, thereby establishing stable reprogrammed target cell phenotypes. Numerous approaches for factor delivery have been used over the past decades including viral vs. non-viral as well as DNA-based and RNA-based. Viral delivery systems like MMLV replication-defective retrovirus (RV), HIV-based self-inactivating lentivirus (LeV), replication-defective non-integrating adenovirus (AV) and adeno-associated virus (AAV) have emerged as powerful tools for transgene delivery over the past decades (Table 1).

AV can deliver genetic material up to a size of 30kb. However, AV provokes a strong immune response (51). To address this issue, AAV was developed, but with a decreased carrier size of 5kb. RV and LeV systems, on the other hand, can efficiently transfer up to 8kb genetic material into the cells, which will then be integrated into the cellular genome. Additionally, LeV and RV can be pseudotyped with a wide variety of envelope proteins to broaden tropism; they have the ability to produce polycistronic vehicles generating less heterogeneous cells. LeV infection has the advantage of high-efficiency infection of dividing and non-dividing cells over RV gene-therapy method.

Other transduction systems are currently being evaluated for reprogramming efficacy by various groups. However, when we initiated this project, the emphasis on LeV appeared justified: (i) the tropism of these vectors is broad and known to include dividing and non-dividing fibroblasts, which can be efficiently transduced at a low MOI, (ii) the cell type specificity can be readily adapted via pseudotyping, and (iii) the relative ease of production.
Therefore, in this study, LeV transfection system was used to target dividing and non-dividing cardiac fibroblasts and for the proof-of-concept. For further advancement, we need to switch to a transfection system with similar or better transfection efficiency as LeV and one that is safe for clinical translation.

	Lentivirus	**Retrovirus**	**Adenovirus**	**Adeno-associated virus**
Genome	ss-RNA (+)	ss-RNA (+)	dsDNA	ssDNA
Genome size	8-10kb	8kb	37.7kb	4.7kb
Packaging capacity	2.5-5kb	2.5-5kb	3-8kb	2.5-4.5kb
Virion size	80-130nm	80-130nm	90-100nm	20-25nm
Virion coat	Enveloped	Enveloped	Naked	Naked
Tropism	Dividing and non-dividing	Dividing	Dividing and non-dividing	Dividing and non-dividing
Gene delivery efficiency	>90%	90%	Low	Low
Replication	No	No	No	No
Genome integration/ Risk insert mutagenesis	Yes	Yes	No	No
Transgene expression pattern	High long-lasting	High long-lasting	Transient	Moderate long-lasting
Immune response	Low	Low	High	Very low
Clinical trials	Ex vivo transduction and Injection of transduced cells	Ex vivo transduction and Injection of transduced cells	Yes	Yes

Table 1**:** Viral vectors used for gene therapy.

5.5. MOLECULAR BEACON TECHNOLOGY

Reprogramming cell cultures contain CFs as well as transdifferentiated target cells. Direct application of these cells cultures in clinical studies could induce arrhythmias, thus sorting methods to obtain a pure population of the target cells are necessary. FACS based cell sorting or enrichment of cells relies on cell surface markers. However, the inability to target and sort MYH6/7 or cTnT specific CMs is a major drawback. Studies have shown that molecular beacons enable detection of live cells by targeting cell-type-specific mRNAs (52-54).
Thereafter, a molecular beacon-based method for the isolation of cardiomyocytes (CMs) from a differentiating culture of iPSCs by targeting highly expressed specific mRNAs was developed. MBs targeting cardiac troponin T (cTnT) and myosin heavy chain beta (MYH6/7) mRNAs, which are highly expressed in CMs were specifically designed and validated (55-58).

Molecular beacons are single-stranded oligonucleotide hybridization probes that form a stem-and-loop structure. The loop contains a probe sequence that is complementary to a target sequence and the stem is formed by complementary arm sequences located on either side of the probe sequence. A fluorophore is linked to the 5' end and a quencher is covalently linked to the 3' end. MBs do not fluoresce in the absence of targets, when the stem places the fluorophore close to the quencher, eliminating the ability to fluoresce. When the probe encounters a target, the MB undergoes a structural change forming a probe-target hybrid that is longer and more stable than the stem hybrid enabling the fluorophore to fluorescence brightly. MBs can be designed to target human genes, mouse genes, or in some cases both. The MBs targeting the MYH6/7 mRNA described in this protocol was designed for both mouse and human genes.

The assumption at the heart of this work was that the MB-based technology followed by FACS based sorting could be a highly specific and efficient method for purifying cells by directly targeting specific mRNA. The MB technology is an innovative and clinically compatible purification system and could potentially also provide pure cell populations for biomedical applications.

6. AIM

iCMs can be generated from iPSC-CMs and direct cardiac reprogramming of fibroblasts. However, there are limitations concerning the iCMs reprogramming efficiency and maturity. We hypothesized that we could improve direct cardiac reprogramming. We thus developed a protocol for the genetic reprogramming of cardiac fibroblasts into iCM precursor cells (iCMPs) with CM lineage commitment. We believe these cells may bypass the problems related to mature iCMs and may represent as a better candidate for cardiac regenerative therapies. Therefore, the following aims were pursued in my project:

Part 1: To achieve baseline cardiac reprogramming – To obtain iCMs from CFs using transcription factor combinations that have already been successful in generating iCMs such as Gata4, Mef2c, Tbx5 (GMT) and Mef2c, Myocd, Tbx5 (MMT).

Part 2: Genetic manipulation of neonatal cardiac fibroblasts that are considered epigenetically more plastic into induced cardiomyocyte precursor cells (iCMPs) via lentiviral transduction with a cocktail of cardiomyogenesis-related transcription factors Gata4, Mef2c, Tbx5, and Myocd.

Part 3: Enrichment, characterization and global transcriptome analysis of iCMPs.

Part 4: In vivo translation: Evaluation of the regenerative and therapeutic potential of iCMPs in a mice model of myocardial infarction.

7. MATERIALS

7.1. Lentivirus

Gene/ Inserts		**Source**
eGFP	IRES-eGFP, VSV-G pseudotyped	Plasmids from Dr. Stephanie Portze
Gata4	IRES-GFP, VSV-G pseudotyped, NEO antibiotic resistance	
Mef2c	IRES-GFP, VSV-G pseudotyped, NEO antibiotic resistance	
Tbx5	IRES-GFP, VSV-G pseudotyped, ZEO antibiotic resistance	
Myocd	IRES-GFP, VSV-G pseudotyped, ZEO antibiotic resistance	

7.2. Bacteria

Bacterial strain	**Source**
Escherichia coli K12 derivatives	Gift from Dr. Manfred Gossen's lab

7.3. Cells

Product	**Source**	**Identifier**
Mouse neonatal cardiac fibroblasts, C57BL/6	PeloBiotech	PB-C57-6049
HT1080	Gift from Dr. Manfred Gossen's lab	
Hek293	Gift from Dr. Manfred Gossen's lab	
αMHC-mCherry CMs	Derived from transgenic αy-mCherry mice	
iPSC-CMs	Gift from Dr. Andreja Brodarac	

7.4. Molecular beacons

Product	Sequence 5'-3'	Fluorophore	Source
DELC (Delivery control)	ACG ACG CGA CAA GCG CAC CGA TAC GTC GT	Cy5	Sequence from Ban K et al. Synthesized by Seqlab/ Microsynth
NEGC (Negative control)	ACG ACG CGA CAA GCG CAC CGA TAC GTC GT		
MYH6/7 (alpha/beta Myosin heavy chain)	CCT CCA TCT TCT TCT TCA CGG AGG		

7.5. Laboratory equipment's

Product	Source
Centrifuge	Eppendorf
CO2 incubator	Binder
Clean bench / Flow hood	Ulf Lippmann Labortechnik
Research Plus Pipettes	Eppendorf/ VWR
Water bath	Thermo Scientific
Ultracentrifuge	Beckman Coulter

7.6. Animal cell and bacterial culture reagents, chemicals and enzymes

Product	**Source**	**Identifier**
DMEM high glucose: 4.5 g/l	Life Technologies	31966
DMEM low glucose: 1 g/l	Life Technologies	21885
FBS (pre-tested lots)	Life Technologies	10270106
Packaging plasmid	Gift from Dr. Manfred Gossen's lab	
Envelope plasmid		
LB-Agar for molecular biology	Roth	X965.1
LB-Medium for molecular biology	Roth	X964.1
Ampicillin	Roth	K029.1
Gelatin	Pan	P06-25200
Matrigel	Corning	354230
Medium 199	Life Technologies	41150-020
PBS	Life Technologies	14040166
Trypan blue dye	Sigma-Aldrich Chemie GmbH	T8154-20
TrypLE Express	Life Technologies	12605010
Penicillin/Streptomycin	Lonza, Basel	DE17-602E
G418 Sulfate	Fisher Scientific	BP673-5
Hexadimethrine bromide (Polybrene)	Sigma-Aldrich Chemie Gmbh	107689
FGF-basic	PeproTech GmbH	100-18B-10
FGF-10	PeproTech GmbH	100-26-25
L-Ascorbic acid	Sigma-Aldrich Chemie GmbH	A8960-5G

BMP-4	R&D Systems	314-BP-010
VEGF	PeproTech GmbH	100-20-10
RPMI 1640	Life Technologies	61870010
IMDM	Gibco	12440053
F12 medium	Gibco	
N2 supplement	Thermo Fisher	17502048
B27 supplement	Thermo Fisher	17504044
B27 supplement without Vitamin A	Thermo Fisher	12587010
GlutaMAX 100X supplement	Gibco	35050061
Bovine serum albumin (BSA)	Roth	CP77.1
β-mercaptoethanol	Carl Roth	4227.3
1-thioglycerol (MTG)	Sigma-Aldrich Chemie GmbH	M6145
4% Formaldehyde	Thermo Scientific Pierce	28908
TritonX-100	Roth	3051.3
Goat serum	Life Technologies GmbH	16210064
IWR-1	Selleckchem	SEL-S7086
IWP2	STEMCELL Technologies	72124
5-Azacytidine	Abcam	AB120842
X-treme GENE HP DNA Transfection Reagent	Sigma-Aldrich Chemie GmbH (previously Roche Diagnostics)	06365752001
PEI (Polyethylenimine)	Polysciences	24765-2
OCT Compound tissue tek	Hartenstein	TTEK

DAPI (4',6-Diamidino-2-Phenylindole, dihydrochloride)	Invitrogen	D1306
Hoechst 33342, trihydrochlorid	Invitrogen	H3570
2,3-Butanedione monoxime (BDM)	Sigma-Aldrich Chemie GmbH	B0753-25
Leibovitz's L-15 Medium	Life Technologies	11415064
Collagenase B	Roche	11088815001

7.7. Antibodies

7.7.1. Primary Antibodies

Target	**Species**	**Source**	**Identifier**
Alpha-actinin (sarcomeric)	Mouse monoclonal	Sigma	A7811
Cardiac troponin T (1C11)	Mouse monoclonal	Abcam	ab8295
Troponin T, Cardiac Isoform Ab-1	Mouse monoclonal	Thermo Fisher Scientific	MS-295-P0
Myosin Heavy Chain, sarcomeric	Mouse monoclonal	DSHB	MF20-supernatant
GFP	Chicken polyclonal	Abcam	ab13970
Smooth muscle actin, alpha	Rabbit polyclonal	Abcam	ab5694
CD31	Mouse monoclonal	Abcam	ab24590

CXCR4	Mouse monoclonal	Santa Cruz Biotechnology, Inc.	sc-53534
Nkx2.5	Mouse monoclonal	Santa Cruz Biotechnology, Inc.	sc-376565
Flk-1	Mouse monoclonal	Santa Cruz Biotechnology, Inc.	sc-6251
PDGFR-a Antibody (C-9)	Mouse monoclonal	Santa Cruz Biotechnology, Inc.	sc-398206
Gata4 (C-20)	Goat polyclonal	Abcam	AB134057
Mef2c (D80C1) XP	Rabbit monoclonal	NEBiolabs	5030 S
Myocardin	Goat polyclonal	Santa Cruz Biotechnology, Inc.	sc-21561
TBX5 (C-20)	Goat polyclonal	Santa Cruz Biotechnology, Inc.	sc-17866

7.7.2. Secondary Antibodies

Product	**Source**	**Identifier**
Donkey Anti-Chicken, FITC	Invitrogen	SA1-72000
Alexa Fluor 647 Goat Anti-Mouse	NEBiolabs	4410S
Alexa Fluor 488 Goat Anti-Mouse	Invitrogen	A10684
Alexa Fluor 647 Goat Anti-Rabbit	Invitrogen	A21245

7.8. Consumables

Product	**Source**
T25, T75 and T175 cell culture flasks	Greiner Bio-One GmbH/ VWR
6, 12, 24 and 48 well cell culture dishes	CELLSTAR
15 and 50ml Falcon tubes	Greiner Bio-One GmbH/ VWR
Hemocytometer	Roth
MicroAmp Optical 96-Well Reaction Plate	Life Technologies
MicroAmp Optical 384-Well Reaction Plate with Barcode	Life Technologies
Stericup-HV, 0,45 µm, PVDF, gamma-sterilisiert	EMD Millipore/ Merck Chemicals GmbH
Cell strainer	VWR
Tube, OptiSeal™, Polypropylene, 32.4 mL, 26 x 77 mm ROTORS: Beckman Coulter SW32 Ti	Beckman Coulter
Spacer, Ultem, Tube, 25 mm ROTORS: Beckman Coulter SW32 Ti	Beckman Coulter
FACS tube with filter cap	Corning/ Falcon
5, 10, 25 and 50ml Serological pipets	Roth
Super frost glass slides	VWR International GmbH

7.9. Instruments

Product	**Source**
MACSQuant Erato analyzer	BCRT, Flow Cytometry Lab
Ariall Calliope Cell Sorter	Miltenyi Biotech GmbH
Operetta high content screener	PerkinElmer, Rodgau, Germany
Zeiss Axio Observer fluorescence microscope	Carl Zeiss Microscopy GmbH, Jena, Germany
Odyssey Infrared Imaging System	LI-COR Biosciences
NanoPhotometer	Implen
2100 Bioanalyzer system	Agilent
Illumina HiSeq 1500 system	Illumina
Eppendorf Mastercycler ep gradient S realplex2	Eppendorf AG
Quant Studio 6 Flex TaqMan	Life Technologies

7.10. Kits

Product	**Source**	**Identifier**
Nucleobond Xtra Midi EF (Plasmid amplification)	Macherey-Nagel GmbH & Co. K	740420.50
BCA Protein Assay Kit	Pierce/Thermo Scientific	23227
RNeasy mini kit	Qiagen	74106
SuperScript III First-Strand Synthesis System	Life Technologies, Carlsbad, California, USA	18080-051
Power SYBR Green PCR Master Mix	Life Technologies, Carlsbad, California, USA	4368706
RNA 6000 Nano Kit	Agilent	M.Sc. Ulrike Krüger BIH core facility Genomics at Charité – Universitätsmedizin Berlin
NEBNext Poly(A)mRNA Magnetic Isolation Module	NEB	
DNA 1000 Kit	Agilent	
NEBNext Ultra RNA Library Prep Kit for Illumina	NEB	
Qubit dsDNA BR Assay Kit and Qubit 3.0	ThermoFisher	
PKH26 Red Fluorescent Cell Linker Mini Kit for General Cell Membrane Labeling	Phanos Technologies/ Sigma-Aldrich Chemie GmbH	MIDI26-1KT

7.11. Software for data analysis

Product	**Source**
FlowJo	BD
AxioVision	Carl Zeiss Microscopy GmbH, Germany
Operetta Harmony (operetta) Columbus (server)	PerkinElmer, Rodgau, Germany
Vevo LAB, ECG-triggered analysis, EKV, M-Mode, B-Mode	Viualsonics Fujifilm

7.12. Animal experiment

Product	**Source**
C57BL/6 mice	Charles River Laboratories
Glucose G-5%	B Braun Melsungen
Isoflurane	AbbVie Inc.
Ventilator System Connecting kit for anesthesia system to Minivent	Hugo Sachs Elektronik-Harvard Apparatus GmbH
Abbocath-T, 20G x 30mm intubation Catheter	Intermed Service GmbH
Prolene blau 7-0 75cm 2XBV175-8 EH7405H (suture thread 9.3mm 3/8c 75cm)	Ethicon Sutures
Ethicon Vicryl 4-0 Plus Viol GEFL (suture thread 19mm 3/8c 70cm)	Ethicon Sutures
Syringe Omnifix-F Solo without cannula, 1 ml (cell injection syringe)	Intermed Service GmbH
BD Micro-fine syringe 0.3ml	BD Medicals
Vevo 2100 Echocardiography	Visualsonics Fujifilm

7.13. Primers for real-time PCR

Oligo Name	**Sequence 5' – 3'**
mGata4_Fw	GCCTGTATGTAATGCCTGCG
mGata4_Rv	CATTGCTGGAGTTACCGCTG
mHand2_Fw	TCATGGATCTGCTGGCCAAG
mHand2_Rv	TCTTGTCGTTGCTGCTCACT
mMef2a_Fw	CTAGGACAAGCAGCCCTCAG
mMef2a_Rv	GGAGGTGAAATTGGCTCTGACT
mMef2c_Fw	ACGAGGATAATGGATGAGCGT
mMef2c_Rv	TGCAATCTCACAGTCGCACA
mMyocd_Fw	AGAATGATGCAGCCTCCCAG
mMyocd_Rv	CGGTTCTTACTGTCACCCAAAG
mTbx5_Fw	ATGAACGTGAACTGTGGCTGA
mTbx5_Rv	GGCCAGTCACCTTCACTTTGT
mNkx2.5_Fw	CCCAAGTGCTCTCCTGCTTT
mNkx2.5_Rv	CCATCCGTCTCGGCTTTGT
mPdgfra_Fw	ACGTTCAAGACCAGCGAGTTT
mPdgfra_Rv	GACCTCGTTGTTAAAGACGGC
mKcnh2_Fw	TCAAGACCACACATGCACCA
mKcnh2_Rv	CCAGGACGGGCATATAGGTTC
mActn2_Fw	TCTACCATGCTTTCGCGGG
mActn2_Rv	CATGGTCTTCTCAGGCGTCC
mMyh6_Fw	GAAGGCCTACAAGCGCCA
mMyh6_Rv	GGTTATTCCTCGTCGTGCATCT
mMyl2_Fw	CCAGGTCCAATTAACTTCACCG

mMyl2_Rv	TCAGCCTTCAGTGACCCTTTG
mMyom1_Fw	GGGCGACACTTACGTTCTCTC
mMyom1_Rv	CACCACATCCAAGGGTGCA
mMki67_Fw	ACCTGGTCTTAGTTCCGTTGAT
mMki67_Rv	CTTGGTTGGCGTTTCTCCTC
mVim_Fw	GATCAGCTCACCAACGACAAG
mVim_Rv	GTTCAAGGTCAAGACGTGCC
mMyl1_Fw	ACCAATCCCACCAATGCAGA
mMyl1_Rv	ACGCAGACCCTCAACGAAAT
mB2m_Fw	TTCTGGTGCTTGTCTCACTGA
mB2m_Rv	CAGTATGTTCGGCTTCCCATTC
mRpl13a_Fw	TGAAGCCTACCAGAAAGTTTGC
mRpl13a_Rv	TCCGATAGTGCATCTTGGCC

8. METHODS

8.1. Cell culture

Cardiac fibroblasts (CFs): Cryopreserved neonatal CFs were purchased from PELOBiotech GmbH. The cells were plated at density of 5,000 cells/cm2. The cells were maintained in basic culture medium, DMEM supplemented with 10% heat-inactivated fetal bovine serum (HI-FBS) and 100U/ml penicillin, 100μg/ml streptomycin (Pen/Strep) in T75 cell culture flasks coated with 0.2% gelatin and incubated at 37°C and 5% CO2 in a humified incubator. All experiments were performed with CFs between passages 2-5.

HT1080 and Hek293 cells were maintained in basic culture medium, DMEM supplemented with 10% fetal bovine serum (FBS) and Pen/Strep in T75 cell culture flasks and incubated at 37°C and 5% CO2 in a humified incubator.

Neonatal α-MHC-mCherry cardiomyocytes were isolated from day 2-5 old mice following a 2 day Jove protocol (59). The hearts were carefully extracted, washed in PBS (- -) supplemented with 20mM 2,3-Butanedione monoxime (BDM). The hearts were then minced thoroughly using a curved scissors and incubated overnight in isolation medium (20mM BDM in L-15 medium) with gentle agitation. The following day tissue digestion was done using a digestion mix (20mM BDM, 1.5 mg/ml collagenase B, 0.125% trypsin in L-15 medium) and the supernatant was filtered through a cell strainer. Red blood cells were removed using the red blood cell lysis solution and the Percoll gradient method was used for CMs purification. The cells were then count and plated at a density of 100,000 cells/cm2.

8.2. Plasmid DNA

p6NST50 lentiviral (LeV) vectors containing the coding regions of Gata4, Mef2c, Tbx5, MyocD and eGFP were a gift from Stephanie Protze. The transcription factors were cloned into the multiple cloning site of the p6NST50-Zeo (Tbx5, MyocD), p6NST-52-Neo (Gata4, Mef2c) lentiviral vectors, containing a spleen focus forming virus (SFFV) U3 promoter and an internal ribosome entry site, driving an enhanced green fluorescent protein (EGFP) fused to a zeomycin,

neomycin or hygromycin resistance protein to facilitate selection of infected cells. As control the p6NST50-Zeo lentiviral vector only expressing EGFP-Zeo was used (30). Stephanie Protze did the cloning.

Lentiviral vectors were eluted from filter paper with double distilled water (ddH2o). LB agar (15g LB agar in 1-liter water) plates were prepared. LB agar plates were streaked with LeV vectors and were used to isolate individual colonies. The bacteria were then cultured in LB medium (20g LB broth powder in 1liter water) containing ampicillin at 37°C as overnight cultures to grow up sufficient numbers of bacteria necessary to isolate enough plasmid DNA. Plasmid DNA was isolated using Machery Nagel Plasmid amplication kits following the manufacturer's recommendations. The plasmids were then sent to SEQlab for verification.
For functional verification, the plasmids were transfected onto Hek293 cells. Two days after transfection, the cells were stained for Gata4, Mef2c, Tbx5 and Myocd respectively to look for the transgene expression in cells.

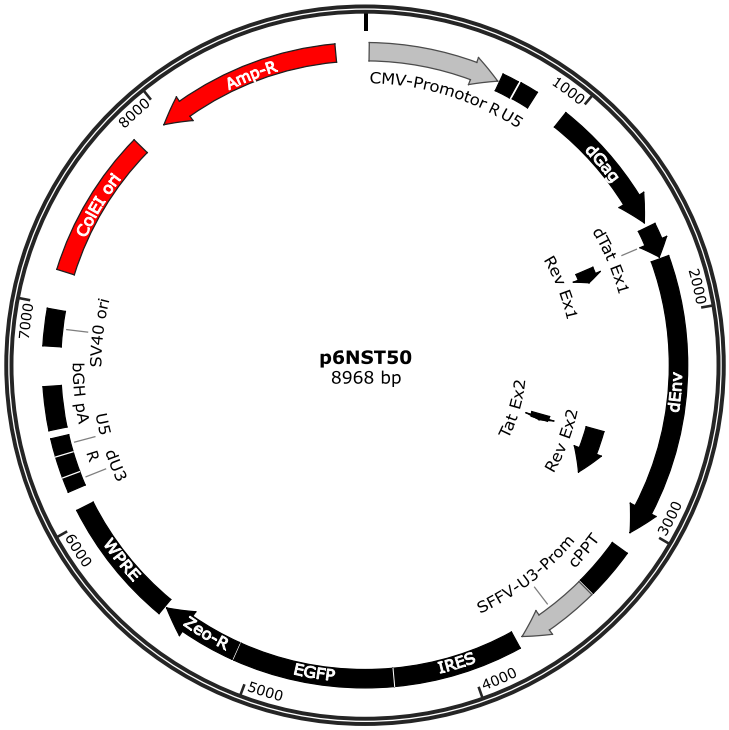

Figure 3**:** Plasmid map of lentiviral vector p6NST50-Zeo (empty IRES-eGFP construct)

8.3. Lentivirus Work

8.3.1. Lentivirus Production

The virus production protocol used was based on the second-generation lentiviral vector system. 2nd generation packaging systems: express the HIV gag, pol, rev, and tat genes all from a single packaging plasmid such as psPAX2, whereas a 3rd generation packaging systems do not express tat, it does not express any viral genes. They are considered safer than 2nd generation systems but maybe more difficult to use because they require transfection with four separate plasmids to create functional lentiviral particles. However, they can be considered for future clinical translation.
Once the plasmid sequence was verified and plasmid function was validated, Hek293 cells were plated at density of 83,333 cells/cm2. The following day the cells were transfected using the PEI transfection method with one of the transgene-containing plasmid, the packaging plasmid psPAX2 and the VSV-G envelope expressing plasmid pMD2.G. Medium (DMEM supplemented with 10% HI-FBS and Pen/Strep) was replaced with fresh media 5-6 hours after transfection.
Virus-containing supernatant was harvested 24 hours after transfection replaced with fresh medium and harvested again 12 hours after medium change. The harvests were filtered with 0.45µm PVDF stericups to remove any cell debris and concentrated up to 100-fold by ultracentrifugation for 2 hours at 22,000 RCF. The viral pellets were resuspended overnight at 4°C in PBS under shaking. Aliquots were prepared and stored at -80°C.

8.3.2. Lentiviral titration

The titers of the produced LeV were determined by infecting HT1080s and CFs. The cells were plated at a density of 5,000 cells/cm2. After 24 hours, the cells were transduced with dilutions of the concentrated virus (0.5, 1, 2.5, 5 and 10µl/well). Medium was replaced after 18-20 hours and cells were incubated for 2-3 days. The percentage of infected cells (GFP+ cells) was determined by flow cytometry. Cells were thoroughly trypsinized to obtain single cell suspensions and centrifuged at 300 RCF for 5 minutes. The pellets were resuspended in FACS buffer (2% BSA and 2 mM in PBS - -) and filtered through a 35µm mesh to remove cell aggregates. Cells were analyzed using the MACSQuant Erato analyzer. Only samples with a concentration between 2 and 20% GFP were included in titer calculation.

The titers were calculated using the following equation:

$$-Transduction\ Units\ per\ ml\ \left(\frac{TU}{ml}\right) = \frac{cell\ number\ on\ transduction\ day * \left(\frac{\%\ of\ GFP + cells}{100}\right)}{volume\ of\ viral\ supernatant\ in\ ml}$$

8.3.3. Lentivirus validation

The competency of each of these transcription factors - Gata4, Mef2c, Tbx5 or Myocd was confirmed by correct transgene expression upon lentiviral infection. Hek293 and HT1080 cells were plated at a density of 5,000 cells/cm2. The following day the cells were infected with the LeVs and the medium was replaced after 12 hours. Three days after infection, the cells were checked by Western blot and immunofluorescence staining for protein size and the nuclear expression.

8.4. Cardiac Reprogramming

CFs were seeded onto gelatin-precoated T75 cell culture flasks at a density of 5,000 cells/cm2. Twenty-four hours later cells were infected with the lentiviral GMTMy cocktail at a multiplicity of infection (MOI) of 10. Basic culture medium, DMEM supplemented with 10% fetal bovine serum (FBS) and Pen/Strep was replaced with cardiac reprogramming medium (CRM) composed of DMEM-LG and M199 (3:1) and supplemented with 10% FBS and Pen/Strep. To enhance lentiviral transduction CRM was supplemented with 8µg/ml Polybrene during LeV addition. As control, CFs were infected with LeV eGFP at a MOI of 10 and treated similarly.

Three days after lentiviral infection the cells were trypsinized, counted and re-plated at a density of 5,000 cells/cm2 onto gelatin-precoated dishes. G418 was added for antibiotic selection at a concentration of 0.5mg/ml as determined by pretests on CFs. CRM was changed every 2 days and cells were monitored regularly.

8.5. Immunofluorescence

8.5.1. Immunofluorescence staining of adherent cells

At indicated time points, cells were washed with PBS and fixed with 4% paraformaldehyde (PFA) for 20 minutes, permeabilized using 0.25% TritonX-100 in PBS (PBST) for 15 minutes and incubated in blocking buffer (PBST + 10% serum) for 30 minutes at room temperature (RT). Thereafter, primary antibodies (Antibody Table 8.5.1) were diluted in blocking buffer and added to the cells for overnight incubation at 4ºC. The following day, secondary antibodies (Secondary Antibody Table 8.5.2) were also diluted in blocking buffer and added to the cells after three PBS washes for, a 2 hour incubation in the dark at RT. Nuclei were counterstained with DAPI for 5 minutes at RT and the cells were finally washed again three times with PBS. Images were acquired using the Operetta high content screener system and the Zeiss Axio Observer fluorescence microscope. The high content screener was used for quantification of the stained cells, while the Axio Observer was used for high-resolution images of protein expression patterns.

8.5.2. Immunofluorescence staining of harvested cells/ FACS

At indicated time points, cells were thoroughly trypsinized to obtain single cell suspensions and centrifuged at 500g for 5 minutes. Cells were washed with PBS, incubated in 4%PFA fixation buffer for 20min. Primary antibody solutions were added to the cells and incubated for 20 minutes at RT. The cells were then washed with PBS and incubated in the secondary antibody solution for 30 minutes at RT. Both primary and secondary antibody solutions were prepared in staining buffer PBST-S (PBS and 0.25% TritonX-100 and 10% BSA). The pellets were then washed 3 times with PBS, centrifuged and resuspended in FACS buffer (2% BSA, 2mM EDTA in PBS--) and filtered through a 35µm mesh to remove cell aggregates. During analysis, cells were counterstained with DAPI to label dead cells. The cells were measured using the MACSQuant Erato analyzer and data were analyzed with FlowJo10 software.

Gating strategy: Forward and side scatter gating was done to obtain the population of interest. A pulse geometry gating was done to get rid of cell clumps if any. Following a subgating using a viability dye (DAPI) to eliminate dead cells, the expression levels of the relevant markers were measured.

8.6. Molecular beacon work

8.6.1. Molecular beacon transfection

MBs that target unique sites in MYH6/7 mRNA in both mouse and human (55) were used. MicroSynth synthesized these MBs, with a Cy5 fluorophore at the 5′ end and a Black Hole Quencher 2 at the 3′ end (Materials table 8.3.)**.** The cells were transfected with Cy5-conjugated DELC (delivery control), NEGC (negative control) and MYH6/7 (myosin heavy chain 6/7) MBs using the XtremeGENE™ HP DNA Transfection Reagent. The DELC MB is modified to have two identical fluorophores instead of a dye-quencher pair and is used as a delivery control probe for delivery studies and the NEGC does not match with any mRNA sequence in the genome of interest, thus any signal from this would be non-specific background signal (57).
For initial concentration tests, the cells were transfected with either - 0.5μM MB or 1μM MB to determine the optimal MB concentration needed for efficient transfection. Additionally, the cells were transfected with a reaction mix of MB and transfection reagent at a ratio of 1:1, 1:2, 1:3 and 1:4 to determine the optimal ratio for our target cell type CFs. The cells were incubated in a humidified, 5% CO2 atmosphere at 37°C for 2-24 hours. The cells were then rinsed thoroughly with PBS and stained with Hoechst 33342 a nuclear dye for 15 minutes. These cells were washed thoroughly again with PBS. Operetta high content screener was used to capture 20X-images that covered the center of the culture surface. Harmony® software was used for quantitative image analysis to determine the Hoechst+ cells for the total cell number and the Cy5+ cells to determine the percentage of MB+ cells.

8.6.2. Molecular beacon-based sorting

Two weeks after LeV infection, target cells were transfected with Cy5-conjugated molecular beacons MYH6/7 using the XtremeGENE™ HP DNA Transfection Reagent. The cells were transfected with a reaction mix containing- 1μM MB and Transfection Reagent at a ratio of 1:4, which was the optimal ratio for our target cell type, determined by initially, conducted protocol establishment experiments. The cells were incubated in a humidified, 5% CO2 atmosphere at 37°C for 4 hours. Thereafter, the cells were washed thoroughly with PBS, harvested by trypsinization and resuspended in sorting buffer (2% BSA and 2mM EDTA in PBS --). iCMPs were sorted using the Ariall Calliope Cell Sorter by, Desiree Kunkel, BCRT FACS core facility.

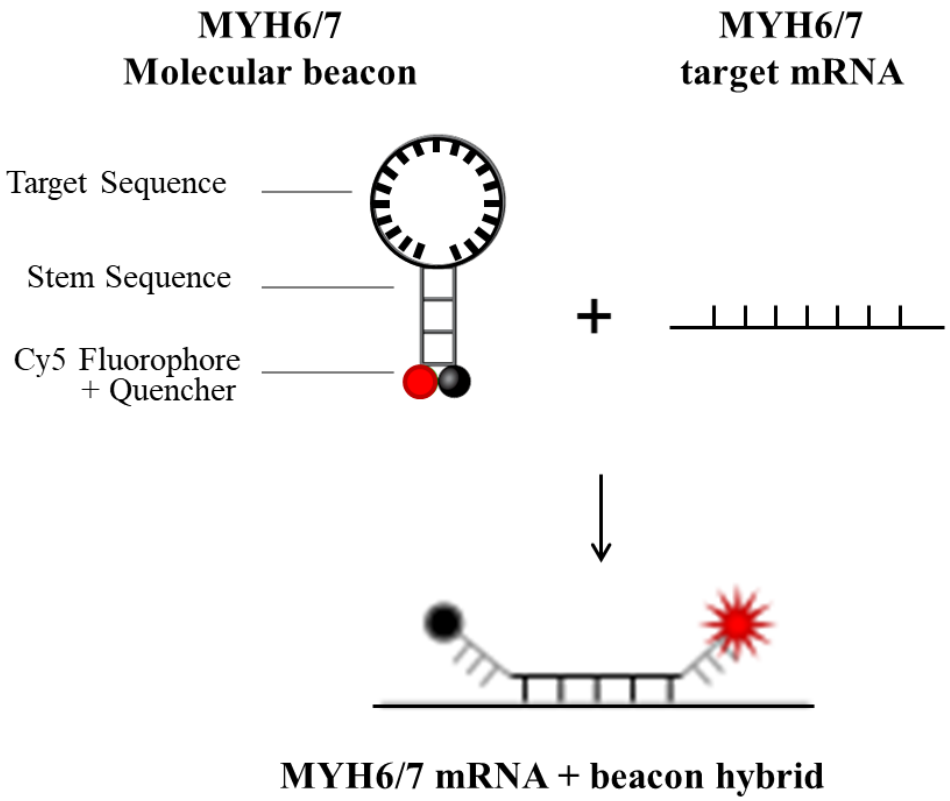

Figure 4**:** Molecular beacon technology

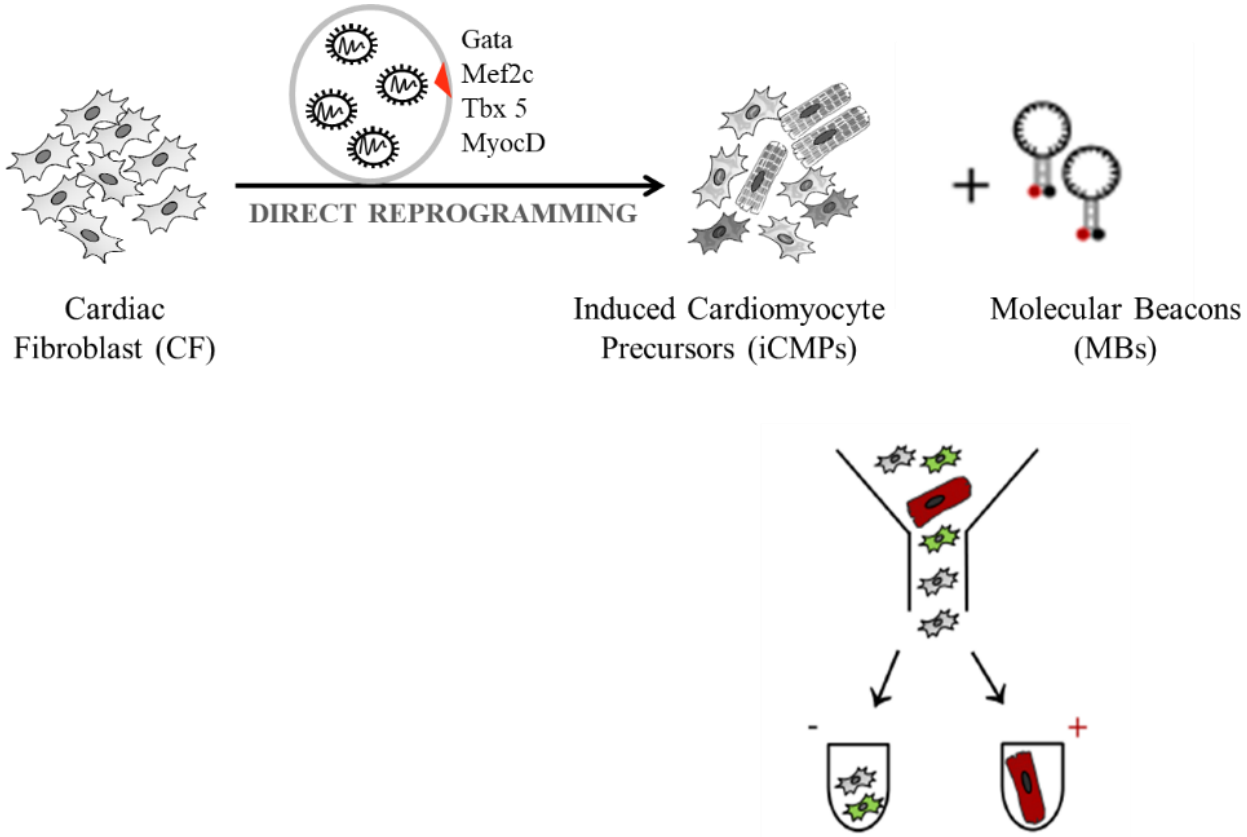

Figure 5**:** Schematic of molecular beacon-based sorting

8.7. RNA Sequencing

RNA sequencing was performed by, M.Sc. Ulrike Krüger of the BIH core facility Genomics at Charité – Universitätsmedizin Berlin.
RNA samples were quantified with a NanoPhotometer and the quality of totalRNA isolates was accessed by the RNA 6000 Nano Kit on 2100 Bioanalyzer system. Poly-(A)-selection was performed from 500ng total RNA utilizing the NEBNext Poly(A)mRNA Magnetic Isolation Module according to the manufacturer's instructions with subsequent library preparation using the NEBNext Ultra RNA Library Prep Kit for the Illumina system. Success of library preparations was confirmed by analyzing the fragment size distribution utilizing the DNA 1000 Kit on a 2100 Bioanalyzer and library concentration was quantified by Qubit® dsDNA BR Assay Kit and Qubit 3.0. After equimolar pooling all samples were sequenced on an Illumina HiSeq 1500 system with Rapid Mode chemistry v2 (50 cycles, single-read).

8.8. Quantitative real-time PCR

Total RNA was isolated from enriched iCMPs 2 weeks after LeV infection and after MB-based sorting, CFs and adult heart tissue, using the Qiagen RNeasy mini kit. Subsequently, 100ng of each RNA sample were random hexamer primed and reverse transcribed into cDNA using the Invitrogen SuperScript III First-Strand Synthesis System. Quantitative real-Time PCR was performed using the Applied Biosystems Power SYBR Green PCR Master Mix and an Applied Biosystems MicroAmp Optical 384 Well Reaction Plate. Each PCR reaction was performed in triplicates. The following PCR program applied in Quant Studio: initial denaturation: 95°C 10 minutes; 50 cycles: 95°C 15 seconds, 60°C 30 seconds, 72°C 30 seconds; final step: melting curve program. PCR primers were purchased from Eurofins Genomics. The following algorithm quantified relative gene expression levels of the markers in iCMPs, parental CFs and heart tissue (embryonic, neonatal and adult): E-Δct.

8.9. iCMPs proliferation

Enriched iCMPs were seeded onto gelatin-precoated culture dishes at a density of 5,000 cells/cm2 and maintained in CRM. The cells were regularly passaged every 3 days and cell counts were performed using a hemocytometer, viability was determined by staining with Trypan blue dye. The total cell numbers per split determined the cell fold increase.

8.10. iCMPs maintenance

Various cardiomyocyte specification factors were screened for maintenance of iCMP phenotype. Considering the sequencing results and heart development knowledge, iCMPs were, maintained in culture medium supplemented with factors/factor cocktails - Ascorbic acid, BMP4, FGF2, FGF10 and VEGF. The cells were then monitored regularly for morphological changes and MYH6/7 expression.

8.11. iCMPs differentiation

For the generation of mature CMs from iCMPs, the effectiveness of previously established differentiation conditions were tested (60-62)
(1) In the first condition, the iCMPs were seeded onto Matrigel coated dishes and cultured in SFDM (IMDM:F12) (3:1) supplemented with 0.5x N2, 0.5x B27 without Vitamin A, 1x GlutaMAX, 0.05% BSA, 450µM 1-thioglycerol (MTG), and 250µM ascorbic acid), and supplemented additionally with 5µM IWP2.

(2) In the second condition, iCMPs were seeded onto 0.2% gelatin coated dishes and cultured in cardiac differentiation medium (CDM) composed of RMPI 1640 supplemented with 0.5x N2, 1x B27, 0.5% GlutaMAX, 0.05% BSA, and 0.1mM β-mercaptoethanol. For the first six days of culture in CDM, the medium was supplemented with 5µM IWR-1.

(3) In the third condition, these cells were cultured on cardiac extra cellular matrix (cECM) to determine, if the exposure to a more cardiac-specific environment in combination with maturation

media and supplement will aid the maturation process. The cells were monitored regularly for morphological changes, spontaneous contractions, and cardiac marker expression.
(4) Additionally, iCMPs were cultured on 0.2% gelatin coated dishes and maintained in differentiation medium (DM) containing ascorbic acid and TGFß with the initially supplement of 5-Azacytidine.

8.11.1. Co culture

Additional mechanical, electrical and paracrine stimulation was provided to proliferative iCMPs by culturing them with either iPSC-derived CMs or mouse neonatal α-MHC-mCherry CMs on 1% gelatin coated dishes. The iPSC-CMs were labeled with the cell labeling dye red in order to distinguish them from the iCMPs. The cells were plated at a ratio of 1:4 and 1:10 iCMPs to CMs and maintained in differentiation medium mentioned above. The co culture was monitored regularly for 10days, for morphological changes, differentiation and spontaneous contraction of the iCMPs stimulated by the CMs.

8.12. Animal experiments

8.12.1. Cell preparations for in vivo experiments

To obtain sufficient number of iCMPs, CFs were plated onto T175 dishes for large-scale cultures. They were reprogrammed with LeV cocktail GMTMy as mentioned in Cardiac Reprogramming. Two weeks after LeV infection the cells were sorted based on MB selection for MYH6/7 as previously mentioned in Molecular beacon work.
The sorted cells were cultured and expanded in CRM to produce cell doses of 500,000 cells/mouse. To obtain control eGFP-CFs, CFs were plated onto T175 dishes and infected with LeV eGFP, and cultured similarly to the iCMPs in CRM but without antibiotic selection. The CFs were sorted based on their eGFP signal. The sorted cells were cultured and expanded to produce cells doses of 500,000 cells/mouse. All cells of passage 3 and 4 were used for cell injections, with cells after sort being passage 1.

8.12.2. Animal care

In this experiment, C57BL/6 male mice of age 8-9 weeks were purchased. The mice were housed in the Forschungeinrichtung für Experimentelle Medizin (FEM) of Charité – Universitätsmedizin Berlin. Two days before the start of experiments the mice were shifted into a new cage with nesting material and drinking water was replaced with 5% glucose. After surgery the mice cages were kept on a heating pad for warmth and recovery. The mice were monitored daily and weighed weekly.

8.12.3. Induction of myocardial infarction in mice and treatment

The project protocol including surgery and all examinations G0288/16 (Table 2) was approved by the Landesamt für Gesundheit und Soziales Berlin (LaGeSo) (State Office of Health and Social Affairs Berlin). Ten to twelve-week-old wild type male C57BL/6J mice were used.

For induction of myocardial infarction (MI), mice were anesthetized 30 minutes before surgery. Sedation depth was considered adequate when there was no response to tactile stimuli and hind limb pedal withdrawal reflex provoked with pinching. The mice were fixed in a supine position, given glucose injection and intubated with an Abbocath-T, 20G x 30mm intubation catheter. The general ventilator settings were 180 strokes/minute, volume 250µl/stroke and Oxygen 2%. Following a left anterolateral thoracotomy and removal of the pericardium, the left anterior descending artery was ligated using a suture thread 7-0 prolene BV175-8 9.3mm. Myocardial ischemia distal to the ligation was evident by the discoloration of the myocardium. Half million iCMPs, eGFP-CFs or PBS only (w/o Ca2+ and Mg2+) was injected at 2 points in the peri-infarct area (5µl each). The chest was closed and mice were given Carprofen subcutaneously after the operation for pain and the animals were allowed to recover. Sham operations with thoracotomy but no manipulation of the heart was performed. The mice were monitored over a period of 6 weeks.

Animal species: C57BL/6J Mouse				
Group Number	**Group Name**	**Group Description**	**Measurement**	**Number of animal's incl. 30% mortality**
1	Sham-Control	Thoracotomy Pericard opening No myocardial infarction No therapy	<u>Histology:</u> After 2 and 6 weeks <u>Heart function measurement</u> (Serial echocardiography: after 2, 4, and 6 weeks; Sacrifice and heart explanation after 6 weeks)	N=16
2	MI-Control	Thoracotomy Pericard opening Myocardial infarction No therapy - PBS injection		N=8 N=16
3	MI-CF intra	Thoracotomy Pericard opening Myocardial infarction Cell therapy		N=8 N=16
4	MI-iCMP intra			N=8 N=16
TOTAL				**88**

Table 2**:** Animal experiment plan

8.12.4. Echocardiography

Echocardiography was performed in mice 2, 4 and 6 weeks after MI and treatment, under light anesthesia with 2-3% isoflurane using the Vevo2100 echocardiography system equipped with a MS550D 22-55 hertz probe. EKV, B-Mode and M-Mode clips were acquired in the parasternal long axis and short axis view of the murine heart. Using the Vevo LAB analysis software left ventricular ejection fraction (LVEF), cardiac output (CO), stroke volume (SV) and volume diastole and volume systole were calculated from EKV based LV tracing. The left ventricular end-diastolic wall thickness and left ventricular fractional shortening (LVFS) were measured from the M-mode tracings of the long and short axis of the heart respectively.

8.12.5. Histology and immunohistochemistry

Six weeks after MI and treatment, experiments were terminated and mice were sacrificed by cardiac puncture, hearts were excised, dehydrated overnight in 15% sucrose solution and frozen in OCT embedding medium the following day. Cryo sections of 7µm were cut from apex to base and mounted onto super frost glass slides for histological analysis. Cryopreserved sections were fixed with 4% PFA and stained with Masson's trichrome and H&E stain according to the manufacturer's instructions. The sections were imaged at 20X magnification using the slide scanner.

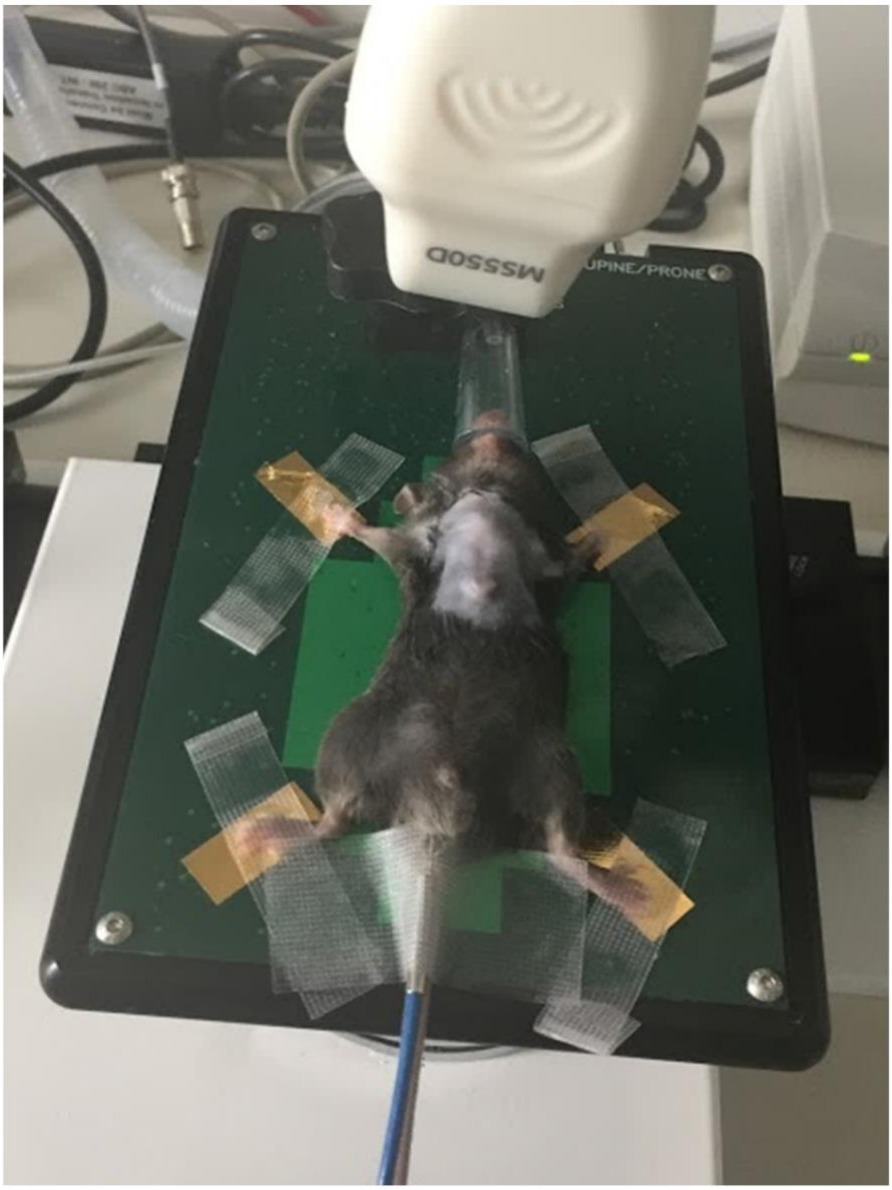

Figure 6**:** Echocardiography analysis of mice heart. Mice placed in supine position on the table for measurements.

A

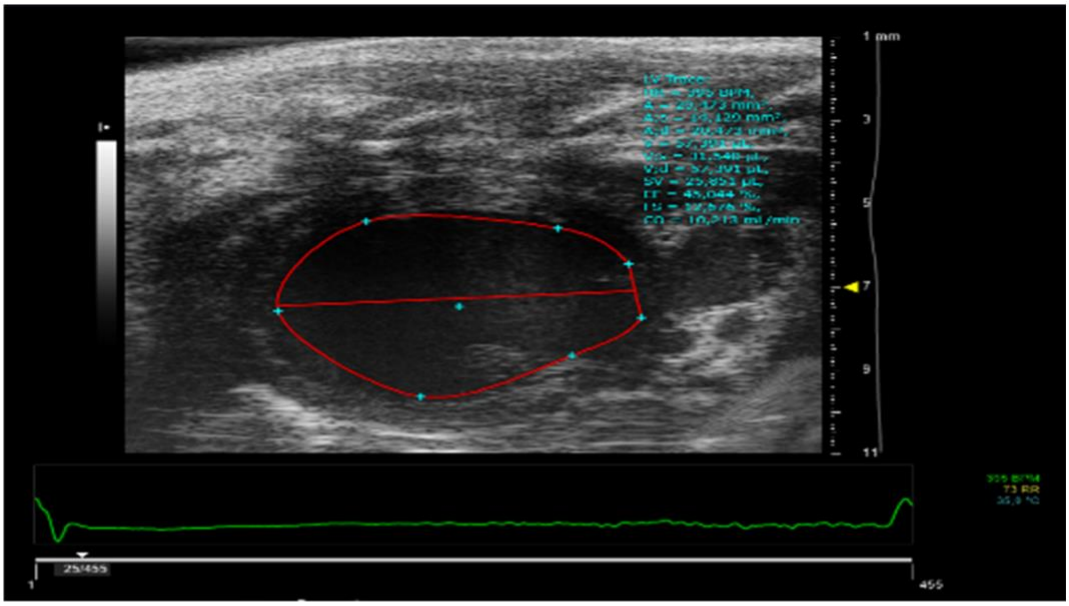

B

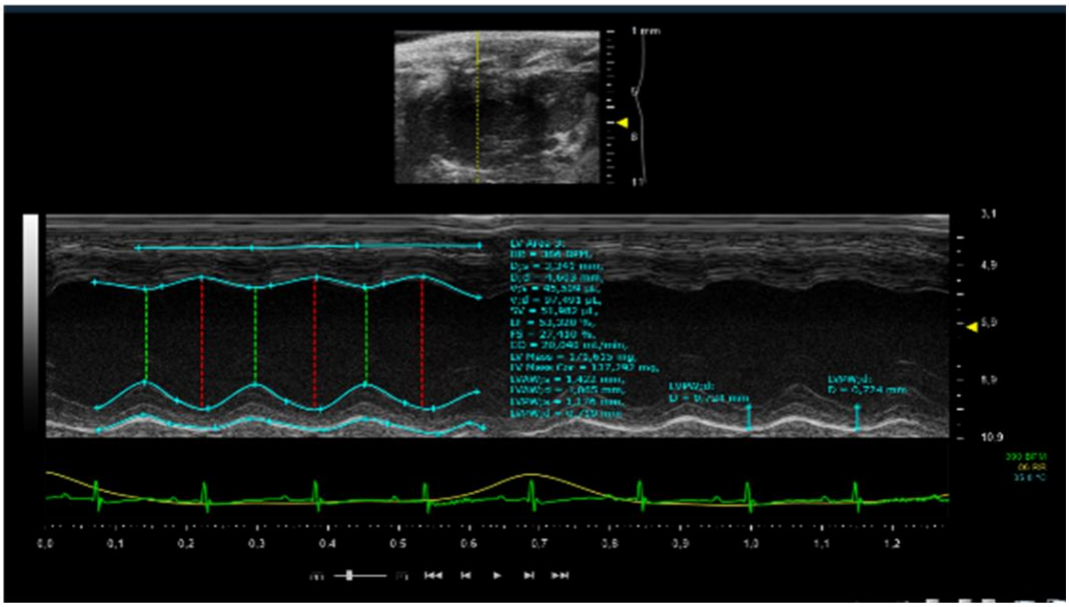

Figure 7**:** Echocardiography analysis of mice heart. (A) Left ventricular tracing of the long axis of the heart in an EKV clip for calculations such as the left ventricular ejection fraction, cardiac output and stroke volume. (B) Left ventricular tracing of the short axis of the heart in an M-mode clip for calculations such as left ventricular fractional shortening and wall thickness.

8.13. Statistics

Statistical analysis was performed using Graph Pad. Data are presented as mean ± standard error of the mean, unless otherwise indicated.

8.13.1. Animal experiment data analysis

Before the start of animal experiments, Sample size calculations was done.
On the basis of our previous experiments average infarct size after 4 weeks in the control group = 38%, in the treatment group = 28%, standard deviation = 5%, significance level $\alpha = 0.05$, power = 0.8, analysis of variance with pairwise comparisons and α-adjustment for multiple comparisons (5 out of 6 possible comparisons). This results in a group size of N = 6.
Based on the expected mortality (according to experience in previous attempts ~ 30%) the resulting total group size was N = 8 for the 2 week histology group.

On the basis of our previous experiments average FS after 4 weeks in treatment group 1 = 22%, in treatment group 2 = 29%, standard deviation = 5%, significance level $\alpha = 0.05$, power = 0.8, analysis of variance with pairs compare and α-adjust for multiple comparisons (5 out of 6 possible comparisons). The result is a group size of N = 12.
Based on the expected mortality (according to experience in previous attempts ~ 30%) the resulting total sample size was N=16 for the 6 week time point.

After animal experiments, for the echocardiographs data, an intergroup difference comparing each group to sham was done by one-way analysis of variance (ANOVA) followed by Bonferroni posttest. A value of $p < 0.05$ was considered statistically significant. P value summery *** <0.0001

8.13.2. RNA Sequencing data analysis

RNA sequencing data was analyzed by Dr. rer. nat. Karsten Jürchott, Bioinformatician of Development & Exploratory Lab (DEL), Charité – Universitätsmedizin Berlin.
Fastq-files were quality controlled using fastqc (version 0.11.7 - Bioinformatics Group at the Babraham Institute). Residual adapter sequences and low quality reads were trimmed using

AdapterRemovel (63). Reads were aligned to the mm10 (GRCm38.82) version of the mouse genome using tophat (64) and bowtie2 (65). Counts per gene were calculated as the sum of all mapped reads within a gene region.

Raw counts of protein-coding genes were normalized and variance stabilizing transformed using the DESeq2 package (66). R: A language and environment for statistical computing. R Foundation for Statistical Computing, Vienna, Austria. URL https://www.R-project.org/.). Variances across all samples were determined for each gene and 1000 genes with the highest variances were selected for unbiased analysis.

Principle component analysis was either done with the plotPCA() function implemented in the DESeq2 package or with the in-built prcomp() function. The first two principle components were shown in the plots. Heat maps were generated after hierarchical clustering of the scaled data using euclidean distances.

Differential expressed genes between treatment groups were defined by fitting negative binomial distribution models to the data. Raw p-values were adjusted for multiple testing by fdr/Bonferoni. An adjusted p-value below 0.05 (and a minimal absolute log2 fold change of 1) was used for selecting significant results.

K-means clustering of differential expressed genes were performed using the in-built kmeans() function in R with 100 randomly defined start sets of 6 clusters in order to a robust reproducible result.

Overrepresentation analysis of selected genes in terms of the gene ontology system was done using the topGO package (Adrian Alexa and Jorg Rahnenfuhrer (2016). topGO: Enrichment Analysis for Gene Ontology. R package version 2.32.0.), in R utilizing classical Fisher tests based on hypergeometric distributions. Due to the high redundancy of the gene ontology system, raw p-values were not adjusted for multiple testing. Overrepresentation analysis of selected genes in gene sets of the Molecular Signature Database (67) was done by applying classical Fisher Tests based on hypergeometric distributions. Due to the high redundancy of some gene set collections with the database, raw p-values were not adjusted for multiple testing.

9. RESULTS

9.1. Lentiviral system

For successful transgene delivery, cellular reprogramming requires overexpression of specific transcription factors and efficient vectors. The initial part of this project was to primarily establish and standardize lentiviral production, concentration, titration, and validation.
Prior to LeV production, plasmid DNA was verified for the correct sequence. Plasmid function was validated was by transfecting Hek293 cells with each of the TF plasmid Gata4, Mef2c, Tbx5, and Myocd. Three days after transfection when stained the cells showed nuclear localization of each of the TFs (Figure 8).

High titer lentiviral vectors were then produced for all TFs Gata4, Mef2c, Tbx5, and Myocd (G, M, T, and My) using the 2nd generation lentiviral packaging system**.**
Nuclear transgene expression was validated by immunofluorescence in Hek293 and HT1080 cells (Figure 9 and 10) and the transgene size was confirmed by western blots (data not shown)**.** Following verification and validation, LeV for each of the TFs was produced in large scale and concentrated using ultracentrifugation. The competency of each of the IRES-eGFP lentiviral vectors was confirmed by infecting HT1080 cells, which resulted in eGFP-positive cells indicating successful transduction of the cells after LeV transduction. The titers of each of these LeV vectors ranged from about 50*10^6 to 300*10^6 TU/ml (Table 3). Titration was also done in CFs, wherein the resulting titers were much lower (data not shown). To determine the amount of virus needed for efficient transduction of CFs, CFs were infected with the LeV at a MOI of 1 to 5 based on the LeV titers obtained from the HT1080 cells. It was seen that at a MOI of 5 a maximum transfection efficiency of 60-90% and a plateau state was achieved as determined by flow cytometry (Figure 11). Further on during the project, when LeV production and titrations were repeated, the MOI tests were done using only eGFP LeV. It was seen that the transfection efficiency was consistent, and at an MOI 5 a transfection efficiency of 90% was obtained (data not shown).

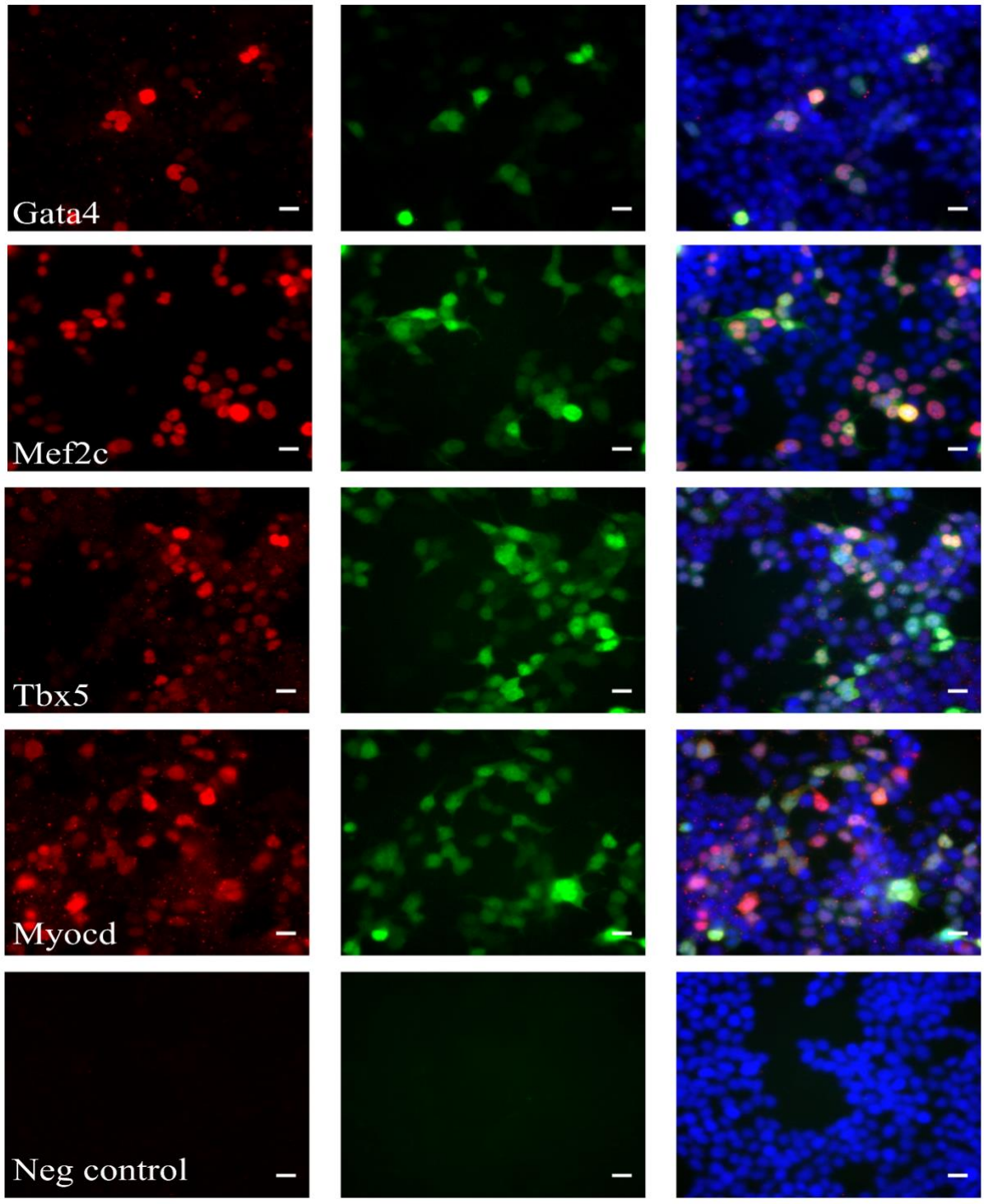

Figure 8: Validation of the lentiviral vectors**:** Immunofluorescence staining of Hek293 cells showing expression of Gata4, Mef2c, Tbx5 and Myocd (red), DAPI (blue) to label the cell nuclei and the eGFP vectors (green) after PEI-based plasmid transfection with the respective plasmids. Scale bars = 20µm.

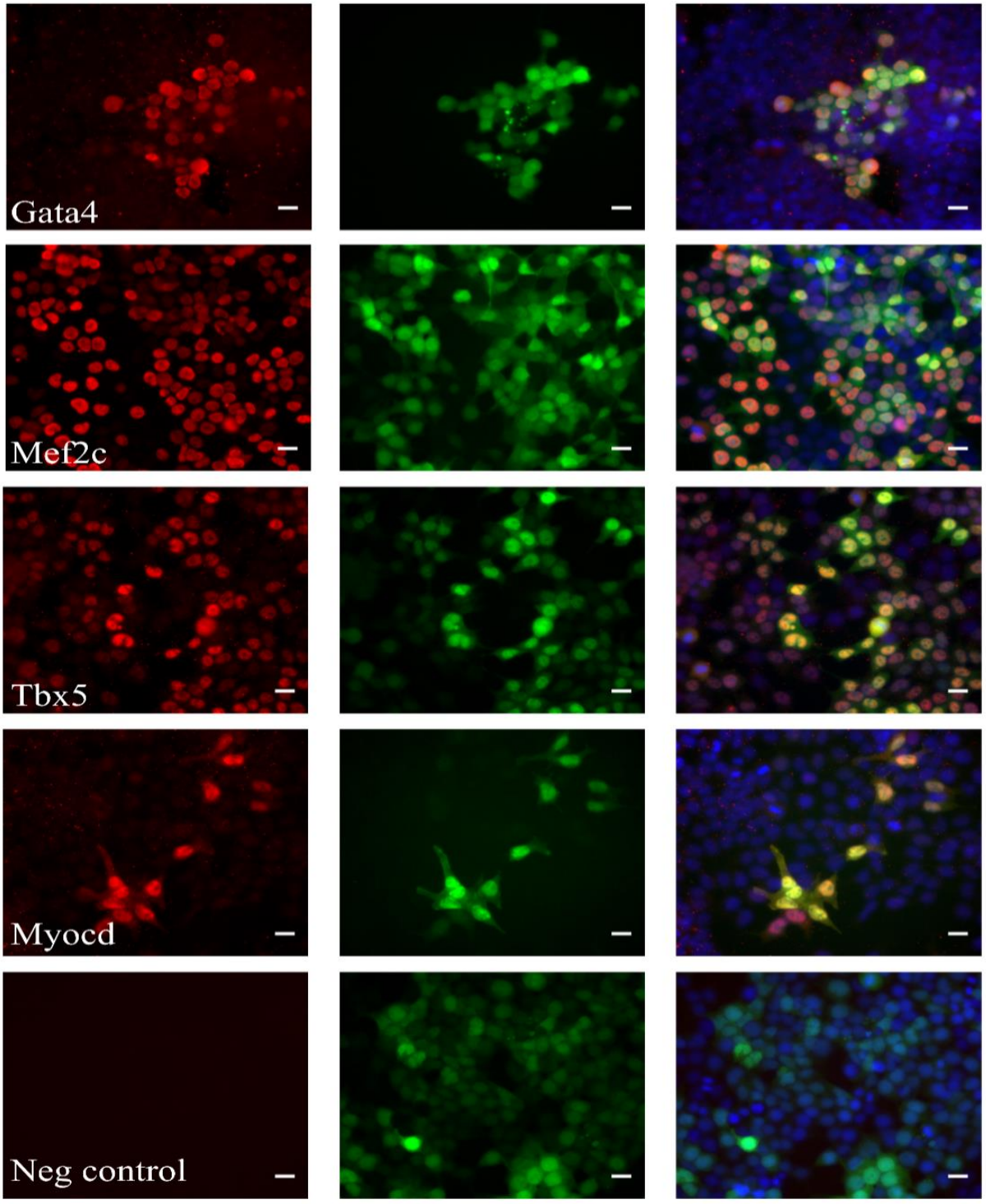

Figure 9: Proof of transgene expression**:** Immunofluorescence staining of Hek293 cells showing expression of Gata4, Mef2c, Tbx5 and Myocd (red), DAPI (blue) to label the cell nuclei and the eGFP vectors (green) after transduction with the respective lentiviruses. Scale bars = 20µm.

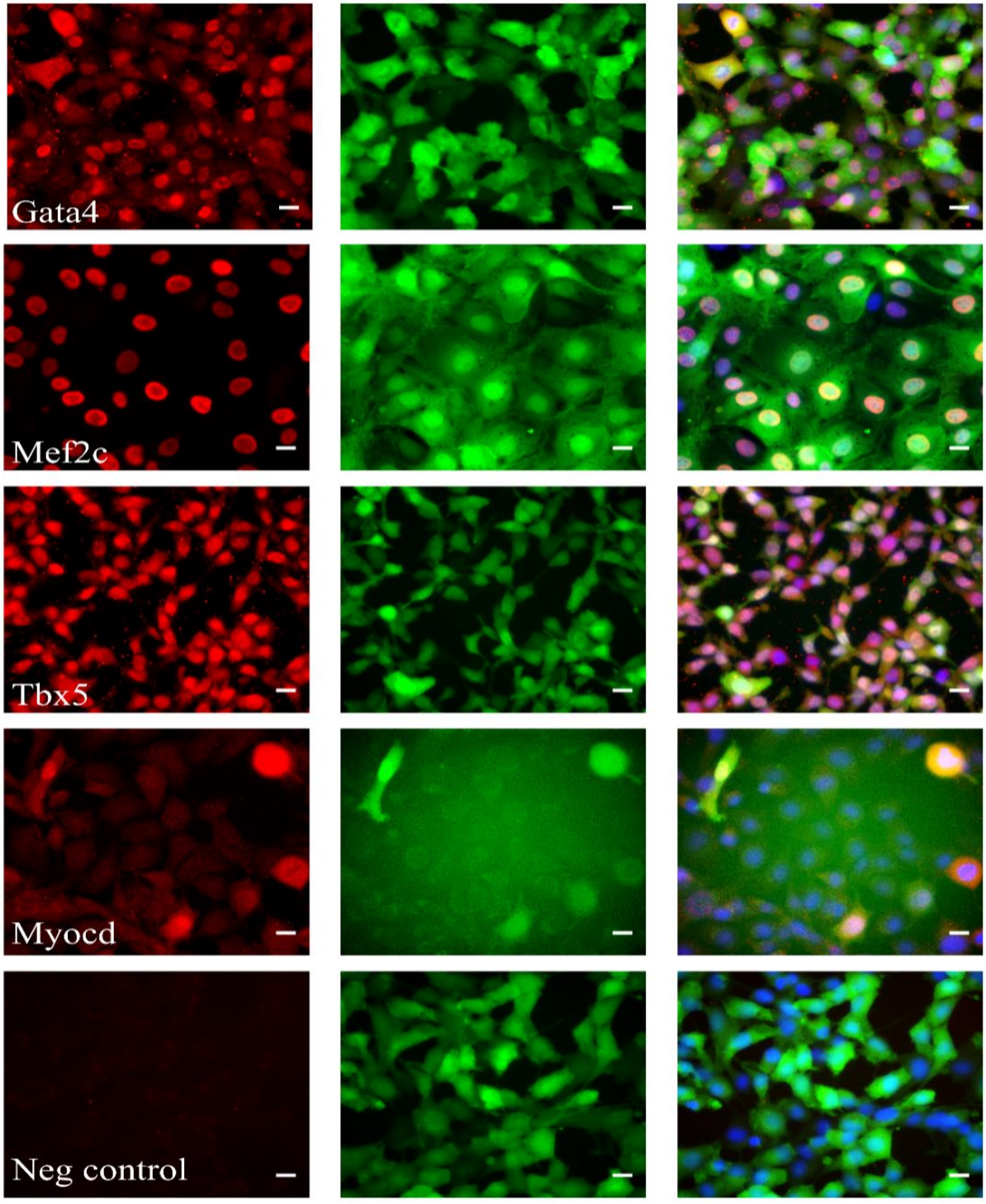

Figure 10: Immunofluorescence staining of HT1080 cells showing expression of Gata4, Mef2c, Tbx5 and Myocd (red), DAPI (blue) to label the cell nuclei and the eGFP vectors (green) after transduction with the respective lentiviruses. Scale bars = 20µm.

Lentivirus titer range (*10^6 TU/ml)*	
Cell Type	**HT1080**
Gata4	58 – 150
Mef2c	55 – 68
Tbx5	104 – 337
Myocd	47 – 79
eGFP	59 – 249

Table 3: Titer range of the concentrated lentiviruses in HT1080 cells.

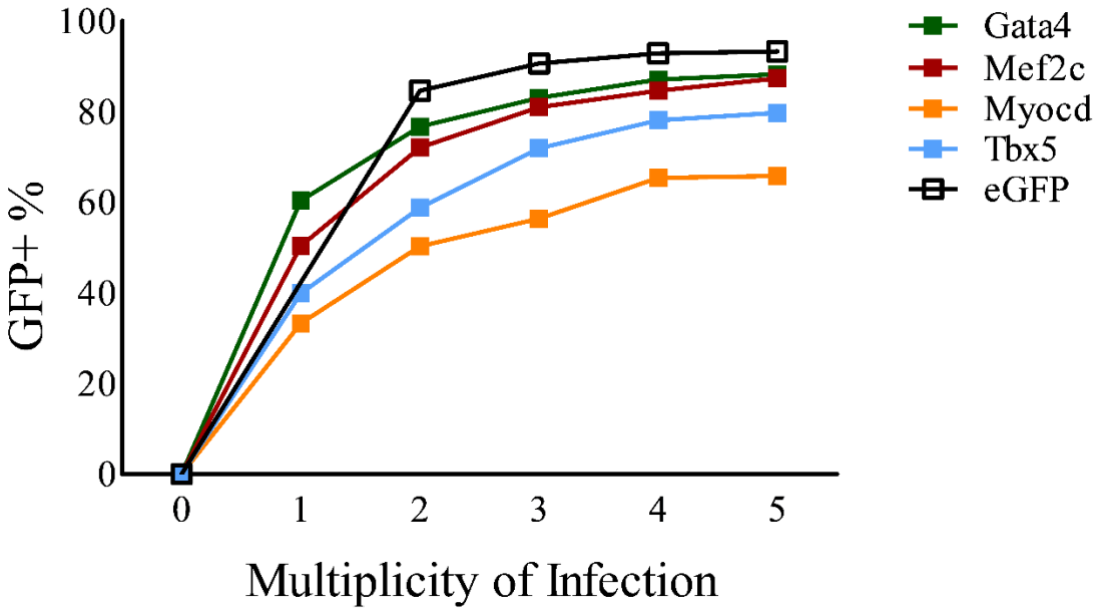

Figure 11**:** Graphical representation of the transduction efficiency of each of the lentiviral vectors at MOI 1 to 5 in cardiac fibroblasts. The maximum transduction efficiency of 60-90% was observed at an MOI of 5 in cardiac fibroblasts.

9.2. Baseline cardiac reprogramming

To achieve baseline cardiac reprogramming of CFs into iCMs as achieved by various other groups like Ieda et al. and Protze et al. (27, 30), we infected CFs with the LeV cocktails GMT and MMT. The cells were positive for GFP indicating successful transduction after infection with both GMT and MMT (data not shown). However, cell viability decreased markedly compared to the non-infected fibroblasts before the onset of reprogramming and relevant cardiomyocyte gene expression. The striking results achieved by various other groups could not be reproduced in our initial attempts.

To counteract cell death after transduction and to optimize reprogramming efficiency initial seeding density (1,000 vs. 5,000 cells/cm2), lentiviral load (MOI of 1 to 10), reprogramming medium (DMEM vs. DMEM/M199, 1 g/l vs. 5 g/l glucose, 2% vs. 10% HI-FBS), antibiotic selection of transduced cells (G418), and subculture were investigated for their influence. Irrespective of seeding density and viral load, cell death occurred in CFs cultures with varying dynamics, starting as early as 4 days after infection (data not shown). LeV induced toxicity, played a minor role, as it would be overcome 4-5 days after infection. Moreover, transduction efficiency with a MOI of 5 ranged approximately from 60-90% for individual viruses as stated previously (Figure 11).

The continuous growth of the non-infected fibroblasts resulted in monolayer confluence, which was the major reason for the dramatic decrease in viability in the transdifferentiating cultures. Regular subculture and antibiotic selection of CFs after infecting with the LeV cocktail prevented cell death (data not shown).

9.3. Direct reprogramming of cardiac fibroblasts into induced cardiomyocyte like cells

To initiate cardiac reprogramming to our desired cell state, CFs were infected with the LeV cocktail GMTMy. Two days after transduction the cells were positive for GFP (Figure 12) and all the transgenes were stably expressed (Figure 13). The cells were subjected to antibiotic selection and were regularly subcultured to prevent cell death.

GMTMy induced expression of mature cardiomyocyte markers such as α-actinin, cTnT and myosin at both mRNA (data not shown) and protein levels starting at 1 week after infection and showed increased expression until 2 weeks after infection. These cells showed expression of α-actinin, cTnT and myosin as determined by immunofluorescence (Figure 14). FACS analysis showed that 23% of the cells were positive for cTnT (Figure 15).

In terms of morphology reprogrammed cell populations appeared heterogeneous with non-organized cTnT positive cells and a few with sarcomeric striations. Most of the cTnT positive cells displayed a rounded epithelial cell-shape while a small fraction of the cells showed mature round like CMs patters (Figure 16). These rounded cells also displayed a proliferative capacity.
No spontaneous contractile activity was detected within 8 weeks of observation. Mature CMs have low proliferation capacity, thus indicating that these epithelial-like troponin positive cells could be a cardiac committed precursor-like cell population – iCM precursor cells (iCMPs).

Additionally, we stained the iCMPs for cardiac progenitor cell (CPC) markers, such as Cxcr4, Flk1, Mesp1, and Nkx2.5, as it is important that these cells show CPC markers. The iCMPs showed bright expression of Nkx2.5, Flk1 and Cxcr4 markers and some cytoplasmic expression of Mesp1 (Figure 17). Mesp1 is a transcription factor and therefore the staining should be seen in the nucleus. However, in my hands, Mesp1 displayed an unexpected expression pattern. Further research is necessary, as it would also be interesting to see what role Mesp1 plays in the reprogramming process.

All these outcomes support our assumption that the reprogrammed cells are a cardiac committed precursor-like cell population.

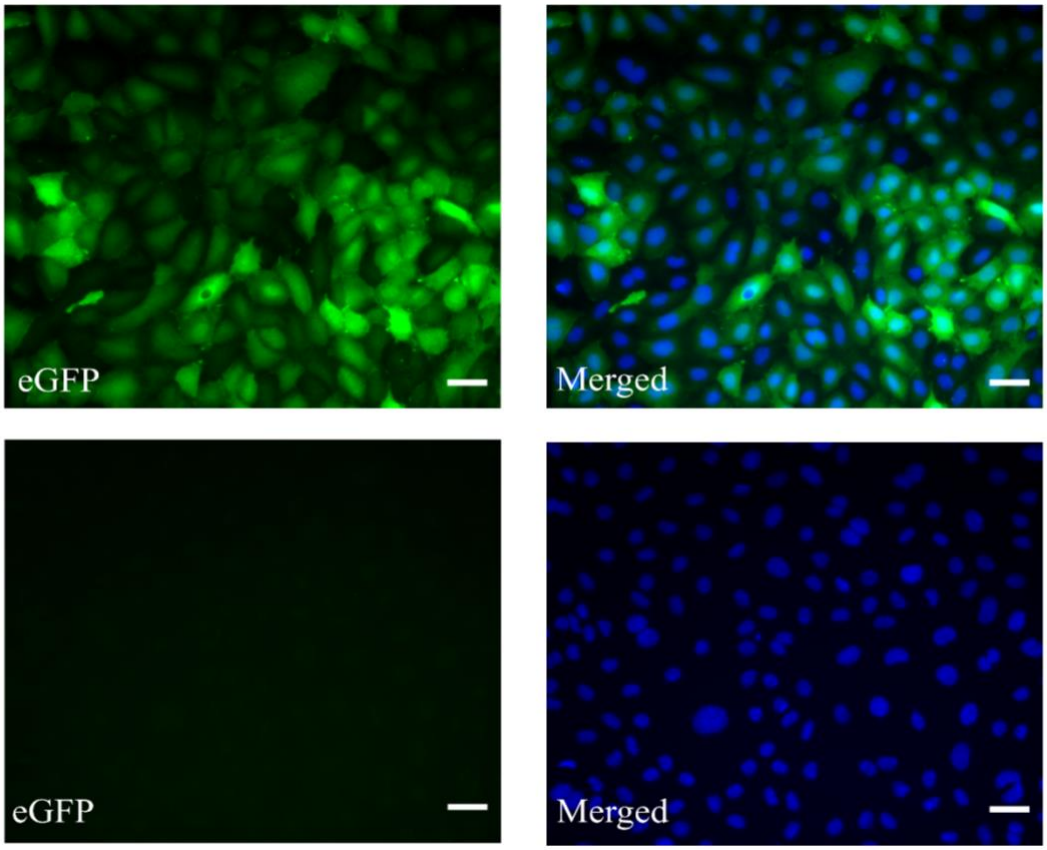

Figure 12**:** eGFP expression in cardiac fibroblasts 3 days after lentivirus cocktail GMTMy infection, indicating successful transduction; and control CFs with no lentivirus infection and therefore no GFP expression. Scale bars = 50μm.

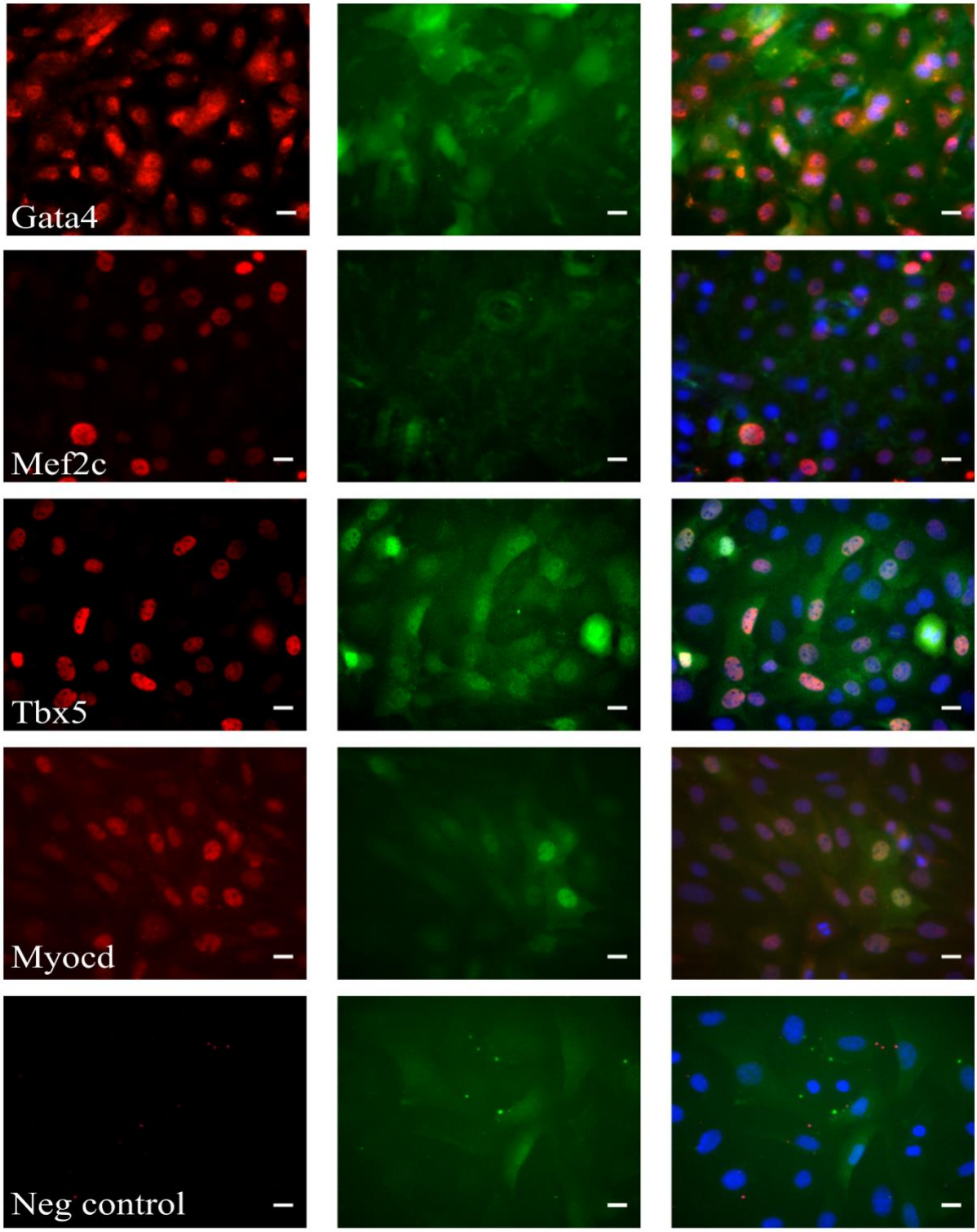

Figure 13**:** Successful LeV transduction: Fluorescence images of CFs after transduction with GMTMy cocktail. The cells were stained for the transcription factors Gata4, Mef2c, Tbx5 and Myocd (red), DAPI (blue) to label the cell nuclei and GFP (green) for LeV. GMTMy were expressed, indicating successful transduction. Scale bars = 20µm

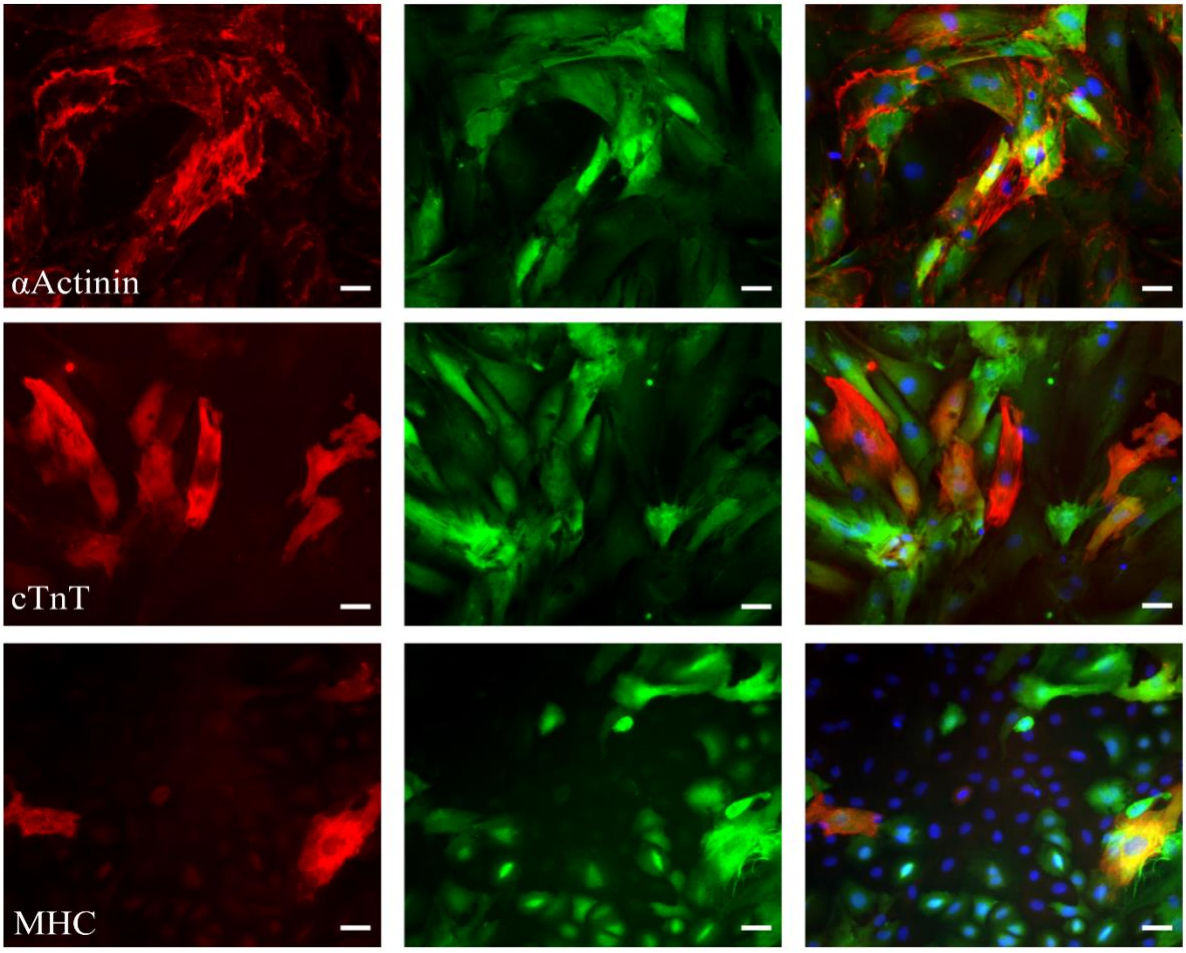

Figure 14**:** Direct cardiac reprogramming: Immunofluorescence images of CFs 2 weeks after LeV transduction showing expression of cardiac markers α-actinin, cTnT and Myosin (red), DAPI (blue) to label the cell nuclei and GFP (green) for LeV. Scale bars = 50μm.

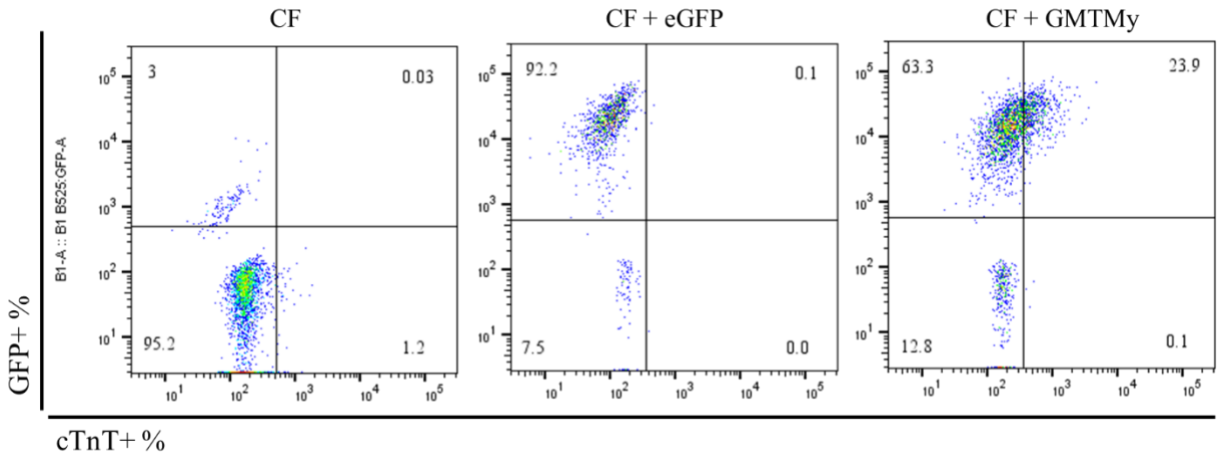

Figure 15**:** Protein expression of cardiac marker cTnT and eGFP in CFs 2 weeks after LeV transduction. CFs transduced with LeV cocktail GMTMy show about 93% GFP+ cells and 23.9% of the eGFP+ cells were cTnT+.

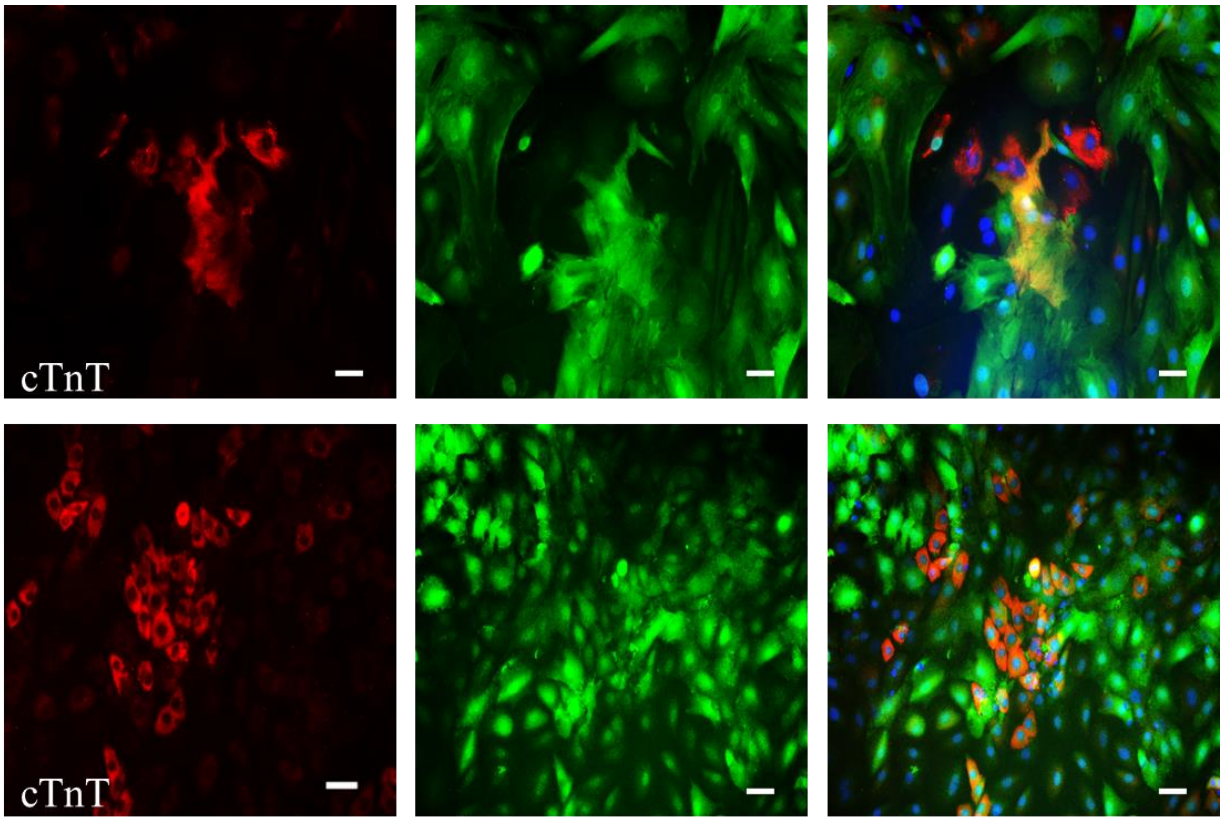

Figure 16**:** Immunofluorescence images 2 weeks after lentivirus transduction showing a heterogenous population cTnT positive cells - Rounded epithelial like cells and rod like straited cells stained positive for cTnT (red), DAPI (blue) to label the Nuclei and lentivirus with GFP (green). These results indicate a heterogeneous population of both mature and dividing cTnT+ cells after reprogramming Scale bars = 50µm.

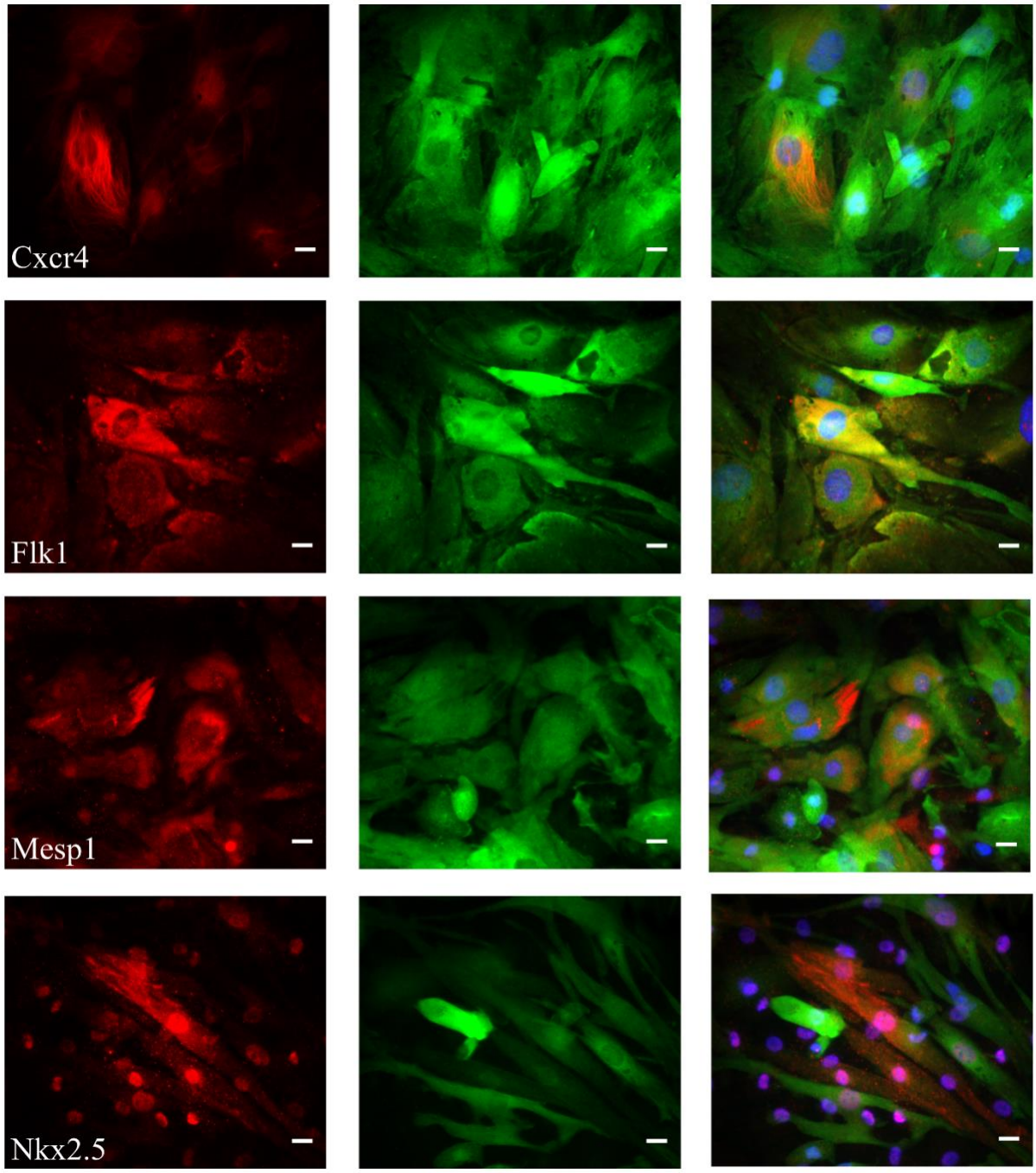

Figure 17**:** Immunofluorescence images of CFs 2 weeks after transduction with lentiviral cocktail GMTMy showing expression of cardiac progenitor markers Cxcr4, Flk1, Mesp1 and Nkx2.5 (red), DAPI (blue) to label the cell nuclei and GFP (green) for lentivirus. Scale bars = 50µm.

9.4. Enriched populations of iCMPs obtained by transcriptional selection

Next, we sought to obtain enriched populations of these iCMPs by using the molecular beacon (MB) technology. The representative cardiac structural genes cardiac troponin T (cTnT) and myosin heavy chain (MYH6/7, α/βMHC) were expressed in the reprogrammed cells and thus were determined optimal candidate genes for MB design. MBs that target unique sites in MYH6/7 mRNA in both mouse and human (55) were used.

To establish an efficient MB-based transfection, it was necessary to, (1) identify an optimal ratio of molecular beacon to transfection reagent (TR); and (2) determine an optimal MB concentration. CFs 70-90% confluent were transfected with, 1:1, 1:2, 1:3 and 1:4 ratios of MB (µM) to TR (µl) and different MB concentrations (0.1, 1, and 10 µM). At a ratio of 1:4 MB:TR and with 1µM MB concentration, about 100% transfection efficiency was achieved as determined by high content screener image analyzer (Figures 18 and 19). Initial experiments were done with HL1 cells, however, HL1 cells were harder to transfect as a result the transfection efficiency was low. Therefore, all further establishment experiments were performed on the target cells CFs.

Furthermore, we sought to determine the specificity of the MBs. In order to do this, CMs were isolated from mCherry transgene mice. These cells were transfected with negative control, positive/ delivery control, and MYH6/7 MB at the optimal working concentration and ratio. MB signals were analyzed by FACS. Approximately 61% of the cells were MYH6/7 positive. The transfection efficiency with the delivery control was about >60%, and CM detection was similar. Indicating that not all cells receive the beacon, but the mCherry positive cells that receive the beacon were MYH6/7+ (Figure 20)**.** Thus, suggests specificity of the MYH6/7 MB for CM specific cells.

Once the MB technology was standardized, cardiac reprogramming using LeV cocktail was initiated. Two weeks after GMTMy, successful reprogramming was confirmed by examining for cardiac marker expression. MB-based sorting yielded an MYH6/7 positive population that corresponded to 33+/-3.2% (Mean + SEM) of the reprogrammed cells (Figure 21). The purity of the sorted cells was confirmed by staining the iCMPs after sorting for cardiac markers α-actinin and cTnT. It was seen that 1 week after sorting the cells maintained stable cTnT and α-actinin expression (Figure 22).

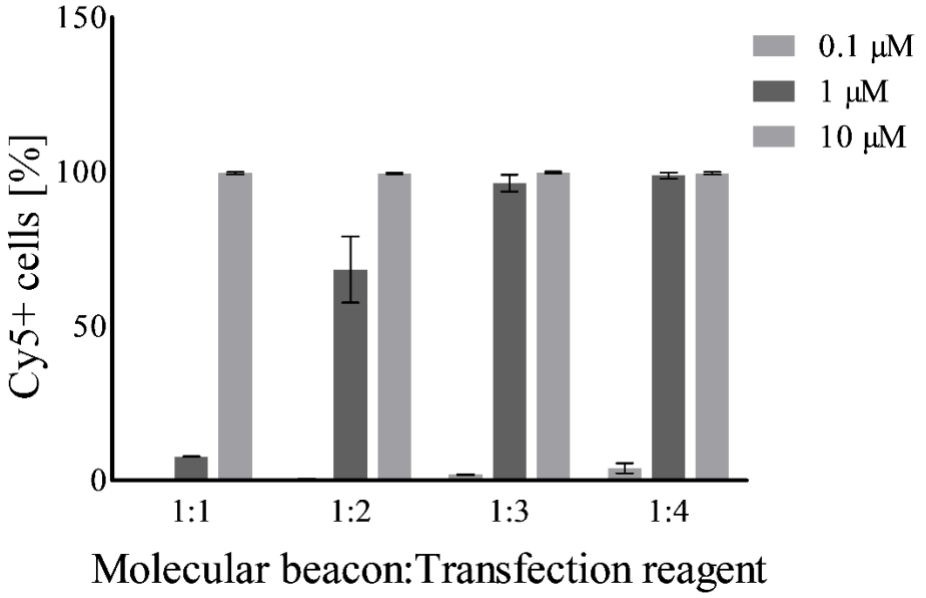

Figure 18**:** Molecular beacon testing**:** Graphical representation of MB transfection efficiency and MB titration as determined by high content screener image analyzer. At an MB concentration of 1µM and at a 1:4 ratio of molecular beacon to transcription reagent, 100% transfection efficiency was achieved in CFs.

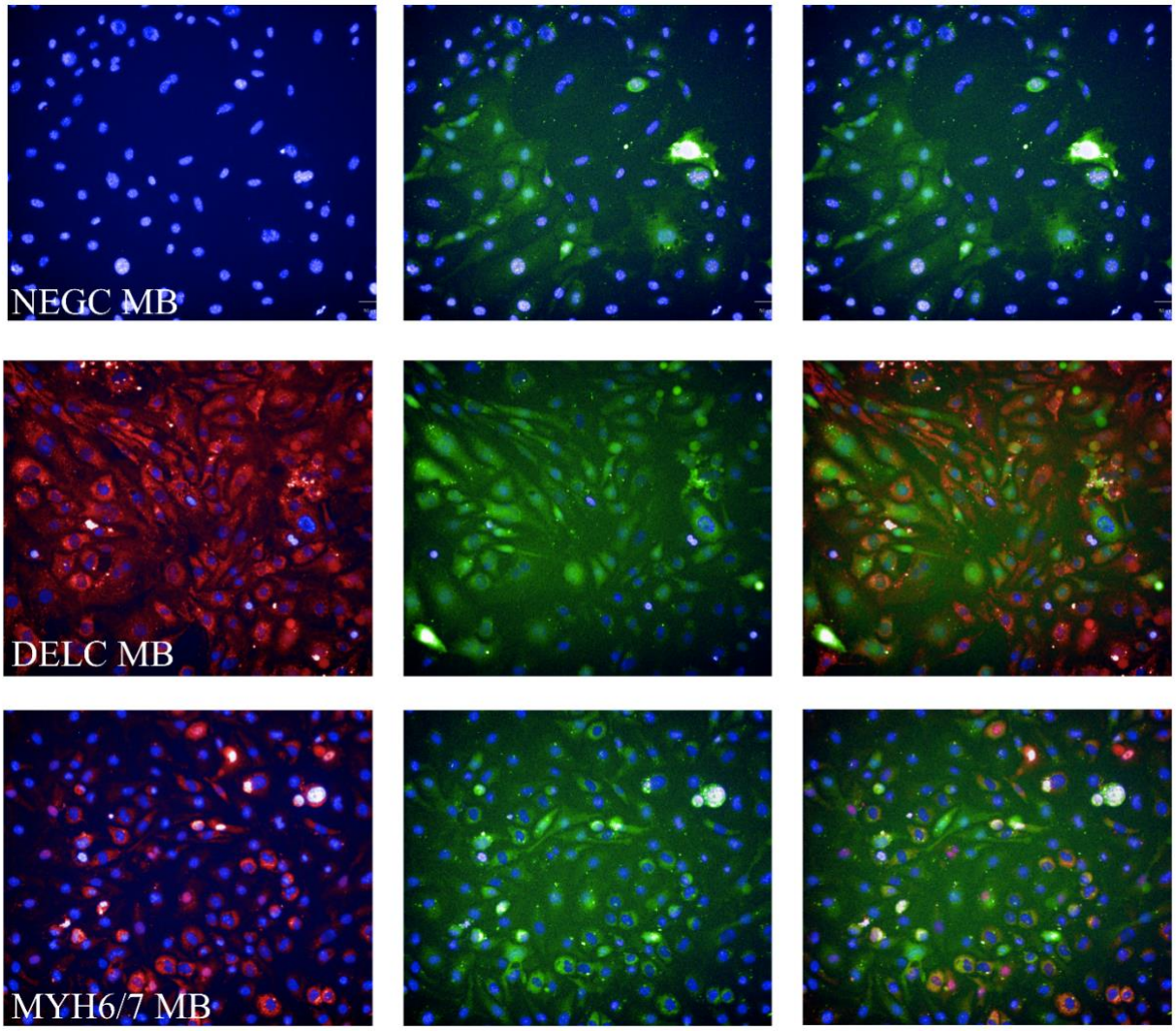

Figure 19**:** Molecular beacon testing**:** High content screener images of CFs expressing Cy5 after transfection with MBs NEGC, DELC and MYH6/7. Cell nuclei were labeled with Hoechst (blue) for visualizing and counting the total cell number and GFP (green) for lentivirus. Scale bars = 50µm.

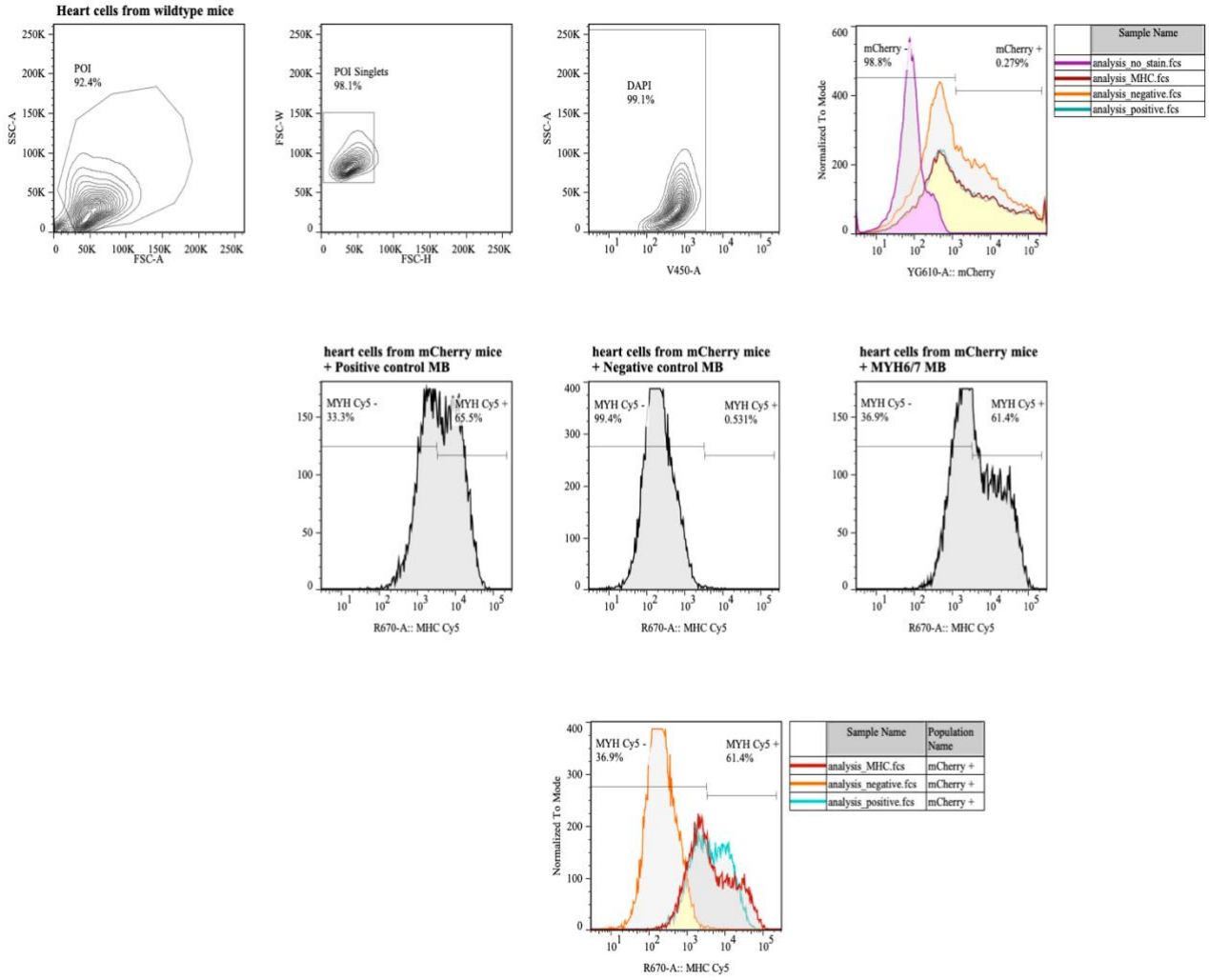

Figure 20**:** Molecular beacon specificity: Neonatal CMs isolated from transgenic α-MHC-mCherry mice transfected with negative control, positive control and MYH6/7 molecular beacon and analyzed by flow cytometry showing mCherry and MYH6/7 (Cy5) expression. Approximately 61% of the cells were MYH6/7+.

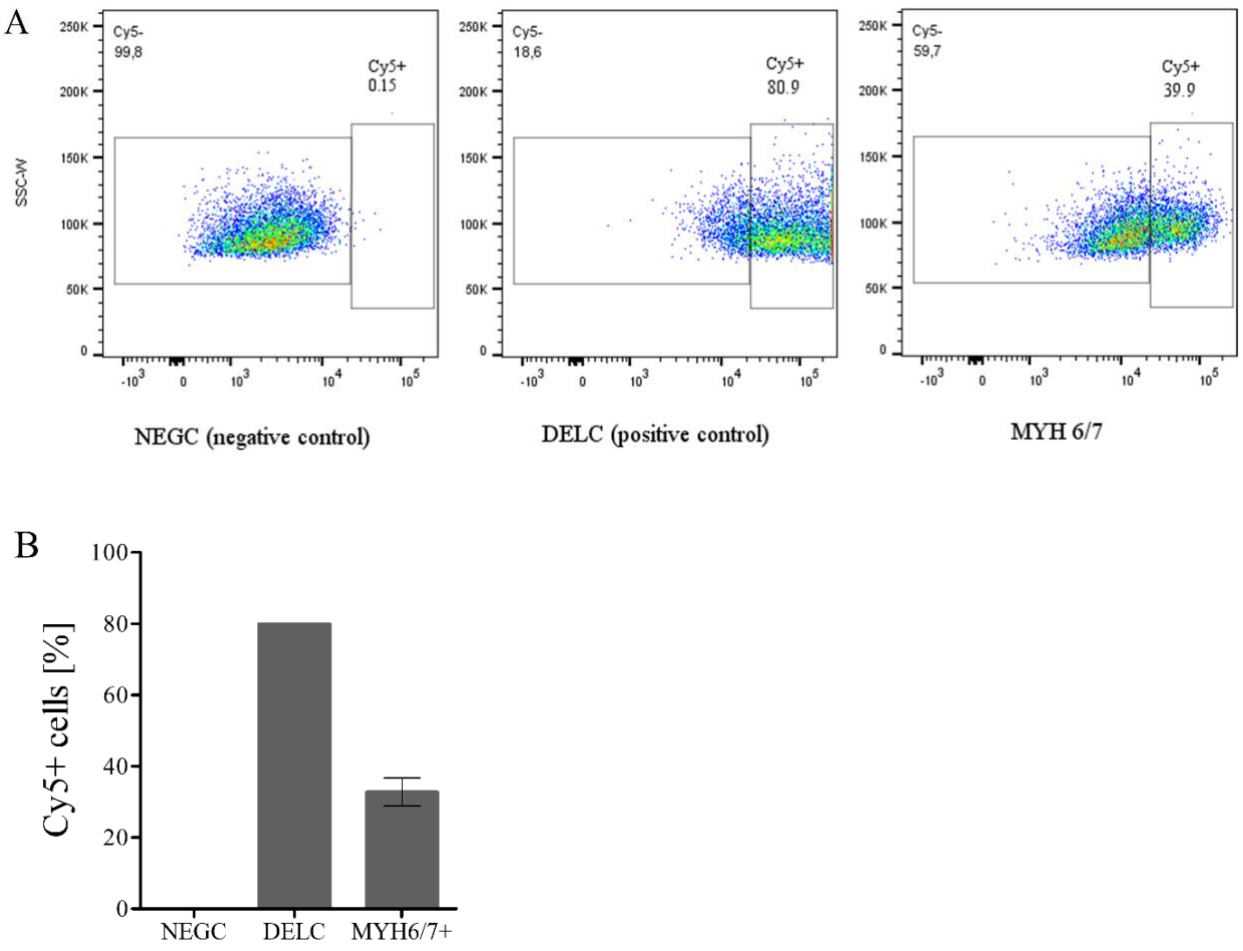

Figure 21**:** Molecular beacon-based iCMP sorting**: (A)** CFs 2 weeks after transduction with lentiviral cocktail GMTMy, transfected with 1µM MYH6/7 MB and sorted yielded approximately 30+/-3% MYH6/7+ cells (Mean +/- SEM). CFs were transfected with NEGC and DELC as control. **(B)** Quantitative data of MB-based sorting of iCMPs.

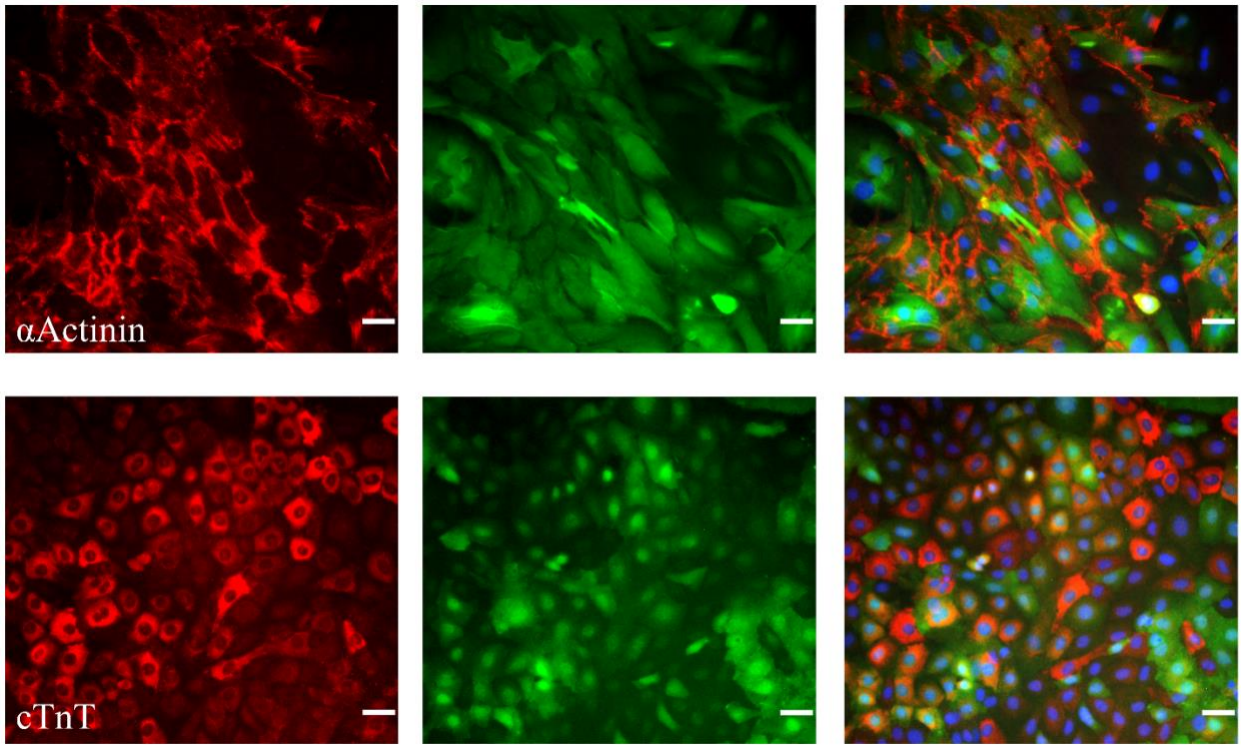

Figure 22**:** Immunofluorescence images after sorting: rounded epithelial like iCMPs expressing cardiac markers cTnT and α-actinin (red), DAPI to label the cell nuclei (blue) and GFP (green) for lentivirus. Scale bars = 50µm.

9.5. Global gene expression analysis of iCMPs unveil their unique transcriptome

Understanding the global gene expression pattern is of paramount importance for future *in vivo* experiments as well as for clinical application of the iCMPs. Therefore, we compared the iCMPs after sorting to their parental CFs and mouse adult heart tissue (AHT) by RNA-Seq. The quality of total RNA isolates was, analyzed using the Agilent RNA 6000 Nano Kit.

Principal component analysis (PCA) plots revealed that iCMPs are different from parental CFs and the biological replicates cluster together. However, the iCMPs move towards AHT CMs. These results indicate low intragroup variation and high intergroup variation indicating that they are in an intermediate state of cardiac development (Figure 23)
Venn diagram revealed the differentially expressed genes and the overlap between differentially expressed genes (Figure 24). Three comparisons were performed, and each circle represents one pairwise comparison, CF versus iCMPs, CF versus AHT and iCMPs versus AHT showing 2402, 6628 and 6197 differentially expressed gene respectively. It was observed that 720 genes were significant in all three comparisons. The Venn diagram shows only the overlap, regardless of the direction of the regulation of the genes. Therefore, it might be that some genes in the overlap between 2 comparisons are significant, but are upregulated in one comparison and downregulated in the other.

This was addressed by K-Means clustering and Gene Ontology (GO) analysis. K-Means clustering of the differentially expressed genes was performed to determine the genes that are upregulated and downregulated generating six gene clusters – cardiac development, cell proliferation, cardiac metabolism/ contraction, embryogenesis/ morphogenesis, and metabolism.
We found that iCMPs show upregulation of genes associated with cardiac development, metabolism, contraction compared to CF. Downregulation of genes associated with cell-proliferation was observed in iCMPs in comparison to their parental CFs. However, in AHT compared to iCMPs, cell proliferation genes were further downregulated, indicating that the iCMPs still maintain some cell proliferation abilities though lower than in CF. Morphogenesis genes were upregulated in iCMP versus CF, but were downregulated in AHT. Genes associated with oxidative metabolism were upregulated in AHT and downregulated in both iCMPs and CF alike (Figure 25).

Evaluation of a selected gene set showed an upregulation of transcription factors that were overexpressed - Gata4, Mef2c, Tbx5, Myocd as well as transcription factors like Hand2 and Mef2a compared to CF indicating on-set of cardiac development. Downregulation of proliferation genes such as Ki67, Plk1, Mcm2 were seen in iCMPs compared to CF, moving them closer to AHT. However, proliferation was still maintained in iCMPs compared to AHT. Cardiac progenitor gene PDGFRa was slight upregulated in iCMPs versus CF. iCMPs compared to CF showed upregulation of cardiac contractile gene such as cTnT as well as and ion channel genes like Kcnh2, Scn5A, Ryr1/2/3. Finally, as expected downregulation of certain non-myocyte genes such as Col3A1 and Vim was seen (Figure 26).

qPCR studies for selected genes were performed to validate our gene expression findings. To understand the gene expression pattern and developmental state of the iCMPs in-depth, we additionally compared them to mouse embryonic heart tissues (mEH) and mouse neonatal heart tissue (mNH) (Figures 27). As seen in the RNA-Seq data, there was upregulation of TFs (Gata4, Mef2c, Tbx5 and Myocd in iCMPs compared to CFs. There was also expression of Mef2a and Hand2 in iCMPs. CPC marker PDGFRa expression was observed in iCMPs, slight expression of this was also seen in CF. No Nkx2.5 expression was observed similar to RNA-Seq, one explanation could be that mRNA production stops, when enough protein is there. Non-myocyte marker VIM expression was downregulated in iCMPs compared to CF. Additionally, expression of cardiac markers such as cTnT, Myh6 was observed.
Gene expression levels in iCMPs are more comparable to mouse embryonic heart tissue rather than adult heart tissue.

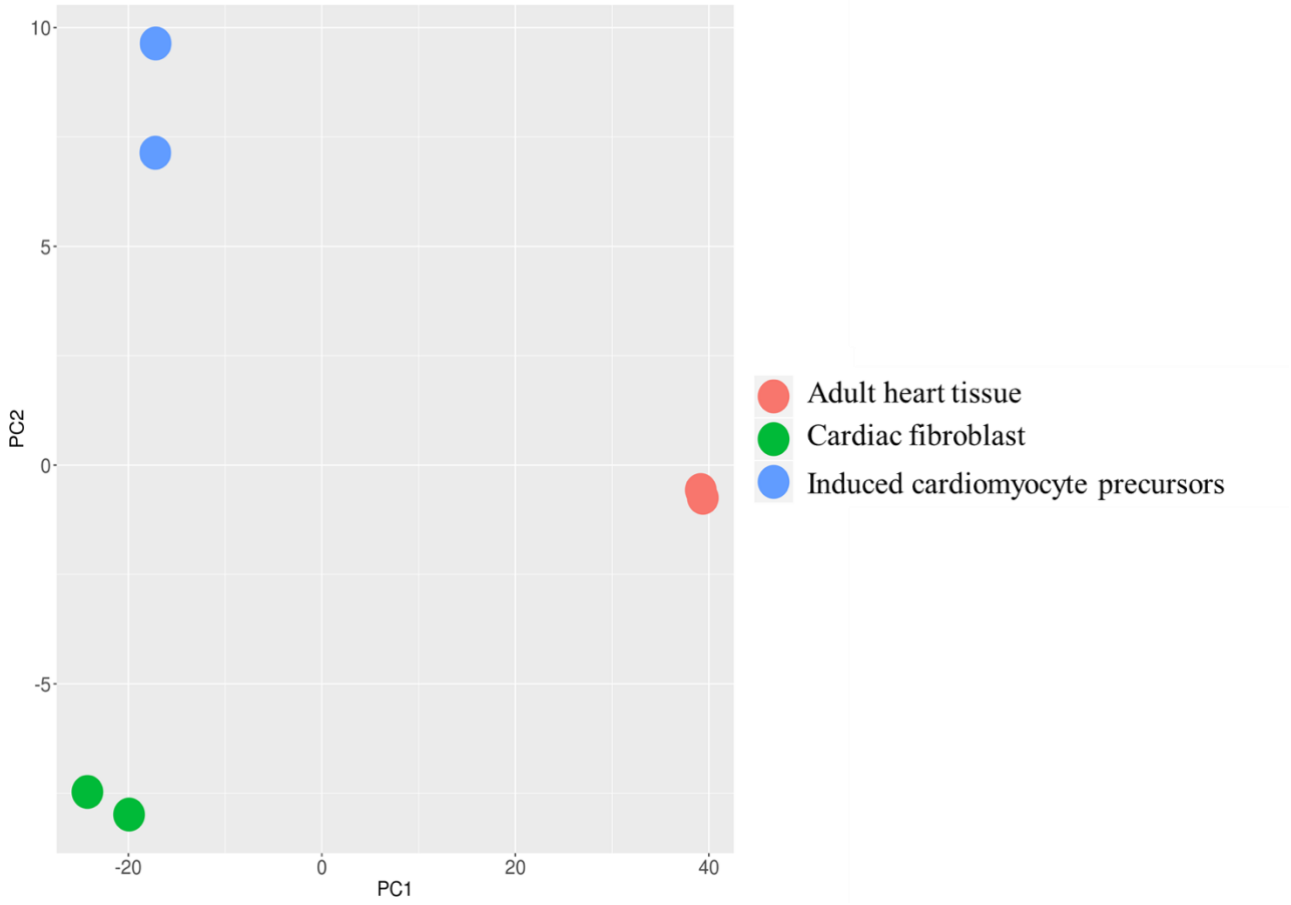

Figure 23**:** Global transcriptome analysis of iCMPs: Principal component analysis (PCA) plots reveal low intra group variation and high inter group variation. The iCMPs are different from the CFs and move towards mouse adult heart tissue, indicating the on-set of cardiac reprogramming.

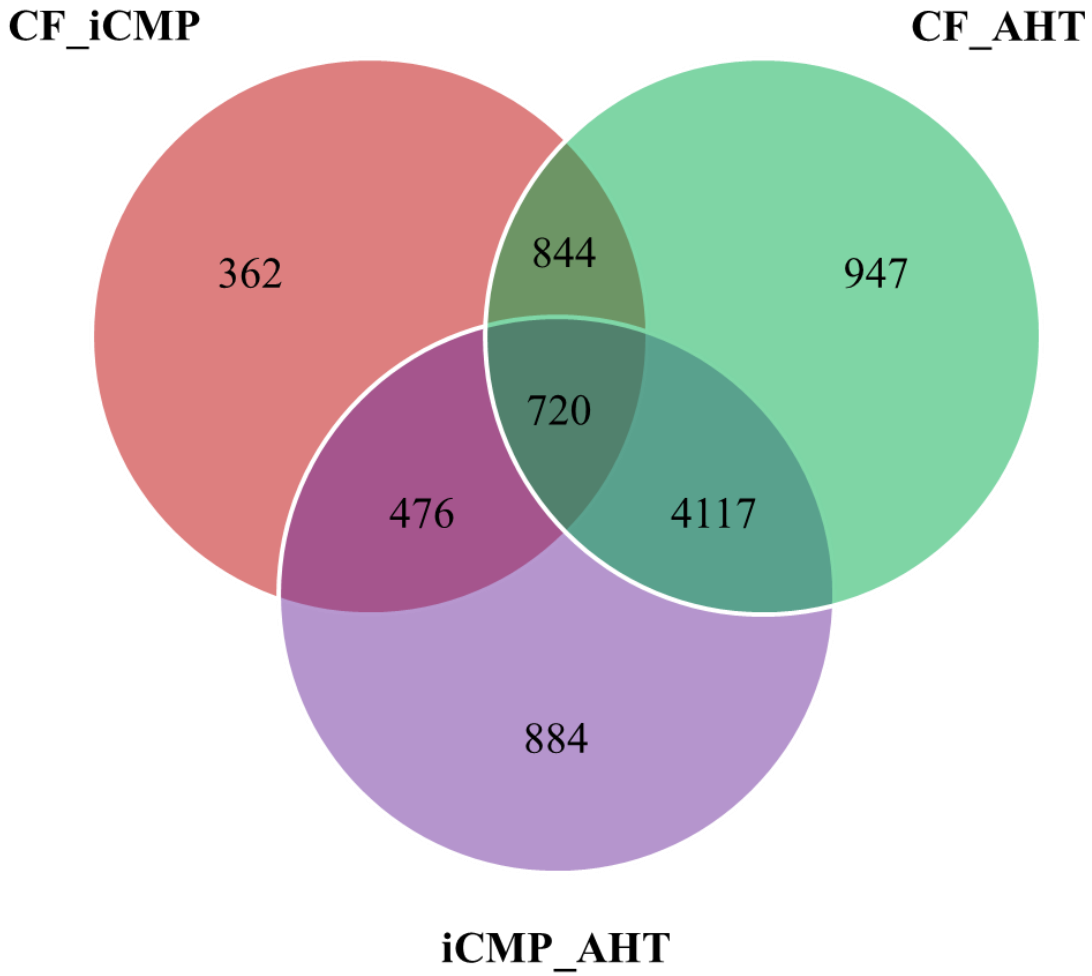

Figure 24**:** Global transcriptome analysis of iCMPs: Venn diagram revealing the differentially expressed genes and the overlap between differentially expressed genes in CFs versus AHT, CFs versus iCMPs and iCMPs versus AHT.

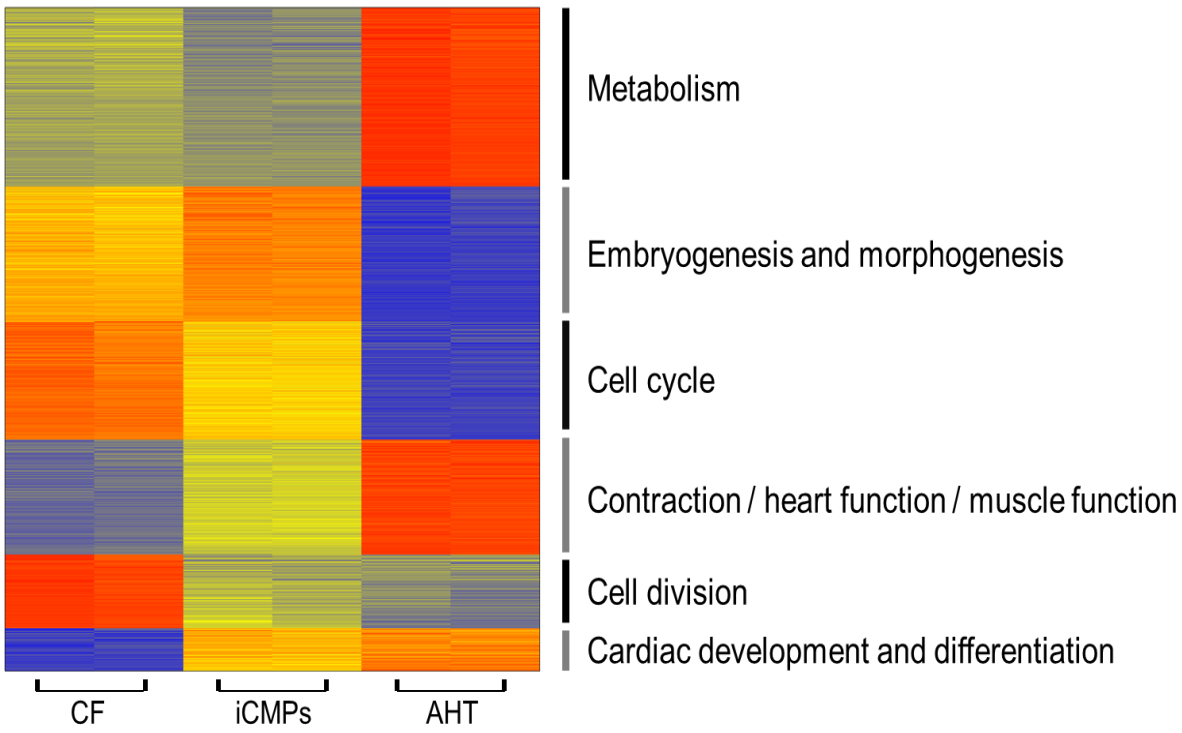

Figure 25**:** K Means clustering and Gene Ontology (GO) analysis: Heat map showing genes that have been categorized into clusters of genes that were upregulated and down regulated in the iCMPs, compared to their parental CFs and AHT. iCMPs show upregulation of genes associated with cardiac development, metabolism, contraction and embryogenesis while they showed down regulation of genes associated to cell-proliferation and metabolism when compared to their parental CFs and AHT respectively.

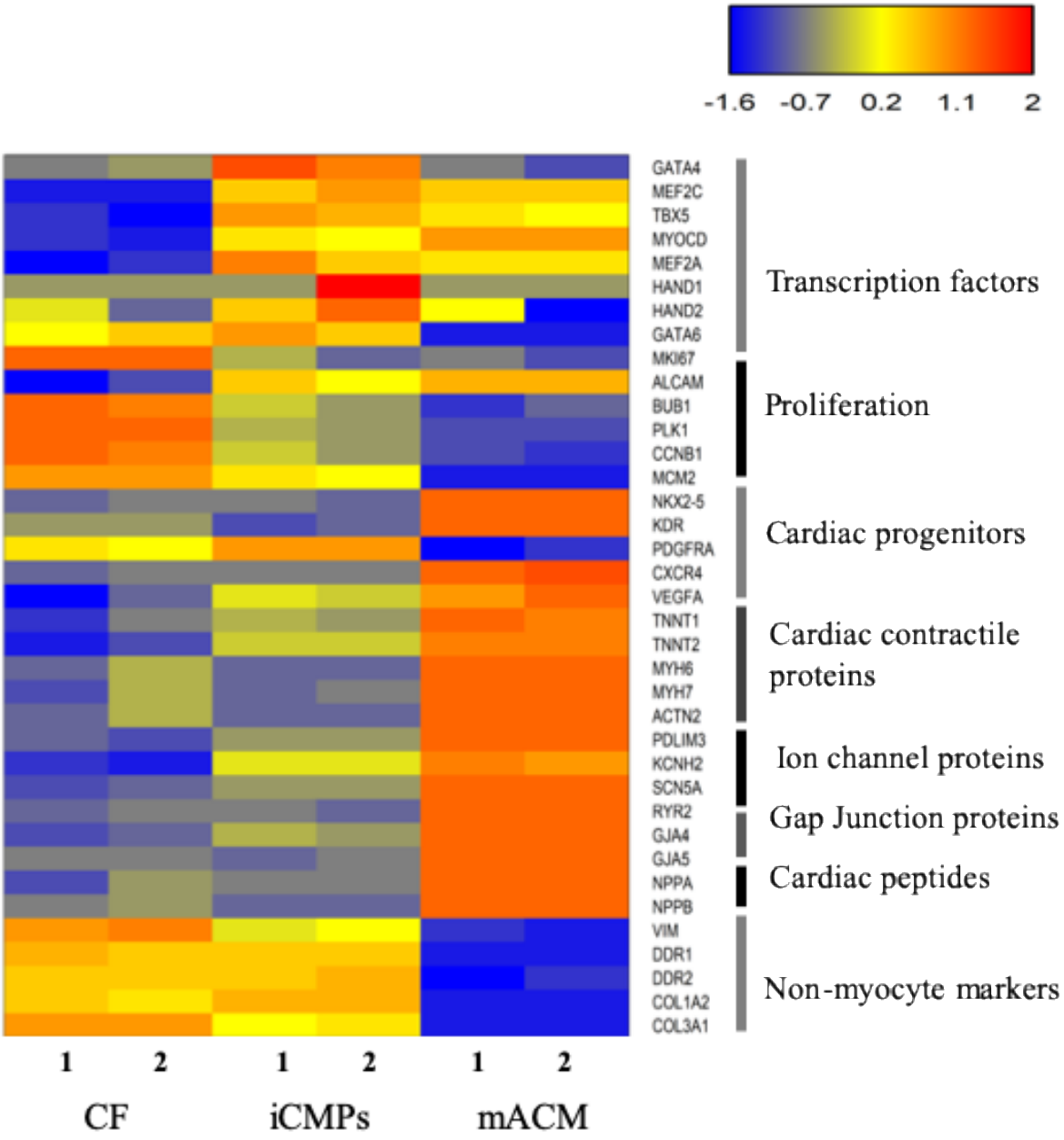

Figure 26**:** Evaluation of selected gene sets: iCMPs showed upregulation of genes associated with transcription factors and cardiac contractile proteins such as cTnT. They also showed upregulation of genes associated to ion channel in comparison to CFs. In contrast, gene encoding non-myocyte markers and proliferation were downregulated in iCMPs when compared to CFs.

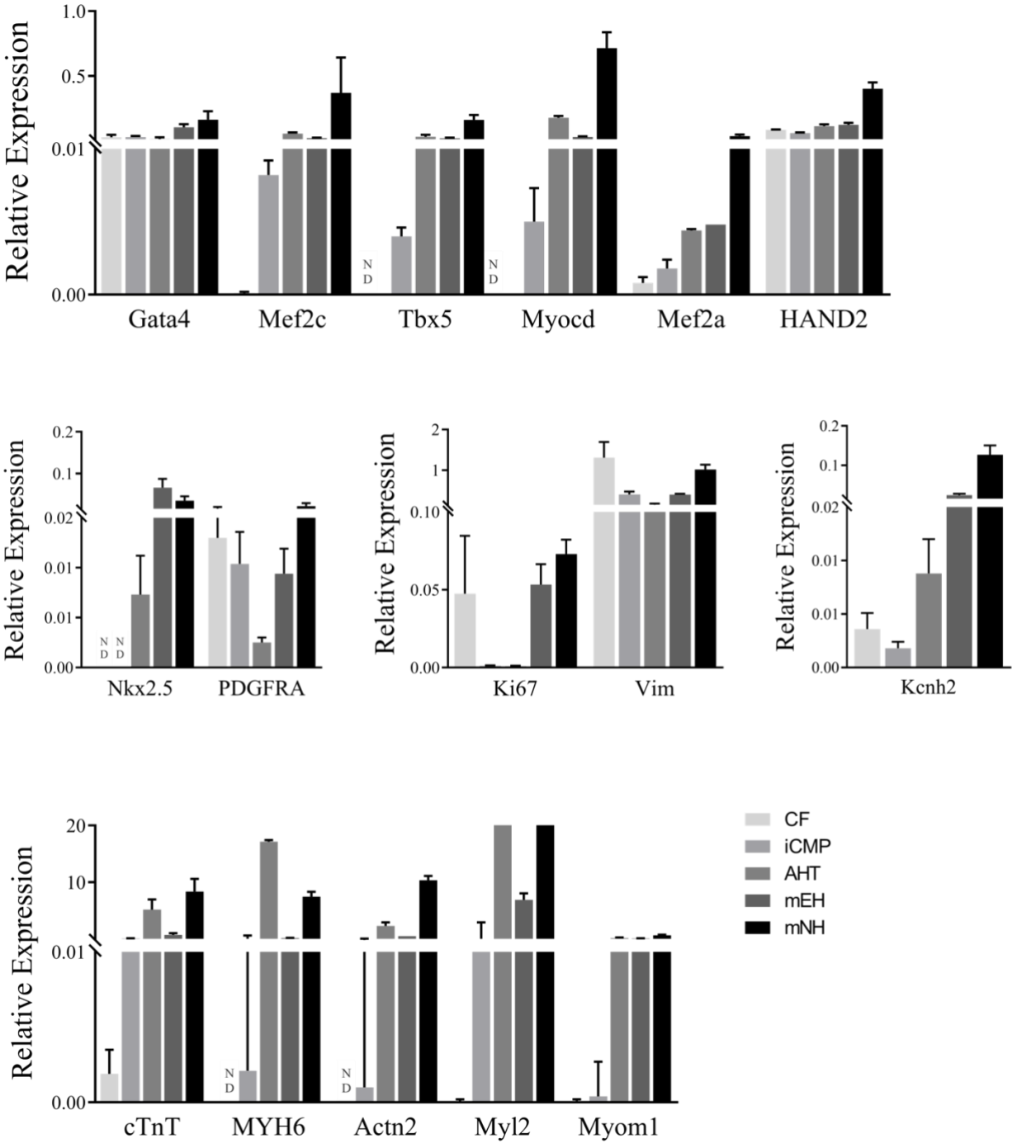

Figure 27**:** Gene expression analysis by qPCR in iCMPs, CFs, mouse adult heart, mouse embryonic heart and mouse neonatal heart tissue. transcription factors: Gata4, Mef2c, Mef2a, Tbx5, Myocd and HAND2; progenitor markers: Nkx2.5, PDGFRa; non-myocyte and proliferation markers: VIM and Ki67; and Cardiac sarcomeric and contractile genes: cTnT, Myh6, Myl2, Actn2, Myom1.

9.6. Long term expansion of iCMPs does not affect proliferation while maintaining a stable phenotype

To monitor proliferation and phenotype stability of iCMPs after sorting was monitored in order to determine the ability to generate large scale cell products and to show the regenerative potential long term. iCMPs were maintained in culture over serial passages while cell growth and cardiac gene expression were assessed. These MYH6/7 positive cells were highly viable as determined by trypan blue staining and cell counting. The iCMPs proliferated up to 57X fold (Figures 28A), that is 22 population doublings in 28 days. With a starting cell number of 50,000 cells we could obtain 3x10^11 cells in 28days (Figures 28B). They maintained a high degree of similarity in growth rate between passages. However, all experiments with these cells were performed at passages 2-4.

MB-based analysis of the iCMPs 1 week after sorting revealed that the MYH6/7+ population dominated the total population (more than 80%). However, over time the positive fraction decreased to about 40-50% in week 2. CF contamination could be one reason, which could be reduced with G418-based antibiotic selection. However, the effect was relatively low (about 10%) to a purity of 65% (Figures 29 and 30). Thus, the contribution of CF impurity was low.

Cells losing iCMP phenotype could be another possible reason for this. Therefore, we sought to counteract this by supplementing the iCMPs with factors that support the maintenance of a cardiomyogenic phenotype. We tested a set of established cardiac specification factors - Ascorbic acid, BMP4+FGF, BMP4+FGF+VEGF and VEGF+FGF. Ascorbic acid addition to iCMP culture medium CRM showed increased MYH6/7 expression in week 2 (99.5%) as compared to the addition of BMP4+FGF (65%), BMP4+FGF+VEGF (74%) or VEGF+FGF (76%) and this trend continued to week 3 of iCMPs in culture (Figures 29 and 30).
Ascorbic acid was therefore determined most effective in preserving a stable iCMP phenotype.

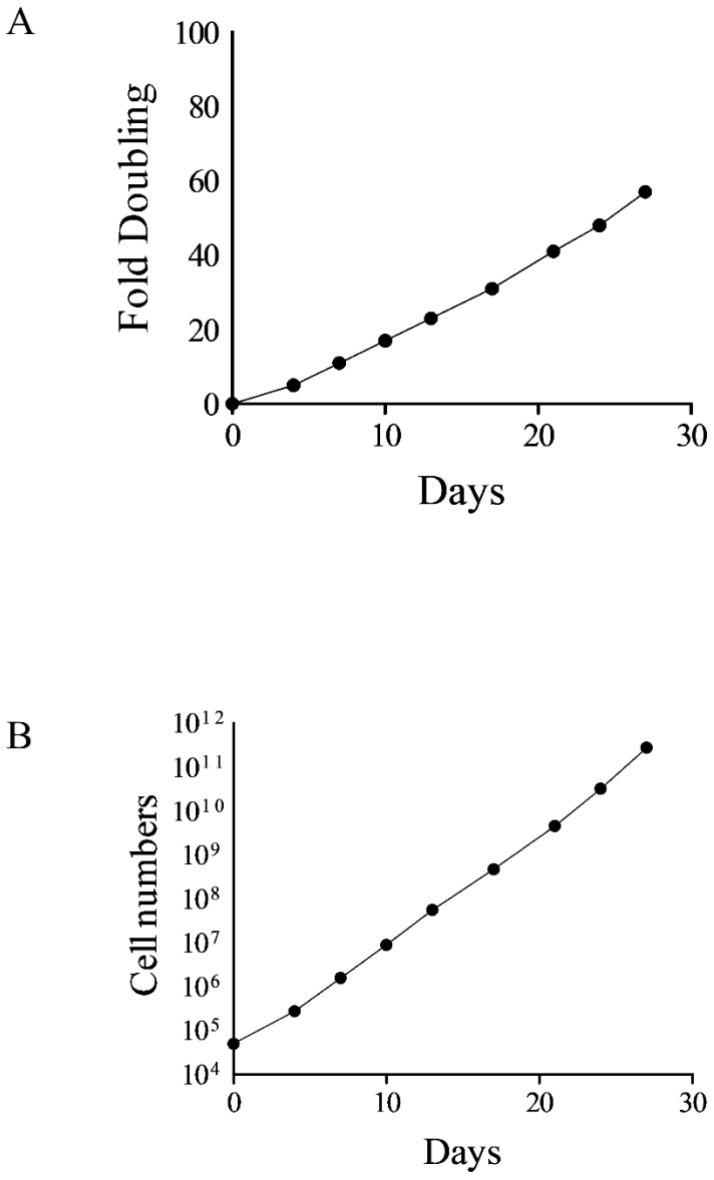

Figure 28**:** Cell proliferation – iCMPs post sorting were highly viable they proliferated **(A)** up to 57X folds in 28 days and **(B)** up to 3x10^11 cells starting from 50,000 cells in 28 days.

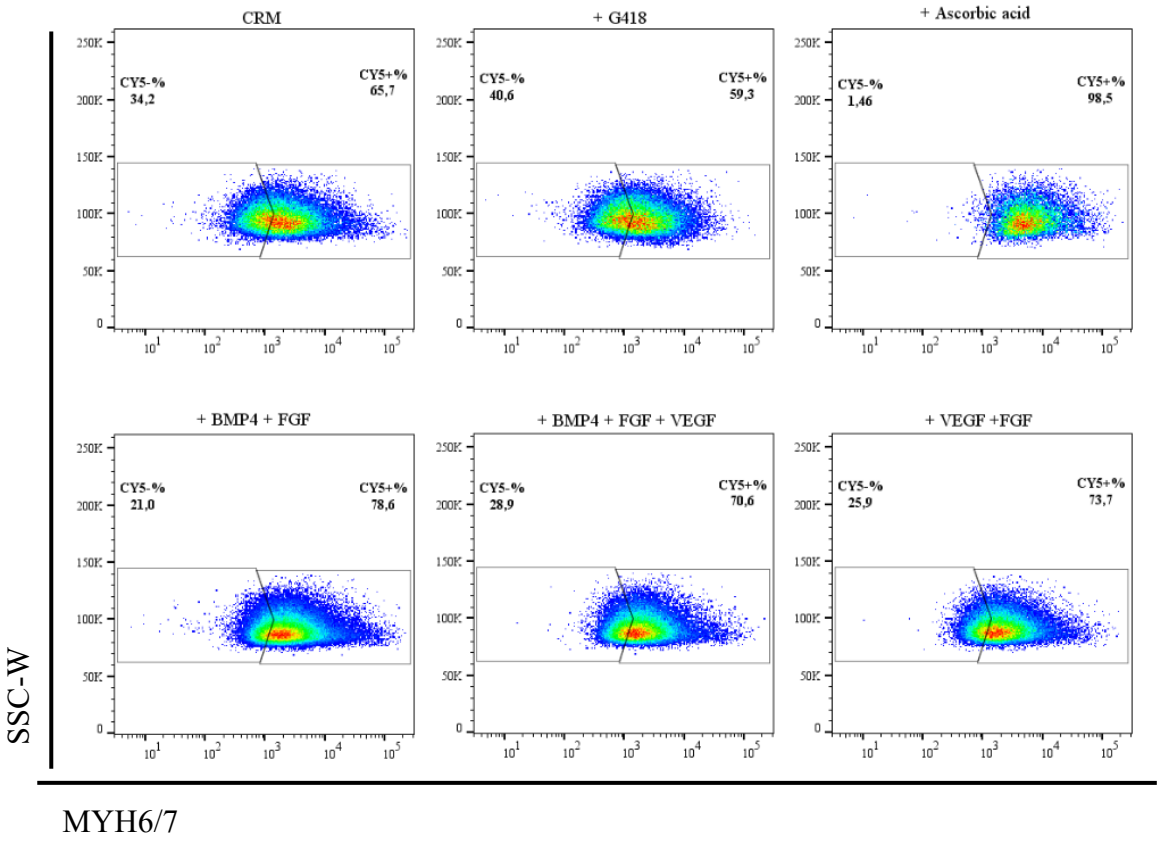

Figure 29**:** Stability of iCMPs 2 weeks after sort: Reduced MYH6/7 expression was observed in iCMPs 2 weeks after sort and when cultured in CRM. Addition of ascorbic acid was seen to best preserve a stable iCMP phenotype as seen by MYH6/7 expression determined by FACS.

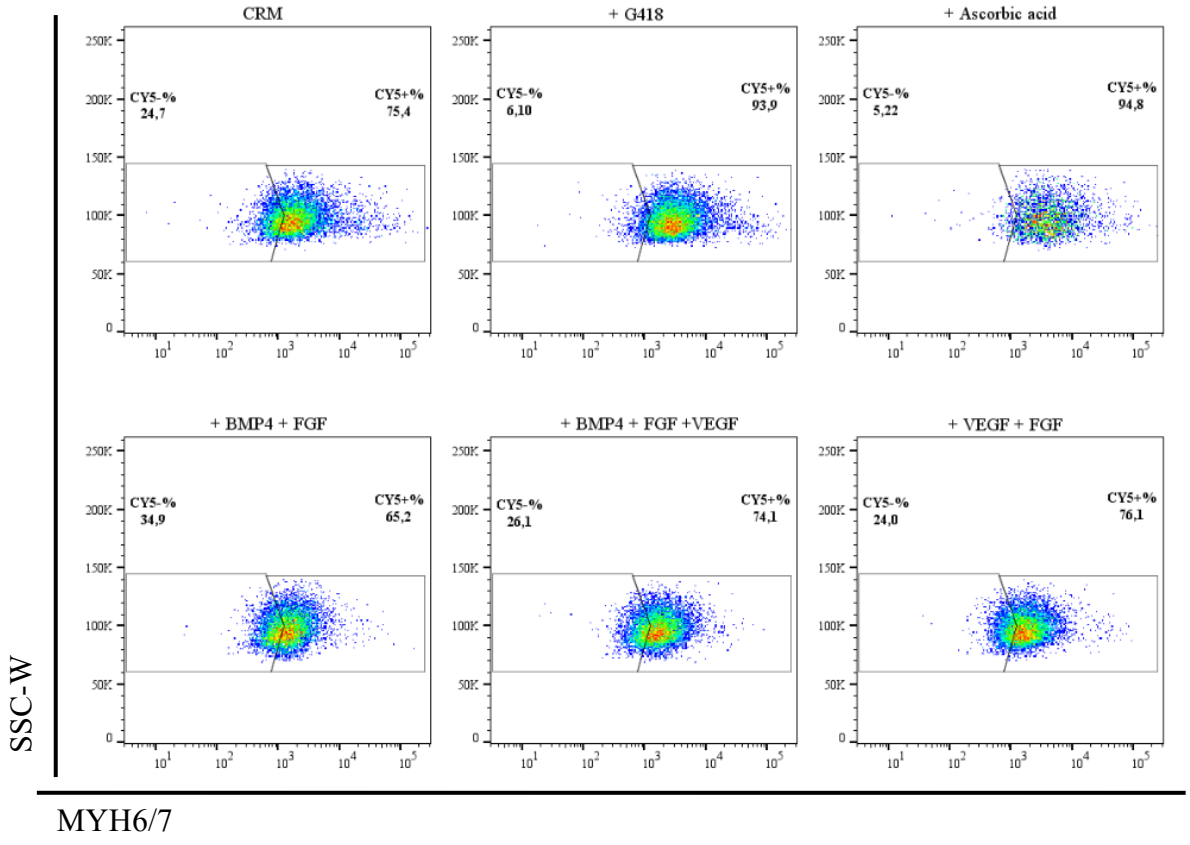

Figure 30**:** Stability of iCMPs 3 weeks after sort: Ascorbic addition helped preserve a stable iCMP population long term as observed by the MYH6/7 expression determined by FACS.

9.7. Differentiation potential of iCMPs

We have a cardiac progenitor population that can proliferate, but if true regeneration is to take place, these cells must be able to differentiate into cardiomyocytes. Therefore, to investigate the differentiation capacity of iCMPs, a couple of established CPC differentiation strategies were explored. iCMPs theoretically have the potential to differentiate into any of the three main cell types found in the heart – cardiomyocytes, smooth muscle cells, or endothelial cells. Thus, we investigated the expression of proteins associated with each of these cell type.

iCMPs, when maintained in serum-free differentiation medium (SFDM) for 20 days with the initial supplementation of the Wnt inhibitor IWP2, showed a slight change in morphology and very low cardiac marker expression. After 20 days in culture with SFDM cells showed smooth muscle marker expression (αSMA), but no endothelial marker (CD31) expression (Figure 31). Similarly, iCMPs when maintained in cardiac differentiation medium (CDM) for 20 days with the initial supplementation of the Wnt inhibitor IWR1, showed smooth muscle marker (αSMA) expression (Figure 31).
Additionally, we chose to investigate the influence of cardiac extracellular matrix cECM in combination with differentiation media on our iCMPs. Our lab (68, 69) has chosen to investigate the use of cECM as a hydrogel and therefore has developed a method for producing a cECM-based coating using limited chemical processing. Its use as a hydrogel can create a more cardiac-specific environment to maintain iCMP phenotype or facilitate differentiation. cECM maintained low cardiac marker expression and showed αSMA expression in both SFDM and CDM, but no CD31 expression (Figure 32).

Apart from Wnt inhibition, 5-Azacytidine and TGFß are known to promote cardiomyogenic differentiation in ESCs and are critical for the expression of cardiac-specific markers. It has been shown that CPC when cultured in differentiation medium (DM) and treated with 5-Azacytidine and TGFß, resulted in beating CMs (62). iCMPs when treated similarly cells showed change in morphology, from rounded epithelial patterns to rod shaped, long straited cells as seen in immunofluorescence staining. Cells expressing the cardiac marker α-actinin showed a dense sarcomeric expression pattern. cTnT and myosin positive cells showed formation of sarcomeric striations. The cells also expressed smooth muscle cells marker αSMA but no endothelial marker

CD31 expressions were seen (Figures 33 and 34). No spontaneous contraction was observed up to 20 days in differentiation medium.

Additional mechanical, electrical and paracrine stimulation was provided to proliferative iCMPs to induce differentiation, by culturing them with either iPSC-derived CMs or mouse neonatal α-MHC-mCherry CMs. The iPSC-CMs were labeled with the cell labeling dye red to distinguish them from the iCMPs. In co-culture set up beating patches of red and green cells were observed (Supplemental Video) via time-lapse imaging. However, despite cell labelling, it was not clear if the iCMPs were contracting themselves or if it was moved by the contracting CMs. The results were inconclusive and demand further research.

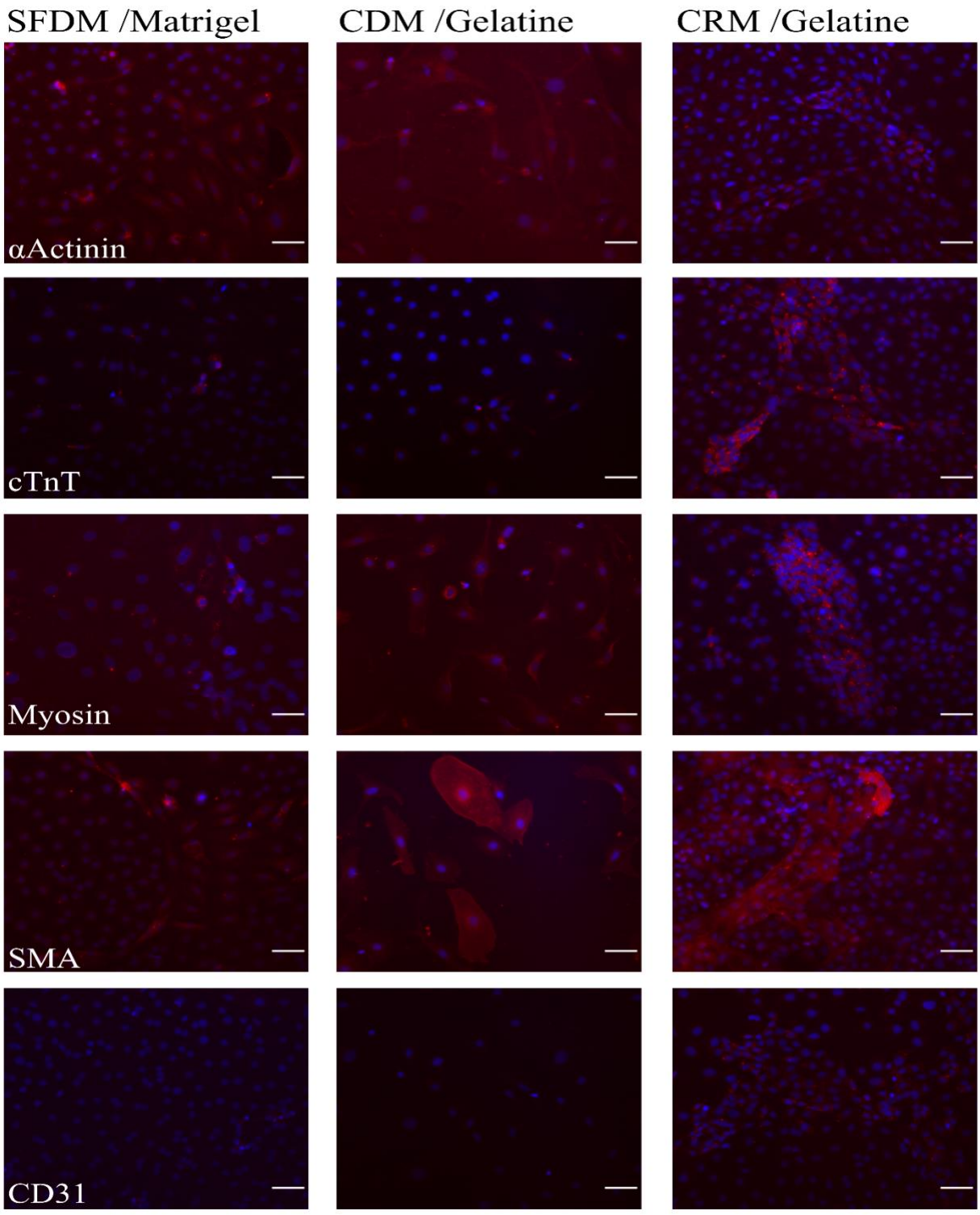

Figure 31**:** Differentiation potential of iCMPs: iCMPs cultured for 20 days on Matrigel in SFDM, on gelatin in CDM, and on gelatin in CRM showing low levels of expression of cardiac markers α-actinin, cTnT and Myosin; smooth muscle marker αSMA; and no endothelial marker CD31 (red). Cells were stained with DAPI (blue) to label the Nuclei. Scale bars = 500µm.

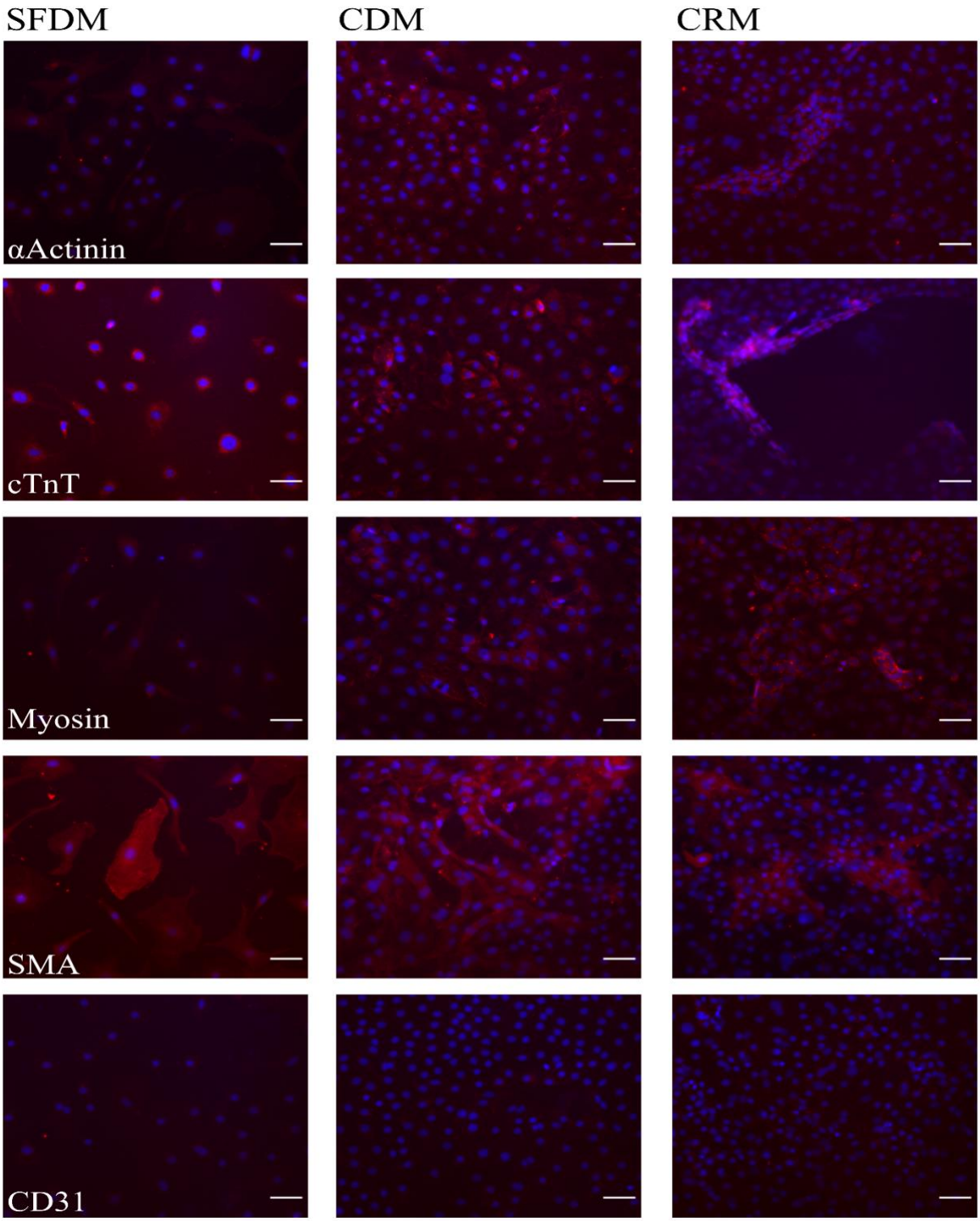

Figure 32**:** Influence of cECM on iCMPs: iCMPs cultured for 20 days on cECM in SFDM, CDM, and in CRM showing low expression of cardiac markers α-actinin, cTnT and Myosin; smooth muscle marker αSMA; and no endothelial marker CD31 (red). Cells were stained with DAPI (blue) to label the Nuclei. Scale bars = 500µm.

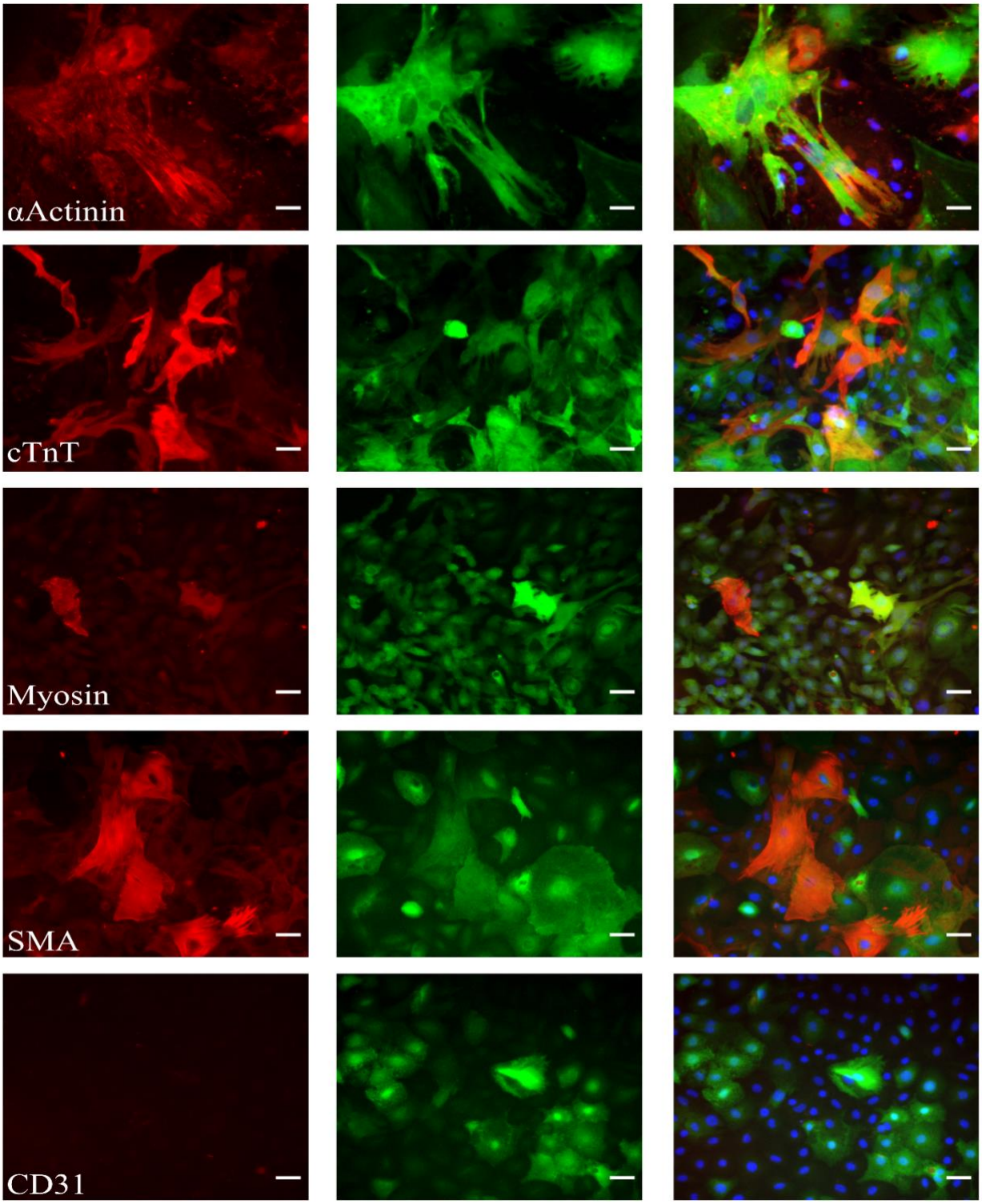

Figure 33**:** iCMP differentiation with 5-Azacytidine and TGFß supplement: Cells showed a dense sarcomeric expression pattern of cardiac markers α-actinin, cTnT and myosin, and smooth muscle marker αSMA (red), DAPI (blue) to label the cell nuclei and GFP (green). No endothelial marker, CD31 expression was observed. Scale bars = 50µm.

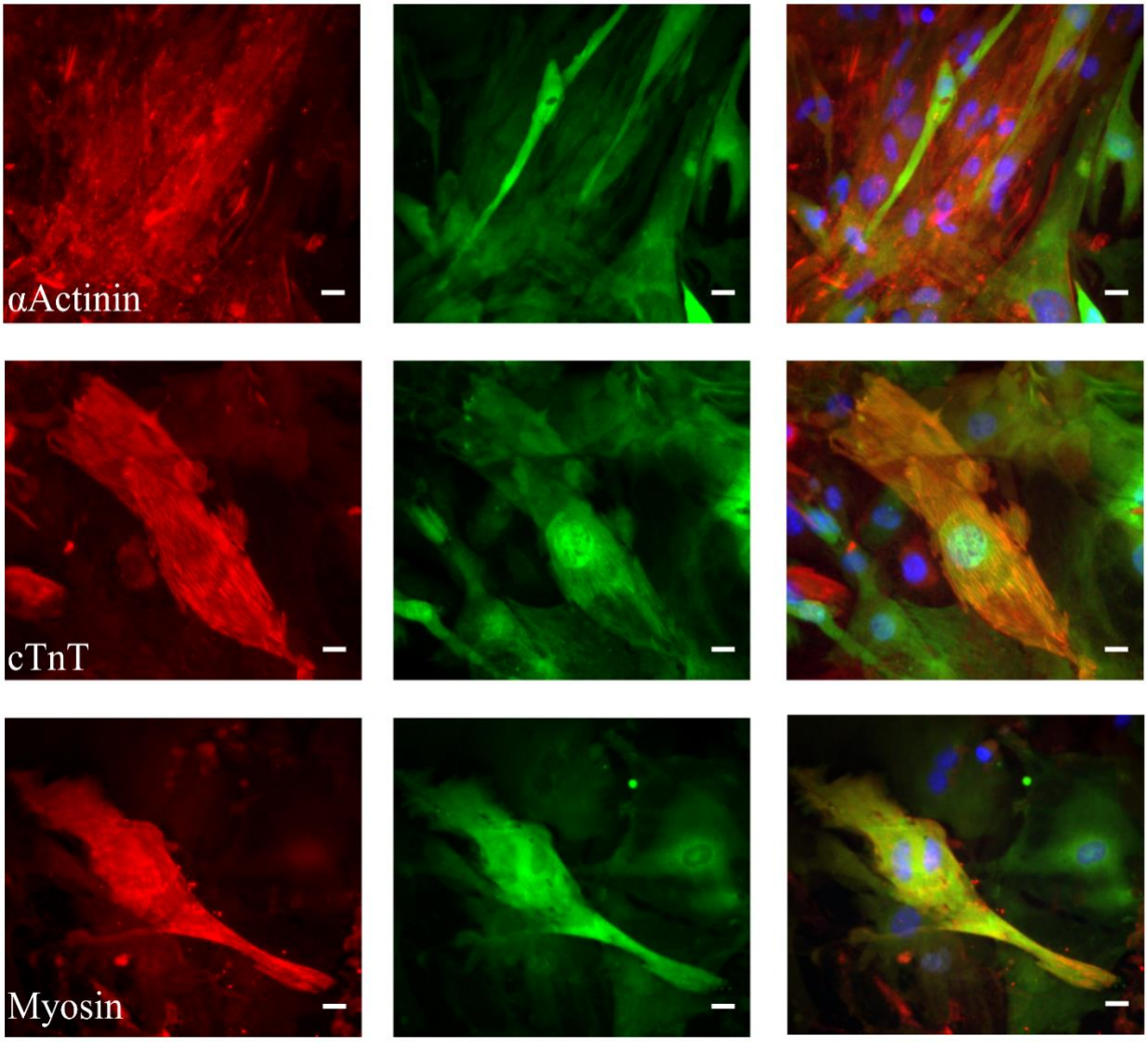

Figure 34**:** iCMP differentiation: Immunofluorescence images of iCMPs at a 40X magnification showing change in morphological characteristics. Cardiac markers α-actinin, cTnT, Myosin, smooth muscle markers αSMA (red), DAPI (blue) to label the cell nuclei and GFP (green). No CD31 expression was observed. Scale bars = 20µm.

9.8. Transplantation of iCMPs into infarcted heart improves cardiac function

The ultimate goal of this study was to evaluate the functional and regenerative potential of the iCM precursor cells in the native heart environment after injury. Therefore, after demonstrating that iCMPs expanded long term and maintained a cardiac committed phenotype, we wished to extend the approach to the native heart environment.

To do so, stocks of iCMPs were produced in large scale. iCMPs, after reprogramming and sorting, were expanded to produce cell doses of 500,000 cells/mouse. eGFP-CFs were produced and treated in ways similar to the iCMPs except for antibiotic selection. eGFP-CFs were obtained by infecting CFs with LeV eGFP and cell-sorted based on their GFP signal. 90% of the infected cells were GFP+ (Figure 35). After sorting the eGFP-CFs were expanded to produce the required cell doses of 500,000 cells/mouse. Cells were trypsinized, thoroughly washed and resuspended in PBS for intramyocardial injections. All cells used were of passage 3-5.

MI was induced by ligating the left anterior descending artery. Immediately thereafter, the mice received intramyocardial injections with either iCMPs or eGFP-CFs or PBS. Cardiac function (Table 4) was monitored and calculated by echocardiography at week 2, 4 and 6 after treatment.

The echocardiography analysis showed improved left ventricular function in iCMP-treated animals compared to the controls eGFP-CFs and PBS. The left ventricular ejection fraction (LVEF) was improved as early as 2 weeks after iCMP injection and was maintained until weeks 6 in comparison to the controls. LVEF of iCMP-treated animals were 38% ± 6.9, whereas the PBS treatment had an LVEF of 20% ± 4.2 and eGFP-CF treatment had an LVEF of 17% ± 4.6 at week 6 (Figure 36 and 37). Left ventricular fractional shortening (LVFS) of the short axis of the heart was 22% ± 3 for iCMPs, 16% ± 2 for PBS and 9% ± 2.2 for eGFP-CF-treated animals at week 6 (Figure 38). The sham groups had an LVEF of 66% ± 4.4 and LVFS of 36% ± 2.4.

Supporting the LVEF and LVFS outcome, an improvement in stroke volume (SV) was observed in mice group treated with iCMPs compared to the control groups (Figure 39). SV of iCMP-treated animals at week 6 were 47% ± 6.8, while the PBS treatment had an SV of 29% ± 6 and eGFP-CF treatment had an SV of 22% ± 3.8.

Additionally, there was less dilation of the hearts when treated with iCMPs as seen in EDV and ESV plots (data not shown). In line with these outcomes, an improvement in cardiac output of the heart was observed showing, 20% ± 3.4 for iCMPs, 13% ± 2.6 for PBS and 11% ± 1.6 for eGFP-CF-treated animals at week 6 (Figure 40). Besides, no abnormal growth was observed up to 6 weeks in the mice hearts.

These results strongly indicated that iCMPs can improve and restore left ventricular function and attenuated remodeling after ischemic myocardial injury.

Echocardiography read outs	
Left ventricular Ejection fraction (LVEF)	Percentage of blood leaving the heart = SV/EDV * 100
Left ventricular Fractional shortening (LVFS)	The fraction of any diastolic dimension that is lost in systole = end-diastole dimension minus end-systole dimension (EDD-ESD)
Left ventricular wall thickness (LVPWd)	Left ventricular posterior wall thickness at end-diastole
Stroke volume (SV)	Volume of blood pumped out = end-diastole minus end-systole
Cardiac output (CO)	Volume blood pumped out per minute
End diastole volume (EDV)	Volume of blood in the right and/or left ventricle at end load or filling in
End systole volume (ESV)	Volume of blood in a ventricle at the end of contraction and the beginning of filling.

Table 4**:** Echocardiography readouts.

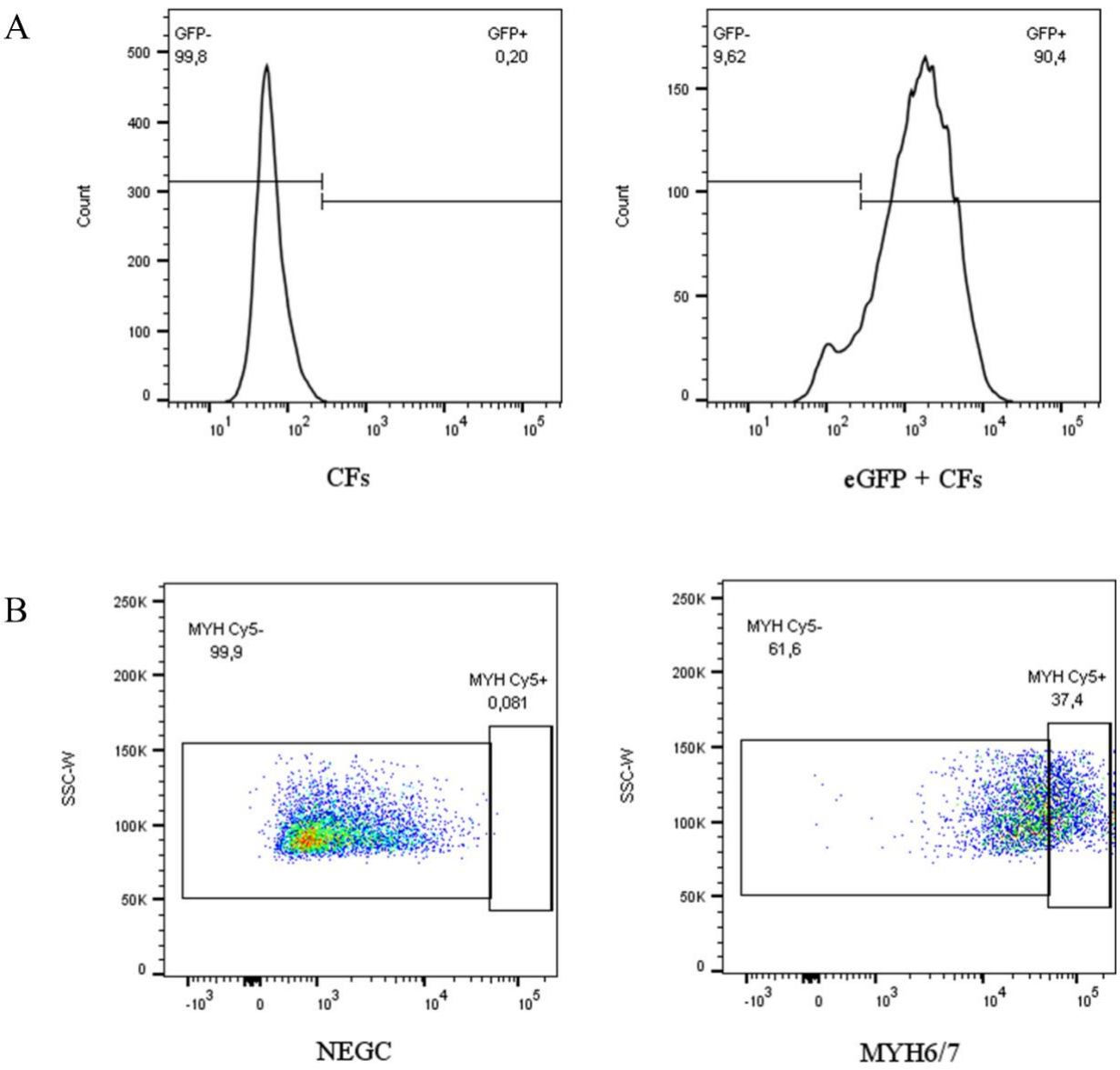

Figure 35**:** Cell preparation for animal experiments: **(A)** Sorting of eGFP-CFs based on their GFP signal post transduction of CFs with LeV-eGFP, 90% of the cells were positive for GFP. **(B)** MB-based sorting of iCMPs 2 weeks after infection with lentiviral cocktail GMTMy yielded 37% MYH6/7 positive cells.

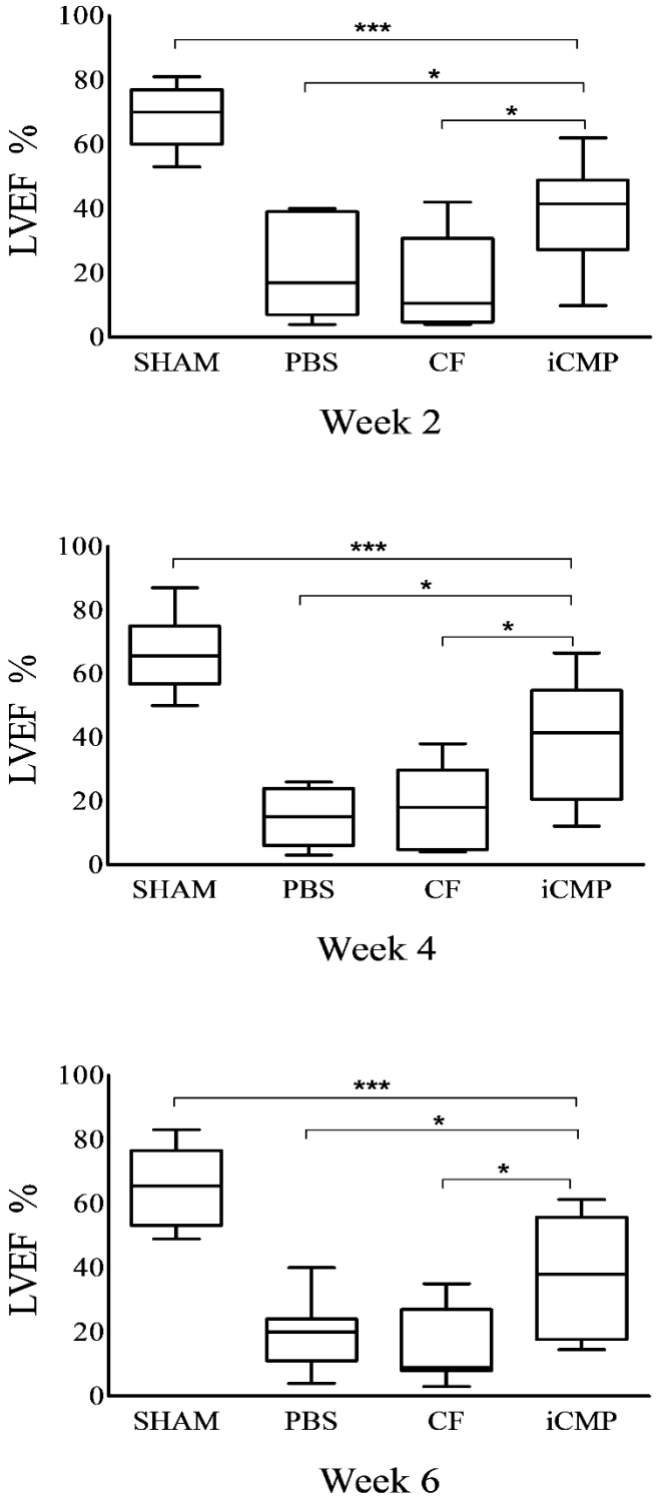

Figure 36**:** Left ventricular ejection fraction: iCMP treatment after MI in a mice model, showed improvement in left ventricular ejection fraction as seen at week 2, 4 and 6 compared to PBS and eGFP-CFs. The boxplots indicate interquartile range (box), median (line), range (min to max) and outliers (+/−). ANOVA, Bonferroni posttest, n=6–10.

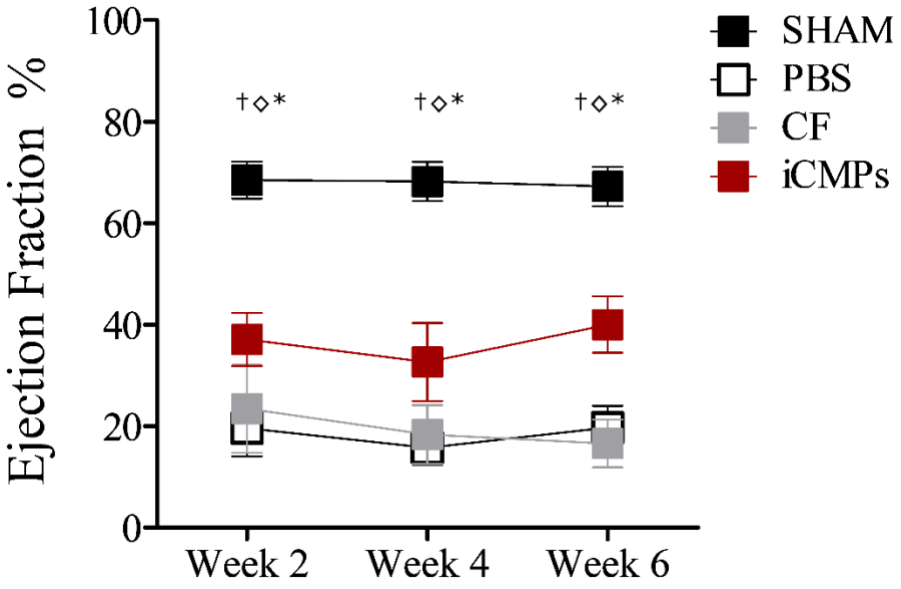

Figure 37**:** Left ventricular ejection fraction: Left ventricular ejection fraction shown overtime at week 2, 4, and 6 as mean ± SEM, * ◊ P<0.05 iCMP vs. CF/PBS, + P<0.001 iCMP vs. Sham. ANOVA, Bonferroni posttest, n=6–10.

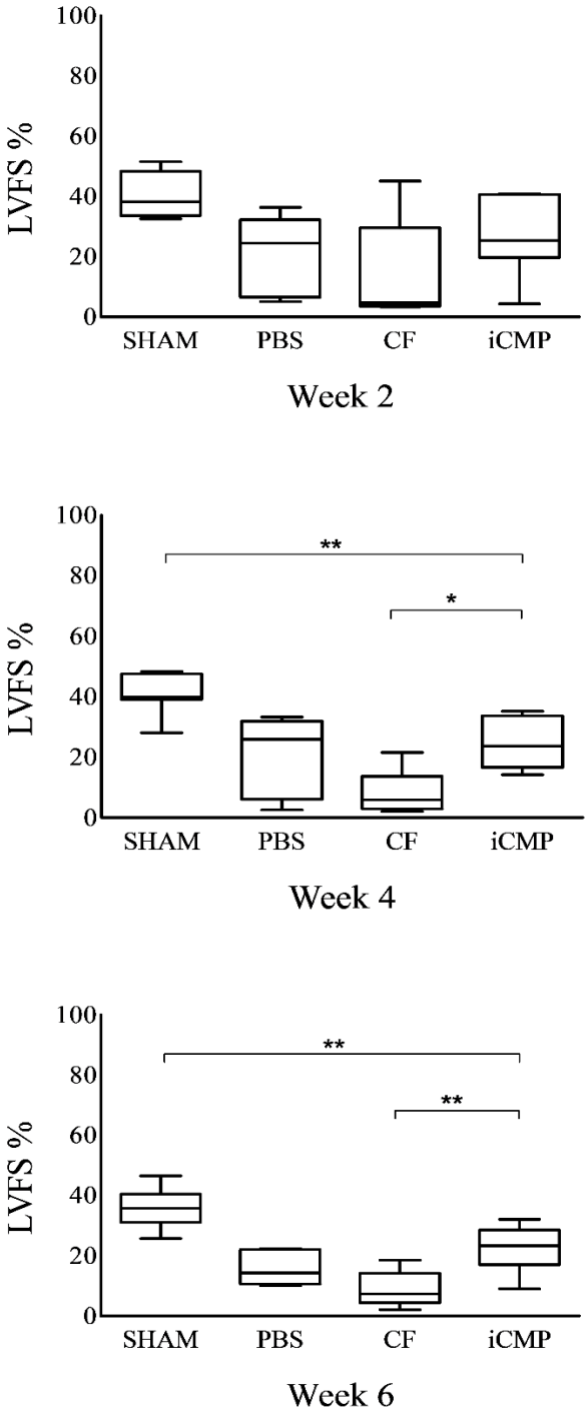

Figure 38**:** Left ventricular fractional shortening: iCMP treatment after MI in a mice model, showed improvement in left ventricular fractional shortening as seen at week 2, 4 and 6 compared to PBS and eGFP-CFs. The boxplots indicate interquartile range (box), median (line), range (min to max). ANOVA, Bonferroni posttest, n=6–8.

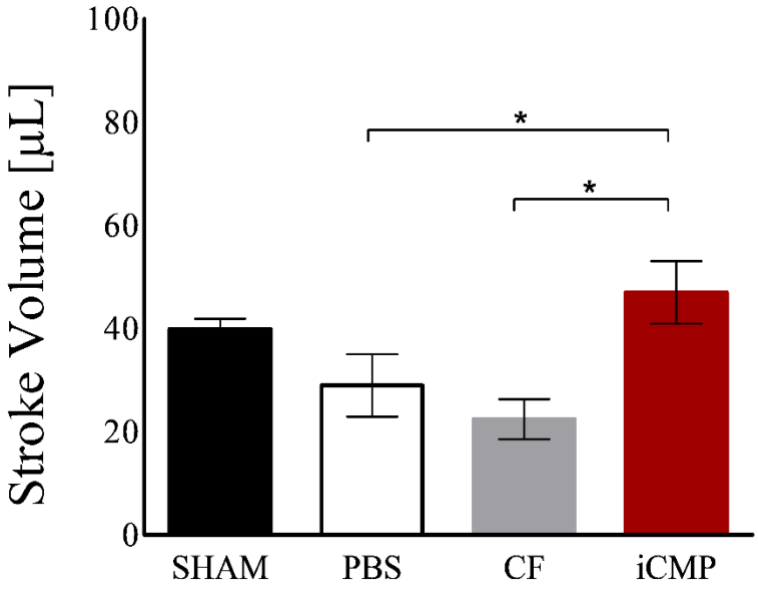

Figure 39**:** Stroke Volume: An improvement in stroke volume was observed in mice treated with iCMPs by week 6 compared to PBS and eGFP-CFs. Data shown as mean ± SEM ANOVA, Bonferroni posttest, n=6–10.

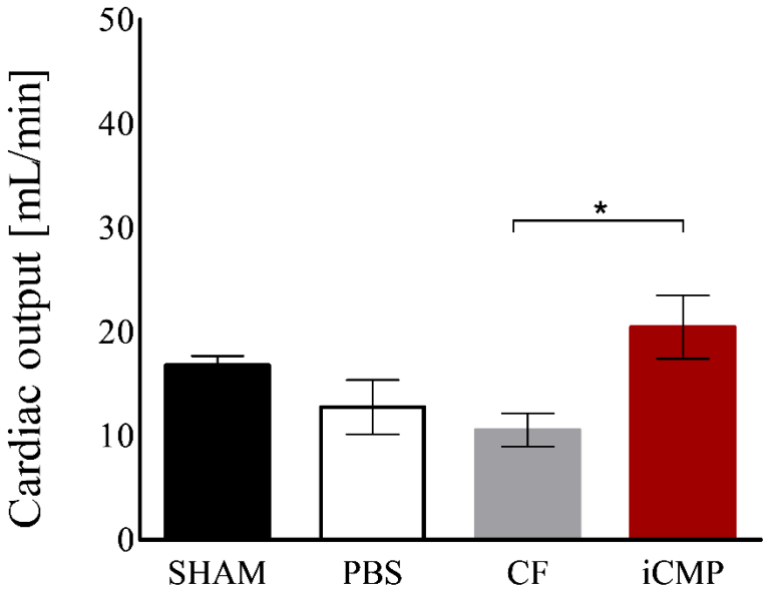

Figure 40**:** Cardiac output: Cardiac output observed in mice treated with iCMPs, PBS, CFs or SHAM at week 6. An improvement in CO was observed in iCMPs compared to CF and PBS groups. Data shown as mean ± SEM, * P≤0.05, iCMP vs. CF. ANOVA, Bonferroni posttest, n=6–10.

10. DISCUSSION

Improving direct cardiac reprogramming

iCM have come across as an appealing CM-like cell for disease modeling, drug testing and also potential therapeutic application in patients to repair or regenerate the injured heart directly through the formation of newly transplanted tissue. When Ieda et al. first reported direct cardiac reprogramming with GMT in 2010, the reprogramming efficiency of generating fully reprogrammed functional iCMs although promising was very low, few iCMs (0.01–0.1% of total cells) showed spontaneous contractions. Huge efforts are underway ever since, to improve the reprogramming efficiency, including modifications of stoichiometry, transcription factors, small molecules, micro-RNAs and epigenetic factors (*3-24*). Wang et al. generated polycistronic vectors, with a possible combination of the three factors in a single transgene to test modifications of stoichiometry. Their findings revealed that a high level of Mef2c and low levels of Gata4 and Tbx5, enhanced cardiac reprogramming, consistent to the findings by Hirai et al. that increasing the transcriptional activity in Mef2c is critical for successful reprogramming for mature iCMs (31, 37). Besides TFs and delivery vectors, a combination of specific microRNAs (miR-1, miR-133, miR-208, and miR-499) and silencing of fibroblast signatures was tested (29, 36). However, despite all these efforts iCM reprogramming efficiency were still low. Moreover, mature iCMs have little or no proliferative capacity, thus, making the regeneration of the heart a difficult process, as the low number of iCMs are insufficient to regenerate heart tissue.

We are therefore in need of a more clinically relevant cardiomyogenic cell type that,

- Has the ability to proliferate
- Is cardiac committed - therefore can generate functional cardiac muscle and vasculature
- Is safe and doesn’t create tumors
- Improves heart function after injury

In this study, I show that - GMT along with Myocd (My) reprogrammed the cardiac fibroblasts towards a phenotype of proliferative, induced cardiomyocyte precursors (iCMPs). The cTnT expressions were strikingly high as seen according to RNA-Seq and according to proteins levels. We were able to purify the iCMPs at high efficiency and specificity from reprogramming cultures with the innovative and clinically compatible MB-based purification system.

A distinct feature of this iCMPs is their ability to proliferate while maintaining similar morphology and gene expression pattern. For cell-based therapies, it is highly desirable to generate expandable sources of committed cells. During iCM reprogramming cell proliferation is suppressed and CM differentiation-specific genes are activated (70). In contrast, global transcriptome analysis and protein expression patterns revealed that iCMPs represent an intermediate state of cardiomyocyte development with preserved mitotic capacity as well as cardiomyogenic lineage commitment.

Different kinds of cardiac progenitor populations have been identified to date, such as Flk1+, Mesp1+, Isl1+, Sca1+, and Nkx2.5+ (71-76). The iCMPs however unlike all other CPCs express a couple of progenitor markers such as Cxcr4, Flk1, Mesp1, PdgfRa and Nkx2.5. These results indicate that our iCMPs similar to the endogenous CPCs population are a mixed cell pool expressing multiple cardiac committed progenitor markers, which could be beneficial for in vivo cell transplantation and cardiac regeneration.

It has been demonstrated that cardiac progenitor cells (CPCs) represent effective cell-based therapy for MI. However, endogenous CPCs are not sufficient for regeneration after injury and the procedure of harvesting for expansion are invasive and could cause more injury to patients. The generation of induced CPCs or iCMPs thus seems attractive. Two groups have reported on the induction of expandable CPCs from mouse fibroblasts with the combination of transcription factors and small molecules (Table 5). Zhang et al. found that the induced CPC (Flk1+ PdgfRα+ population) could be generated from mouse fibroblasts with overexpressing Sox2, Klf4, Oct4, and c-Myc. Lalit et al. adopted a straightforward approach to reprogram fibroblasts into Nkx2.5+ iCPCs through lineage-specific transcription factors Mesp1, Tbx5, Gata4, Nkx2.5, and Baf60c. However, one of the primary problems of long-term cell culture of transdifferentiated cells is the overgrowth by contaminating fibroblasts and residual fibroblast identity. Zhang et al, reported BMP4, Activin A, CHIR99021 (GSK3beta inhibitor) and SU5402 (FGF, VEGF, and PDGF inhibitor) stimulation for stable maintenance. While Lalit et al. state that the addition of (leukemia inhibitory factor) LIF and BIO stimulation were necessary for stable expansion and maintenance of iCPCs.

In case of the iCMPs MB-based FACS sorting after reprogramming circumvented fibroblast contamination and growth. Additionally, I found that ascorbic acid supplementation maintained a pure and cardiac committed proliferative iCMPs population. Ascorbic acid is and has been used

in several studies proving its role in cardiogenesis crucial. Ascorbic acid induces pluripotent stem cells at different phases of differentiation, it induces cardiac progenitor specification and proliferation and it is known to induce cardiomyocyte maturation at both the structural and functional levels (15, 48, 77).

Reference	**Zhang et al. (60)**	**Lalit et al. (78)**	**This study**
Starting cell type	MEF, TF	CF, TF	CF
Transcription factors	Sox2, Klf4, Oct4, c-Myc	Mesp1, Tbx5, Gata4, Nkx2.5, Baf60c	Gata4, Mef2c, Tbx5, Myocd
Delivery method	CASD-lineage conversion	LeV	LeV
Chemicals or specification factors	BMP4, Activin A, CHIR99021, SU5402 (BACS)	LIF, BIO	Ascorbic acid
CPC Marker expression	Flk1, PdgfRα	Nkx2.5, Irx4	Cxcr4, Flk1, Mesp1, Nkx2.5
CM Marker expression	-	-	cTnT, Myosin, α-actinin
Purification	Flk1+ PdgfRα+ based FACS sorting	Nkx2.5+ FACS sorting	Molecular beacon Myh6/7 based FACS sorting
Proliferation	$>10_{10}$ fold expansion in 18 passages	-	57X fold, 22 population doubling in 28days
Differentiation characterization	Action potential, Calcium transient, Contractility	CM marker expression	CM marker expression with sarcomeric striations
Therapeutic application in an MI model	Improved heart function	Improved survival	Improved cardiac function – LVEF, LVFS, SV and CO

Table 5**:** Generation of cardiac progenitor and precursor cells via direct reprogramming

Modification of signaling pathways and environmental cues for CM differentiation

iCMPs with the addition of 5-Azacytidine and TGFß induced increased expressions of cardiac and contractile genes such as cTnT and α-actinin, additionally, they showed an assembly of sarcomeric bundles on the protein level. Which is in line to studies by Goumns et al. that 5-Azacytidine and TGFß enhance cardiomyocyte differentiation of cardiomyocyte progenitor cells (hCMPCs) from human heart tissue and resulted in functional beating CMs (62, 79).
Consistent with this Gearhart et al. showed that inhibition of fibroblast-related signaling pathways, such as transforming growth factor-β (TGFβ), enhanced cardiac reprogramming efficiency and maturation through silencing of fibroblast signatures (46).

In our hands, an effort to obtain mature contracting iCMs from iCMPs using Wnt inhibition as reported by Zhang et al. and Li et al. (60, 61) was not successful. A possible factor influencing the maturation of iCMPs to iCM is the timing of Wnt inhibition. Previous work examining the effects of Wnt/β-catenin signaling on mouse ES cell differentiation into cardiomyocytes deduced that this pathway exhibits developmental stage-specific, biphasic, and antagonistic effects on cardiomyogenesis and hematopoiesis/vasculogenesis (16, 60).
Activation of the Wnt/β-catenin pathway in the early phase of development enhanced ESC differentiation into CMs, but the reverse is observed in the late phase after embryonic body formation (80). The timely activation and deactivation of particular genes and signaling molecules have repeatedly been shown to have a strong influence on cell fate decisions during development. Therefore, it may be necessary to refine the timing and duration of Wnt inhibition to efficiently promote cardiomyocyte differentiation.

No spontaneous contraction was observed up to 20 days in the differentiation conditions. However, in an in vitro heart model such as the co-culture set up beating patches of red and green cells were observed. Thus indicating that upon stimuli, the iCMPs could contract. It would be interesting to investigate this further.

Environmental cues, such as extracellular matrix (ECM), 3D hydrogels and scaffolds are also important for cardiac maturation. There are wide varieties of hydrogel materials and delivery methods currently in use and each approach carries with it its advantages and disadvantages. For

example, studies have shown that using a microgroove substrate or using a 3D fibrin hydrogel culture enhances reprogramming efficiency (81, 82).

We chose to investigate the influence of cECM based-hydrogel in combination with differentiation media on our iCMPs. Its use as a hydrogel can create a more cardiac-specific environment to maintain iCMP phenotype or facilitate differentiation. In our experiments, the use of cECM maintained cardiac marker expression on protein level indicating its supportive effect on the differentiation. Our lab has previously shown that cardiac lineage commitment was favored when ESCs or iPSCs were grown on cECM (83). In the future, it would be interesting to investigate the influence of cECM on transduction and reprogramming efficiency as well, proving a cardiac environment from the start.

The iCMPs are a heterogeneous population of cells that express cardiac progenitor genes such as Cxcr4, Flk1, Mesp1, Nkx2.5; cardiac mesoderm genes such as Gata4, Tbx5, Tbx20, Mef2c, Mef2a, HAND2; and mature cardiac genes such as cTnT and α-actinin as seen in immunofluorescence staining and RNA-Seq. This could also explain why at present, none of the Wnt differentiation stimuli singularly is sufficient to induce complete maturation equivalent to that of adult CMs. A combination of stimuli may bypass the problems associated with iCMP differentiation.

Nevertheless, cardiomyocytes are not the only cell type required for heart regeneration. Cardiogenesis requires the generation of diverse muscle and nonmuscle cell lineages: atrial and ventricular cardiomyocytes, smooth muscles cells, endothelial cells, cells of the coronary arteries and veins, endocardial cells, valvular components, and connective tissue. One of the major sources of heart cell precursors in the embryo is the cardiogenic mesoderm. The cardiogenic mesoderm, with distinct contributions to the mature heart, ultimately forms the majority of the working myocardium in the ventricular and atrial chambers (84).

Cardiac reprogramming in vivo

To examine the efficiency of iCMPs for cardiac regenerative medicine, we tested the potency of iCMPs in an adult mouse heart. iCMPs were transplanted intramyocardialy into a mice model of MI, resulting in preservation of cardiac function. iCMP treatment showed improvement in LVEF and LVFS whereas PBS and CF treated groups showed a decline. Similarly, iCPC transplantation studies by Zhang et al. and Lalit et al. have shown improvement in heart function and improved survival after treatment. With iCMPs treatment cardiac functional improvement was seen at an early stage (2 weeks) and was maintained long term in mice after acute myocardial injury (6 weeks). This improvement may be a result of iCMP engraftment, differentiation to CMs to restore heart contractility, contributing to blood-vessel formation and integration into surrounding tissues (84). Similarly, Zhang et al. showed that iCPC induced a sudden increase in heart function as early as 3days after treatment, which then reduced at week 2 up to week 4 and was then maintained consistent up to week 12.

Other than LVEF and LVFS our results showed an improvement in LVPWd and CO as compared to the control groups. However, the CO values were slightly higher in iCMPs than that of SHAM. As part of the tissue dies and loses function after MI the remaining heart tissue overcompensates resulting in hypertrophy, which might explain the iCMPs CO.

In vivo differentiation may have been possible due to additional environmental cues such as ECM and/or secreted proteins, exosomes or paracrine effect. The discovery of cardiovascular precursor cells in mammalian embryos, human hearts, as well as in intermediate stages of differentiation of ESCs and iPSCs offers exciting opportunities in the field of cardiac translational medicine. Cardiovascular precursors offer an advantage over iCMs, as they might be able to proliferate and differentiate into diverse mature cardiovascular lineages, thus contributing to both remuscularization and revascularization (84).

Ieda et al. in their first study transplanted GMT overexpressing CFs one day after viral transduction and showed that within 2 weeks they were able to detect the injected cells and these cells also expressed α-actinin and had sarcomeric structures; while no functional improvement was reported (27). In contrast, Chen et al showed that transplantation of GMT overexpressing CFs into injured murine hearts resulted in poor cell survival and minimal expression of cardiac genes (85).

Ever since, alternate to cell therapy, other groups have demonstrated that gene transfer of appropriate reprogramming factors can better improve cardiac function and suppress fibrosis after MI (41, 42, 86-88). It is understandable that gene transfer might be preferred, as engraftment of transplanted cells could be a major limitation for cardiac cell therapies. However, different routes such as cells immobilized on bioengineered scaffolds or cECMs could be an option to overcome this. Moreover, ex vivo transduction circumvents in vivo off-target effects, an immune response to viral vectors and it allows the cells to be examined and tested for insertional mutagenesis. Moreover, large amounts of an individual's fibroblasts can be grown from a cardiac biopsy or skin biopsy in vitro for transduction with the defined factors, followed by expansion to produce millions of cells and delivery of cells to damaged hearts. Most importantly, it allows cell expansion and off the shelf storage.

This study shows that iCMPs can improve and restore left ventricular function after acute myocardial injury. Further studies are underway testing the use of cECM patch in aiding iCMP engraftment and enhancing functional improvement. As an alternative to just intramyocardial iCMP injections, we plated iCMPs on to cECM patches and cultured them overnight in CRM allowing the cells to adhere to the cECM surface. The cECM patches with cells were sutured on to the mice heart after induction of MI. The mice were monitored regularly. However, this study is still ongoing.

11. CONCLUSION

In summary, cardiac reprogramming is a promising strategy for cardiac cell therapy and there has been significant progress in the past years to increase the efficiency and function of iCMs.

In this project, we were able to generate a cardiac committed proliferative cell type – iCMPs by direct reprogramming of cardiac fibroblasts, using the cardiac transcription factors Gata4, Mef2c, Tbx5, Myocd (GMTMy). The iCMPs are a heterogeneous population of cells with high cardiac troponin expression along with multiple cardiac progenitor markers such as Cxcr4, Flk1, Mesp1, and Nkx2.5. Next, pure iCMP populations were obtained by transcriptional selection with MYH6/7-targeting molecular beacons.

iCMPs can be expanded to yield therapeutic cell doses. Structural abilities such as sarcomeric formations upon 5-Azacytidine addition were ascertained. Furthermore, they exert therapeutic benefits in vivo - Serial transthoracic echocardiographic analyses revealed long term functional benefits such as improvement in heart function after MI in mice treated with iCMPs compared to the no treatment and control groups.

Taken together, iCMPs generated via direct cellular reprogramming followed by transcriptional selection display a phenotype compatible with an intermediate state of cardiogenic development and beneficially aid post-infarct myocardial remodeling in a rodent model. Thus, cardiac regeneration with iCMPs might be a potential cell therapy option for heart diseases.

In the near future, to translate the iCMP strategy into clinical studies, a shifted focus on human cell reprogramming and approaches for transcriptional delivery system should be considered.

12. LIST OF REFERENCE

1. Konstam MA, Kramer DG, Patel AR, Maron MS, Udelson JE. Left ventricular remodeling in heart failure: current concepts in clinical significance and assessment. JACC Cardiovasc Imaging. 2011;4(1):98-108.
2. Awada HK, Hwang MP, Wang Y. Towards comprehensive cardiac repair and regeneration after myocardial infarction: Aspects to consider and proteins to deliver. Biomaterials. 2016;82:94-112.
3. Medical Advisory S. Left ventricular assist devices: an evidence-based analysis. Ont Health Technol Assess Ser. 2004;4(3):1-69.
4. Karimov JH, Sunagawa G, Horvath D, Fukamachi K, Starling RC, Moazami N. Limitations to Chronic Right Ventricular Assist Device Support. Ann Thorac Surg. 2016;102(2):651-8.
5. Toyoda Y, Guy TS, Kashem A. Present status and future perspectives of heart transplantation. Circulation journal : official journal of the Japanese Circulation Society. 2013;77(5):1097-110.
6. Lin Z, Pu WT. Strategies for cardiac regeneration and repair. Science translational medicine. 2014;6(239):239rv1.
7. Bergmann O, Bhardwaj RD, Bernard S, Zdunek S, Barnabe-Heider F, Walsh S. Evidence for cardiomyocyte renewal in humans. Science. 2009;324(5923):98-102.
8. Wang WE, Li L, Xia X, Fu W, Liao Q, Lan C, et al. Dedifferentiation, Proliferation, and Redifferentiation of Adult Mammalian Cardiomyocytes After Ischemic Injury. Circulation. 2017;136(9):834-48.
9. Fisher SA, Doree C, Mathur A, Taggart DP, Martin-Rendon E. Stem cell therapy for chronic ischaemic heart disease and congestive heart failure. Cochrane Database Syst Rev. 2016;12:CD007888.
10. Takahashi K, Yamanaka S. Induction of pluripotent stem cells from mouse embryonic and adult fibroblast cultures by defined factors. Cell. 2006;126(4):663-76.
11. Hou P, Li Y, Zhang X, Liu C, Guan J, Li H, et al. Pluripotent stem cells induced from mouse somatic cells by small-molecule compounds. Science. 2013;341(6146):651-4.
12. Zwi L, Caspi O, Arbel G, Huber I, Gepstein A, Park IH. Cardiomyocyte differentiation of human induced pluripotent stem cells. Circulation. 2009;120(15):1513-23.

13. Hartman ME, Dai DF, Laflamme MA. Human pluripotent stem cells: Prospects and challenges as a source of cardiomyocytes for in vitro modeling and cell-based cardiac repair. Advanced drug delivery reviews. 2016;96:3-17.
14. Talkhabi M, Aghdami N, Baharvand H. Human cardiomyocyte generation from pluripotent stem cells: A state-of-art. Life Sci. 2016;145:98-113.
15. Burridge PW, Matsa E, Shukla P, Lin ZC, Churko JM, Ebert AD, et al. Chemically defined generation of human cardiomyocytes. Nature methods. 2014;11(8):855-60.
16. Burridge PW, Keller G, Gold JD, Wu JC. Production of de novo cardiomyocytes: human pluripotent stem cell differentiation and direct reprogramming. Cell Stem Cell. 2012;10(1):16-28.
17. Sheehy SP, Pasqualini F, Grosberg A, Park SJ, Aratyn-Schaus Y, Parker KK. Quality metrics for stem cell-derived cardiac myocytes. Stem cell reports. 2014;2(3):282-94.
18. Davis RL, Weintraub H, Lassar AB. Expression of a single transfected cDNA converts fibroblasts to myoblasts. Cell. 1987;51(6):987-1000.
19. Kulessa H, Frampton J, Graf T. GATA-1 reprograms avian myelomonocytic cell lines into eosinophils, thromboblasts, and erythroblasts. Genes & development. 1995;9(10):1250-62.
20. Xie H, Ye M, Feng R, Graf T. Stepwise reprogramming of B cells into macrophages. Cell. 2004;117(5):663-76.
21. Izumikawa M, Minoda R, Kawamoto K, Abrashkin KA, Swiderski DL, Dolan DF. Auditory hair cell replacement and hearing improvement by Atoh1 gene therapy in deaf mammals. Nature medicine. 2005;11(3):271-6.
22. Zheng JL, Gao WQ. Overexpression of Math1 induces robust production of extra hair cells in postnatal rat inner ears. Nat Neurosci. 2000;3(6):580-6.
23. Pinto AR, Ilinykh A, Ivey MJ, Kuwabara JT, D'Antoni ML, Debuque R. Revisiting Cardiac Cellular Composition. Circulation research. 2016;118(3):400-9.
24. Ruskoaho VTaH. Cardiac fibrosis in myocardial infarction-from repair and remodeling to regeneration. 2016 Jun 21.
25. Byun J, Huh JE, Park SJ, Jang JE, Suh YL, Lee JS. Myocardial injury-induced fibroblast proliferation facilitates retroviral-mediated gene transfer to the rat heart in vivo. The journal of gene medicine. 2000;2(1):2-10.
26. Aydin B, Mazzoni EO. Cell Reprogramming: The Many Roads to Success. Annu Rev Cell Dev Biol. 2019.

27. Ieda M, Fu JD, Delgado-Olguin P, Vedantham V, Hayashi Y, Bruneau BG. Direct reprogramming of fibroblasts into functional cardiomyocytes by defined factors. Cell. 2010;142(3):375-86.
28. Efe JA, Hilcove S, Kim J, Zhou H, Ouyang K, Wang G, et al. Conversion of mouse fibroblasts into cardiomyocytes using a direct reprogramming strategy. Nature cell biology. 2011;13(3):215-22.
29. Jayawardena TM, Egemnazarov B, Finch EA, Zhang L, Payne JA, Pandya K. MicroRNA-mediated in vitro and in vivo direct reprogramming of cardiac fibroblasts to cardiomyocytes. Circulation research. 2012;110(11):1465-73.
30. Protze S, Khattak S, Poulet C, Lindemann D, Tanaka EM, Ravens U. A new approach to transcription factor screening for reprogramming of fibroblasts to cardiomyocyte-like cells. Journal of molecular and cellular cardiology. 2012;53(3):323-32.
31. Hirai H, Katoku-Kikyo N, Keirstead SA, Kikyo N. Accelerated direct reprogramming of fibroblasts into cardiomyocyte-like cells with the MyoD transactivation domain. Cardiovascular research. 2013;100(1):105-13.
32. Addis RC, Ifkovits JL, Pinto F, Kellam LD, Esteso P, Rentschler S. Optimization of direct fibroblast reprogramming to cardiomyocytes using calcium activity as a functional measure of success. Journal of molecular and cellular cardiology. 2013;60:97-106.
33. Smith AW, Hoyne JD, Nguyen PK, McCreedy DA, Aly H, Efimov IR. Direct reprogramming of mouse fibroblasts to cardiomyocyte-like cells using Yamanaka factors on engineered poly(ethylene glycol) (PEG) hydrogels. Biomaterials. 2013;34(28):6559-71.
34. Christoforou N, Chellappan M, Adler AF, Kirkton RD, Wu T, Addis RC. Transcription factors MYOCD, SRF, Mesp1 and SMARCD3 enhance the cardio-inducing effect of GATA4, TBX5, and MEF2C during direct cellular reprogramming. PloS one. 2013;8(5):e63577.
35. Xie M, Cao N, Ding S. Small molecules for cell reprogramming and heart repair: progress and perspective. ACS chemical biology. 2014;9(1):34-44.
36. Muraoka N, Yamakawa H, Miyamoto K, Sadahiro T, Umei T, Isomi M. MiR-133 promotes cardiac reprogramming by directly repressing Snai1 and silencing fibroblast signatures. The EMBO journal. 2014.
37. Wang L, Liu Z, Yin C, Asfour H, Chen O, Li Y. Stoichiometry of Gata4, Mef2c, and Tbx5 influences the efficiency and quality of induced cardiac myocyte reprogramming. Circulation research. 2015;116(2):237-44.

38. Fu JD, Stone NR, Liu L, Spencer CI, Qian L, Hayashi Y, et al. Direct Reprogramming of Human Fibroblasts toward a Cardiomyocyte-like State. Stem cell reports. 2013;1(3):235-47.
39. Wada R, Muraoka N, Inagawa K, Yamakawa H, Miyamoto K, Sadahiro T. Induction of human cardiomyocyte-like cells from fibroblasts by defined factors. Proceedings of the National Academy of Sciences of the United States of America. 2013;110(31):12667-72.
40. Nam YJ, Song K, Luo X, Daniel E, Lambeth K, West K. Reprogramming of human fibroblasts toward a cardiac fate. Proceedings of the National Academy of Sciences of the United States of America. 2013;110(14):5588-93.
41. Qian L, Huang Y, Spencer CI, Foley A, Vedantham V, Liu L. In vivo reprogramming of murine cardiac fibroblasts into induced cardiomyocytes. Nature. 2012;485(7400):593-8.
42. Mathison M, Gersch RP, Nasser A, Lilo S, Korman M, Fourman M. In vivo cardiac cellular reprogramming efficacy is enhanced by angiogenic preconditioning of the infarcted myocardium with vascular endothelial growth factor. J Am Heart Assoc. 2012;1(6):e005652.
43. Brown RD, Ambler SK, Mitchell MD, Long CS. The cardiac fibroblast: therapeutic target in myocardial remodeling and failure. Annual review of pharmacology and toxicology. 2005;45:657-87.
44. Camelliti P, Borg TK, Kohl P. Structural and functional characterisation of cardiac fibroblasts. Cardiovascular research. 2005;65(1):40-51.
45. Baudino TA, Carver W, Giles W, Borg TK. Cardiac fibroblasts: friend or foe? Am J Physiol Heart Circ Physiol. 2006;291(3):H1015-26.
46. Ifkovits JL, Addis RC, Epstein JA, Gearhart JD. Inhibition of TGFbeta signaling increases direct conversion of fibroblasts to induced cardiomyocytes. PloS one. 2014;9(2):e89678.
47. Hirai H, Kikyo N. Inhibitors of suppressive histone modification promote direct reprogramming of fibroblasts to cardiomyocyte-like cells. Cardiovascular research. 2014;102(1):188-90.
48. Talkhabi M, Pahlavan S, Aghdami N, Baharvand H. Ascorbic acid promotes the direct conversion of mouse fibroblasts into beating cardiomyocytes. Biochemical and biophysical research communications. 2015.
49. Morez C, Noseda M, Paiva MA, Belian E, Schneider MD, Stevens MM. Enhanced efficiency of genetic programming toward cardiomyocyte creation through topographical cues. Biomaterials. 2015;70:94-104.

50. Wang L, Liu Z, Yin C, Zhou Y, Liu J, Qian L. Improved Generation of Induced Cardiomyocytes Using a Polycistronic Construct Expressing Optimal Ratio of Gata4, Mef2c and Tbx5. J Vis Exp. 2015(105).
51. CHOOI MAY LAI YKYL, and P. ELIZABETH RAKOCZY. Adenovirus and AAV vectors.pdf. 2002.
52. Nitin N, Santangelo PJ, Kim G, Nie S, Bao G. Peptide-linked molecular beacons for efficient delivery and rapid mRNA detection in living cells. Nucleic acids research. 2004;32(6):e58.
53. Santangelo P, Nitin N, Bao G. Nanostructured probes for RNA detection in living cells. Ann Biomed Eng. 2006;34(1):39-50.
54. Rhee WJ, Bao G. Simultaneous detection of mRNA and protein stem cell markers in live cells. BMC Biotechnol. 2009;9:30.
55. Ban K, Wile B, Kim S, Park HJ, Byun J, Cho KW. Purification of cardiomyocytes from differentiating pluripotent stem cells using molecular beacons that target cardiomyocyte-specific mRNA. Circulation. 2013;128(17):1897-909.
56. Ban K, Wile B, Cho KW, Kim S, Song MK, Kim SY. Non-genetic Purification of Ventricular Cardiomyocytes from Differentiating Embryonic Stem Cells through Molecular Beacons Targeting IRX-4. Stem cell reports. 2015;5(6):1239-49.
57. Wile BM, Ban K, Yoon YS, Bao G. Molecular beacon-enabled purification of living cells by targeting cell type-specific mRNAs. Nature protocols. 2014;9(10):2411-24.
58. Jha R, Wile B, Wu Q, Morris AH, Maher KO, Wagner MB, et al. Molecular beacon-based detection and isolation of working-type cardiomyocytes derived from human pluripotent stem cells. Biomaterials. 2015;50:176-85.
59. Ehler E, Moore-Morris T, Lange S. Isolation and culture of neonatal mouse cardiomyocytes. Journal of visualized experiments : JoVE. 2013(79).
60. Zhang Y, Cao N, Huang Y, Spencer CI, Fu JD, Yu C. Expandable Cardiovascular Progenitor Cells Reprogrammed from Fibroblasts. Cell Stem Cell. 2016;18(3):368-81.
61. Li XH, Li Q, Jiang L, Deng C, Liu Z, Fu Y. Generation of Functional Human Cardiac Progenitor Cells by High-Efficiency Protein Transduction. Stem cells translational medicine. 2015;4(12):1415-24.
62. Goumans MJ, de Boer TP, Smits AM, van Laake LW, van Vliet P, Metz CH. TGF-beta1 induces efficient differentiation of human cardiomyocyte progenitor cells into functional cardiomyocytes in vitro. Stem cell research. 2007;1(2):138-49.

63. Schubert M, Lindgreen S, Orlando L. AdapterRemoval v2: rapid adapter trimming, identification, and read merging. BMC Res Notes. 2016;9:88.

64. Kim D, Pertea G, Trapnell C, Pimentel H, Kelley R, Salzberg SL. TopHat2: accurate alignment of transcriptomes in the presence of insertions, deletions and gene fusions. Genome biology. 2013;14(4):R36.

65. Langmead B, Salzberg SL. Fast gapped-read alignment with Bowtie 2. Nature methods. 2012;9(4):357-9.

66. Love MI, Huber W, Anders S. Moderated estimation of fold change and dispersion for RNA-seq data with DESeq2. Genome biology. 2014;15(12):550.

67. Subramanian A, Tamayo P, Mootha VK, Mukherjee S, Ebert BL, Gillette MA. Gene set enrichment analysis: a knowledge-based approach for interpreting genome-wide expression profiles. Proceedings of the National Academy of Sciences of the United States of America. 2005;102(43):15545-50.

68. Becker M, Maring JA, Oberwallner B, Kappler B, Klein O, Falk V. Processing of Human Cardiac Tissue Toward Extracellular Matrix Self-assembling Hydrogel for In Vitro and In Vivo Applications. J Vis Exp. 2017(130).

69. Becker M, Maring JA, Schneider M, Herrera Martin AX, Seifert M, Klein O. Towards a Novel Patch Material for Cardiac Applications: Tissue-Specific Extracellular Matrix Introduces Essential Key Features to Decellularized Amniotic Membrane. Int J Mol Sci. 2018;19(4).

70. Qian L, Berry EC, Fu JD, Ieda M, Srivastava D. Reprogramming of mouse fibroblasts into cardiomyocyte-like cells in vitro. Nature protocols. 2013;8(6):1204-15.

71. Kattman SJ, Huber TL, Keller GM. Multipotent flk-1+ cardiovascular progenitor cells give rise to the cardiomyocyte, endothelial, and vascular smooth muscle lineages. Developmental cell. 2006;11(5):723-32.

72. Yang L, Soonpaa MH, Adler ED, Roepke TK, Kattman SJ, Kennedy M. Human cardiovascular progenitor cells develop from a KDR+ embryonic-stem-cell-derived population. Nature. 2008;453(7194):524-8.

73. Bondue A, Lapouge G, Paulissen C, Semeraro C, Iacovino M, Kyba M. Mesp1 acts as a master regulator of multipotent cardiovascular progenitor specification. Cell stem cell. 2008;3(1):69-84.

74. Cai CL, Liang X, Shi Y, Chu PH, Pfaff SL, Chen J. Isl1 identifies a cardiac progenitor population that proliferates prior to differentiation and contributes a majority of cells to the heart. Developmental cell. 2003;5(6):877-89.

75. Oh H, Bradfute SB, Gallardo TD, Nakamura T, Gaussin V, Mishina Y. Cardiac progenitor cells from adult myocardium: homing, differentiation, and fusion after infarction. Proceedings of the National Academy of Sciences of the United States of America. 2003;100(21):12313-8.
76. Wu SM, Fujiwara Y, Cibulsky SM, Clapham DE, Lien CL, Schultheiss TM. Developmental origin of a bipotential myocardial and smooth muscle cell precursor in the mammalian heart. Cell. 2006;127(6):1137-50.
77. Cao N, Liu Z, Chen Z, Wang J, Chen T, Zhao X. Ascorbic acid enhances the cardiac differentiation of induced pluripotent stem cells through promoting the proliferation of cardiac progenitor cells. Cell research. 2012;22(1):219-36.
78. Lalit PA, Rodriguez AM, Downs KM, Kamp TJ. Generation of multipotent induced cardiac progenitor cells from mouse fibroblasts and potency testing in ex vivo mouse embryos. Nature protocols. 2017;12(5):1029-54.
79. Smits AM, van Laake LW, den Ouden K, Schreurs C, Szuhai K, van Echteld CJ. Human cardiomyocyte progenitor cell transplantation preserves long-term function of the infarcted mouse myocardium. Cardiovascular research. 2009;83(3):527-35.
80. Naito AT, Shiojima I, Akazawa H, Hidaka K, Morisaki T, Kikuchi A. Developmental stage-specific biphasic roles of Wnt/beta-catenin signaling in cardiomyogenesis and hematopoiesis. Proceedings of the National Academy of Sciences of the United States of America. 2006;103(52):19812-7.
81. Sia J, Yu P, Srivastava D, Li S. Effect of biophysical cues on reprogramming to cardiomyocytes. Biomaterials. 2016;103:1-11.
82. Li Y, Dal-Pra S, Mirotsou M, Jayawardena TM, Hodgkinson CP, Bursac N. Tissue-engineered 3-dimensional (3D) microenvironment enhances the direct reprogramming of fibroblasts into cardiomyocytes by microRNAs. Scientific reports. 2016;6:38815.
83. Oberwallner B, Brodarac A, Anic P, Saric T, Wassilew K, Neef K. Human cardiac extracellular matrix supports myocardial lineage commitment of pluripotent stem cells. European journal of cardio-thoracic surgery : official journal of the European Association for Cardio-thoracic Surgery. 2015;47(3):416-25; discussion 25.
84. Lam JT, Moretti A, Laugwitz KL. Multipotent progenitor cells in regenerative cardiovascular medicine. Pediatr Cardiol. 2009;30(5):690-8.
85. Chen JX, Krane M, Deutsch MA, Wang L, Rav-Acha M, Gregoire S. Inefficient reprogramming of fibroblasts into cardiomyocytes using Gata4, Mef2c, and Tbx5. Circ Res. 2012;111(1):50-5.

86. Inagawa K, Miyamoto K, Yamakawa H, Muraoka N, Sadahiro T, Umei T. Induction of cardiomyocyte-like cells in infarct hearts by gene transfer of Gata4, Mef2c, and Tbx5. Circulation research. 2012;111(9):1147-56.
87. Mathison M, Singh VP, Gersch RP, Ramirez MO, Cooney A, Kaminsky SM. "Triplet" polycistronic vectors encoding Gata4, Mef2c, and Tbx5 enhances postinfarct ventricular functional improvement compared with singlet vectors. The Journal of thoracic and cardiovascular surgery. 2014.
88. Mohamed TM, Stone NR, Berry EC, Radzinsky E, Huang Y, Pratt K. Chemical Enhancement of In Vitro and In Vivo Direct Cardiac Reprogramming. Circulation. 2016.

13. STATUTORY DECLARATION

I, Dipthi Bachamanda Somesh, by personally signing this document in lieu of an oath, hereby affirm that I prepared the submitted dissertation on the topic “Induced cardiomyocyte precursor cells obtained by direct reprogramming of cardiac fibroblasts”, independently and without the support of third parties, and that I used no other sources and aids than those stated.
All parts, which are based on the publications or presentations of other authors, either in letter or in spirit, are specified as such in accordance with the citing guidelines. The sections on methodology (in particular regarding practical work, laboratory regulations, statistical processing) and results (in particular regarding figures, charts and tables) are exclusively my responsibility.

My contributions to any publications to this dissertation correspond to those stated in the below joint declaration made together with the supervisor. All publications created within the scope of the dissertation comply with the guidelines of the ICMJE (International Committee of Medical Journal Editors; www.icmje.org) on authorship. In addition, I declare that I am aware of the regulations of Charité – Universitätsmedizin Berlin on ensuring good scientific practice and that I commit to comply with these regulations.

The significance of this statutory declaration and the consequences of a false statutory declaration under criminal law (Sections 156, 161 of the German Criminal Code) are known to me.”

Date: 20.04.2020

Signature:

14. DECLARATION OF YOUR OWN CONTRIBUTION TO ANY PUBLICATIONS

Dipthi Bachamanda Somesh contributed to the Abstract publications listed below:

D Bachamanda Somesh, K Klose, JA Maring, K Juerchott, U Krueger, D Kunkel, A Kurtz, V Falk, M Gossen, C Stamm

Generating proliferative induced cardiomyocyte precursor cells

EMJ Cardiology 2019

O. Reidell, D. B. Somesh, K. Klose, S. Protze, D. Kunkel, U. Krüger, K. Jürchott, V. Falk, M. Gossen, C. Stamm

Maturation of Induced Cardiomyocyte Precursor Cells Created by Direct Reprogramming

In: Thorac cardiovasc Surg 2018; 66(S 01): S1-S110

DOI: 10.1055/s-0038-1627947

Somesh DB, Klose K, Kunkel D, Krüger U, Protze S, Falk V, Gossen M, Stamm C

Induced cardiomyocyte progenitor cells created by direct reprogramming and transcriptional selection

In: Clin Res Cardiol 106, Suppl 1, April 2017-P475.

DOI: 10.1007/s00392-017-1105-2

D.B. Somesh, K. Klose, S. Protze, D. Kunkel, U. Krüger, K. Jürchott, M. Gossen, V. Falk, C. Stamm

Next generation sequencing reveals a committed but immature phenotype of induced cardiomyopcyte progenitor cells

In: Thorac cardiovasc Surg 2017; 65(S 01): S1-S110

DOI: 10.1055/s-0037-1598858

D.B. Somesh, K. Klose, S. Protze, D. Kunkel, U. Krüger, K. Jürchott, M. Gossen, V. Falk, C. Stamm

Maintenance and expansion of induced cardiomyocyte precursor cells created by direct reprogramming

In: Thorac cardiovasc Surg 2017; 65(S 01): S1-S110

DOI: 10.1055/s-0037-1598945

D.Somesh, K.Klose, S.Protze, D.Kunkel, V.Falk, M.Gossen, C.Stamm

Transcriptional selection and maintenance of induced cardiomyocyte precursor cells created by direct reprogramming

Submitted to: XLIII Annual Congress of the European Society for Artificial Organs 2016 (ESAO Congress 2016)

D.Somesh, K.Klose, S.Protze, D.Kunkel, A.Kurtz, V.Falk, Y.H.Choi, M.Gossen, C.Stamm

Transcriptional selection of induced cardiomyocyte precursor cells

In: The Thoracic and Cardiovascular Surgeon 64(S 01) · January 2016

DOI: 10.1055/s-0036-1571714

D. Bachamanda-Somesh, K. Klose, S. Protze, A. Kurtz, M. Gossen, C. Stamm

Direct in vitro lineage reprogramming of murine fibroblasts into cardiomyocytes induces cell death

In: The Thoracic and Cardiovascular Surgeon 62(S 01) · February 2014

DOI: 10.1055/s-0034-1367447

Contribution - Study design, performing the experiments, animal experiments, data analysis, interpretation of data and writing the abstracts.

_____

Signature, date and stamp of supervising university professor / lecturer

_____

Signature of doctoral candidate

15. CV

For reasons of data protection law, my curriculum vitae will not be published in the electronic version of my work.

For reasons of data protection law, my curriculum vitae will not be published in the electronic version of my work.

For reasons of data protection law, my curriculum vitae will not be published in the electronic version of my work.

16. ACKNOWLEDGEMENT

Marie Curie warned that “The way of progress is neither swift nor easy”. The true difficulty of a graduate school lies in the mental challenge that extends beyond the intellectual and into the psychological. The only thing swift and easy about science is how quickly everything call fall apart. In the lab, you work hard, work early, work late, work weekends and still fail. No one warns us how it feels to fail constantly.
However, as many times as I was knocked down, I have been able to stand up, brush off my lab coats and keep pipetting, because of all the support I got from my family, friends, lab mates, and supervisors.

I am grateful for my supervisors Prof. Dr. Christof Stamm, Prof. Andreas Kurtz, and Dr. Manfred Gossen, without whom this project would not have been. They made this project what it is. I am lucky to have had them to guide and support me with remarkable expertise and assistance with objective insights and answers to my questions and troubles. Special thanks to Christof Stamm, for giving me the opportunity to pursue my Ph.D. research under his guidance. He gave me all the freedom to pursue my research and silently steered me in the right direction whenever he thought I needed it. An extended thanks to Dr. Manfred Gossen for always having his office door open for guidance with research and writing this thesis.

I am very grateful to the Berlin Brandenburg School for Regenerative Therapies (BSRT) for allowing me to be a part of the prestigious graduate school. I am also thankful for all the funding bodies, without which I would not have been able to pursue my PhD research.

Special gratitude to the following staff of the institute for their gracious help and assistance: Dr. rer. nat. Désiree Kunkel, of the BCRT FACS core facility, Ulrike Krüger of the BIH core facility Genomics, and Dr. rer. nat. Karsten Jürchott, Bioinformatician of Development & Exploratory Lab (DEL).

I would also like to acknowledge all my scientific colleagues Rajika Roy, Kristin Klose, Andreas Bader, Zhiyi Xu (Daisy), Barbara Oberwallner, Matthias Becker, Ana Gracia Duran, Liu Zihou, Donald Hanssen, Timo Nazari, Sebastian Neuber and Olivia Reidell for the regular progress meetings, journal clubs, all the fruitful discussions, the lunch breaks, cake sessions and all the little things we did to make PhD life fun.
Special thanks to our post doc Dr. Janita Aline Maring, for performing all animal surgeries and teaching in the process. It was a fantastic experience to assist with animal surgeries.

A very special thanks to Kris for being there at every step of my Ph.D. work and for helping me in myriad different ways. I am grateful for all our long coffee break conversations. Every PhD student should be so lucky to have a friend like her.

My acknowledgement would be incomplete without thanking my family. This journey would have not been possible without their support and encouragement.

I am very thankful to my mom, dad, and Jagjith for their unending love and support. They let me be and do what I want and kept me going on my path to success.

Thanks to Achen, Amma, Sandhya, Shreejith, and my adorable little niece Naina for their support and patience along the way.

I am grateful to Sreesanth for being the moral and emotional support in my life, for making sure there wasn't a dull day, and for always being there. I thank him for putting up with me in difficult moments where I felt stumped and for goading me on to follow my dream of getting this degree. Without his unwavering love, support, and belief in me I never would have made it this far.